Hepatitis B virus production is modulated through the autophagy pathway in response to glucose

Inaugural-Dissertation

zur

Erlangung des Doktorgrades

Dr. rer. nat.

der Fakultät für

Biologie

an der

Universität Duisburg-Essen

Vorgelegt von

Xueyu Wang

Aus Loudi, P.R.China

September 2019

Die der vorliegenden Arbeit zugrunde liegenden Experimente wurden am Institut für Virologie der Universität Duisburg-Essen durchgeführt.

1. Gutachter: Prof. Astrid Westendorf

2. Gutachter: Prof. Mengji Lu

3. Gutachter: Prof. Matthias Gunzer

Vorsitzender des Prüfungsausschusses: Prof. Astrid Westendorf

Tag der mündlichen Prüfung: 07.02.2020

DOI: 10.17185/duepublico/71422
URN: urn:nbn:de:hbz:464-20210303-101020-1

Table of contents

1. Introduction

1.1 Glucose metabolism

In living organisms, glucose metabolism signifies the various biochemical processes responsible for the formation, breakdown, and interconversion of carbohydrates. These processes provide energy and biosynthetic precursors to maintain cellular homeostasis and function. Metabolism consists of catabolism, which breaks down macromolecules (such as polysaccharides, lipids, nucleic acids and proteins) into smaller units (such as monosaccharides, fatty acids, nucleotides, and amino acids, respectively) to produce energy, and anabolism, which constructs essential building blocks for macromolecule production.

1.1.1 Glycolysis

Glycolysis is the main catabolism pathway, where a glucose molecule breaks down into two pyruvate molecules, while releasing energy as adenosine triphosphate (ATP) and nicotinamide adenine dinucleotide hydride (NADH) (Figure 1.1) [1]. Nearly all living organisms that break down glucose utilize glycolysis. This pathway is anaerobic, because it does not require oxygen.

The first step in glucose metabolism is its entrance in the cell through the action of glucose transporters (GLUT) that belong to the SLC2A family of membrane transport proteins. Glycolysis consists of ten steps, split into two phases. The first phase requires the breakdown of two ATP molecules. During the second phase, chemical energy from the intermediates is transferred into ATP and NADH. The breakdown of one molecule of glucose results in two molecules of pyruvate, which can be further oxidized to provide more energy in later processes. The first step relies on the phosphorylation of glucose by the rate-limiting enzyme hexokinase (HK), which yields glucose-6-phosphate. The quick phosphorylation of intracellular glucose prevents its cellular efflux as well as the enzymatic conservation of high-energy bonds through the formation of phosphate esters. Additionally, phosphoryl groups destabilize glucose and facilitate its consequent metabolism. HK is regulated through a negative feedback loop by glucose-6-phosphate that when in high intracellular quantity signals for excess of cellular energy. Glucose-6-phosphate is then reversibly isomerized to fructose-6-phosphate, which can be further phosphorylated by phosphofructokinase (PFK), at the cost of one ATP molecule, to fructose-1,6-bisphosphate. The irreversible

step mediated by PFK is a very important pacemaker of glycolysis being allosterically positively regulated by AMP and negatively by ATP, fructose-2,6-phosphate, and citrate. This balance points out the importance of the ATP/AMP ratio for the rate of glycolysis, as well as its regulation to channel carbon molecules through the oxidative branch of the pentose phosphate pathway (PPP) for maintaining the NADPH pool for fatty acid synthesis. Ultimately, FK is also capable of indirectly inhibiting hexokinase. If PFK is inactive, fructose-6-phosphate and glucose-6-phosphate accumulate, thus inhibiting hexokinase. However, this dynamic may be variable depending on the final destination of glucose-6-phosphate. Although the latter is an important intermediate, since it can modulate the glycolytic flux, it may also be shuttled to feed glycogenesis or the pentose phosphate pathway. The other irreversible step of glycolysis is mediated by pyruvate kinase where phosphoenolpyruvate is converted into the end glycolytic product, pyruvate. In fact, pyruvate kinase isoforms have been suggested to support divergent energetic and biosynthetic outputs, and thus fulfilling differential requirements of cellular metabolism. As such, this catalytic activity plays a crucial role in energy metabolism and has recently been associated with cell proliferation and tumor growth[2, 3]. Although glucose represents a high-energy substrate, only a small portion of free energy is released during glycolysis: most of it remains in the end product, pyruvate, that needs to be further catabolized.

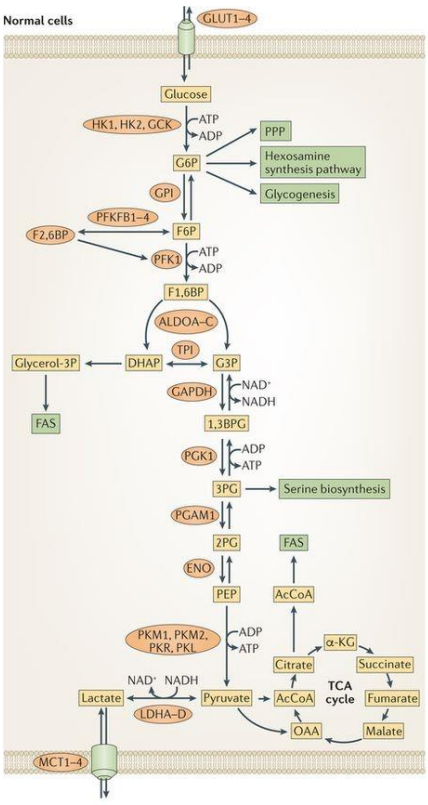

Figure 1.1 Glycolysis pathways and the integration of multiple metabolic pathways

Glycolysis is a series of metabolic processes, driven by nine specific enzymes, by which one molecule of glucose is catabolized into two molecules of pyruvate, two moles of NADH with a net gain of two ATP. It is separated into two parts, the energy investment phase and the energy generation phase. The energy investment phase has five reactions, two of which are reversible and the other three are irreversible. During this phase, two ATP are converted into two ADP. The energy generation phase also has five reactions, one of these reactions is irreversible and the rest are reversible. Four ADP are converted to four ATP and two NAD+ into two NADH. For every molecule of glucose entering glycolysis, two ATP and NAD+ are used and four ATP and NADH are generated. The net gain in glycolysis is two ATP and two NADH.[1]

1.1.2 Tricarboxylic Acid (TCA) Cycle

In mammalian organisms, the end product of glycolysis, pyruvate, shuttles to the mitochondria to yield acetyl-Coenzyme A, which will sustain the TCA cycle (also named citric acid cycle or Krebs cycle) (Figure 1.2)[4, 5]. The TCA cycle is a series of chemical reactions used by all aerobic organisms to release stored energy through the oxidation of acetyl-CoA into carbon dioxide and chemical energy in the form of ATP. The first primary control point in the TCA cycle occurs in the decarboxylation of isocitrate to α-ketoglutarate. NADH and ATP inhibit this reaction, which under certain circumstances (excess of pyruvate and excess of acetyl-CoA) may culminate in accumulation of citrate, triggering lipid synthesis. The allosteric inhibition of α-ketoglutarate dehydrogenase, by succinyl-CoA and NADH, hampers its activity to convert α-ketoglutarate into succinyl-CoA. It is also a key metabolic pathway that connects carbohydrate, fat, and protein metabolism.

TCA cycle is an amphibolic pathway that generates several biosynthetic precursors for *de novo* synthesis of macromolecules. Oxaloacetate and α-ketoglutarate are precursors for aspartate and glutamate synthesis, which in turn may originate other amino acids, such as asparagine, arginine, proline, and glutamine. Furthermore, these intermediates can also contribute to the synthesis of pyrimidines and purines, which are the main building blocks of nucleic acids[6]. Oxaloacetate may also be converted into phosphoenolpyruvate, by phosphoenolpyruvate carboxykinase, thus completing the first step of gluconeogenesis. Succinyl-CoA withdrawal is responsible for the central metabolism that originates the synthesis of porphyrin rings, essential for hemoglobin production[7]. Citrate production may have a vital role in *de novo* fatty acid synthesis. However, when these intermediates are withdrawn from the TCA cycle, its rate is reduced and only their replenishment will allow the continuation of the oxidative capacity of this cycle. This exquisite and dynamic balance is mainly assured

by pyruvate carboxylase that produces oxaloacetate via carboxylation of pyruvate, which guarantees the maintenance of homeostatic levels of TCA intermediates.

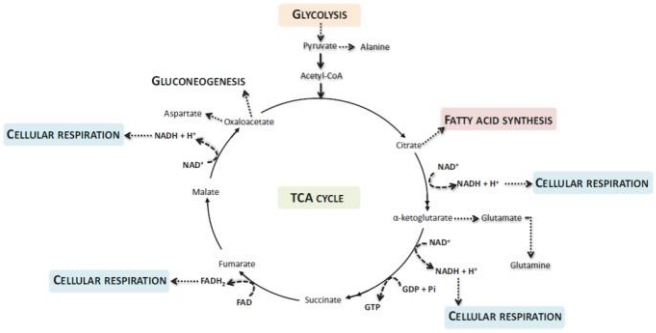

Figure 1.2 The tricarboxylic acid cycle and the integration of multiple metabolic pathways

CoA=Coenzyme A, FAD=flavin adenine mononucleotide, GDP=guanosine diphosphate, GTP=guanosine triphosphate, NAD=nicotinamide adenine dinucleotide

1.1.3 Pentose phosphate pathway

The pentose phosphate pathway (PPP) is a major glycolytic-divergent pathway that shifts metabolic reactions towards the production of precursors for nucleotide and amino acid synthesis as well as the mostly studied product, the reducing co-factor NADPH. This pathway supports cell proliferation and survival[8, 9]. The PPP comprises an oxidative (Figure 1.3) and a non-oxidative branch. The rate limiting step of the oxidative branch is mediated by glucose-6-phosphate dehydrogenase (G6PD) that through the oxidative decarboxylation of glucose-6-phosphate, produces two molecules of NADPH and one ribose-5-phosphate. As expected, this branch relies on the availability of $NADP^+$, as the final electron acceptor, while excess of NADPH is a negative regulator. The non-oxidative branch includes several reversible reactions that interchange carbons from three-carbon and six-carbon molecules to five-carbon molecules, depending on the cellular concentration of NADPH and ribose-5-phosphate, being rate limited by transketolase and transaldolase. The fine balance between PPP and glycolysis is tightly regulated. Whereas ribose-5-phosphate can be produced for nucleotide synthesis, NADPH production mainly supports fatty acid synthesis and has an important action in counteracting oxidative stress. For the latter, six molecules of ribose-5-phosphate are shifted towards production of two molecules of glyceraldehyde-3-phosphate and four molecules of fructose-6-phosphate, thus fuelling glycolysis. The maintenance of redox homeostasis is a vital requisite for cell survival, particularly in aerobic organisms. Taken together, PPP is essential not only in the coordination of cellular metabolism

(catabolism/anabolism) but also for fulfilling intermediaries that are needed for cellular defense and detoxification.

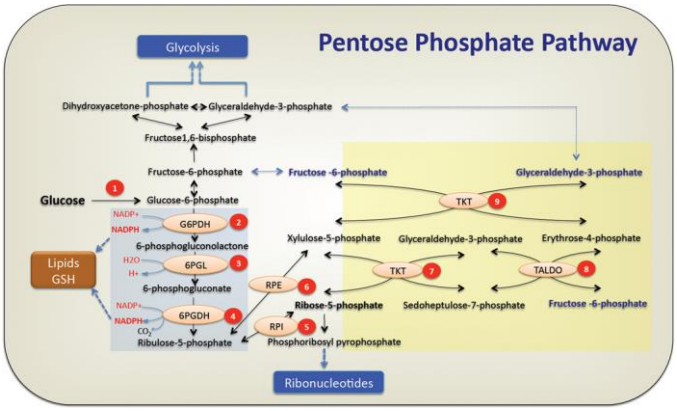

Figure 1.3 The pentose phosphate pathway

The oxidative arm of the pentose phosphate pathway is initiated by conversion of glucose to glucose-6-phosphate (G6P) by hexokinases. Fructose-6-phosphate (F6P) can either be used for glycolysis or be converted back to G6P to replenish the oxidative PPP, while G3P can be utilized in glycolysis, depending on the cellular requirements. The oxidative and nonoxidative branches of the PPP are highlighted by a blue and yellow background, respectively.[9]

1.1.4 Hexosamine biosynthesis pathway

The hexosamine biosynthetic pathway (HBP) is a side branch of glycolysis, which controls *O*-GlcNAc modification of proteins (Figure 1.4). A fraction (2-5%) of the glucose entering the cell is directed into this pathway for UDP-GlcNAc biosynthesis[10]. Then, glutamine D-fructose-6-phosphate amidotransferase (GFPT) uses glutamine to convert fructose-6-phosphate into glucosamine-6-phosphate, which is then used for the synthesis of UDP-GlcNAc. OGT uses UDP-GlcNAc as a substrate to add GlcNAc on serine or threonine residues, and its activity is tightly dependent on the concentration of UDP-GlcNAc in the cell. These modifications can be reversed by OGA, which removes the *O*-GlcNAc moiety from *O*-GlcNAc-modified proteins. In experiment, the level of *O*-GlcNAc in proteins can be increased by culturing cells with a high concentration of glucose, glucosamine (which bypasses allosteric inhibition of the ratelimiting enzyme GFAT) or with PUGNAc, which inhibits deglycosylation of proteins by OGA. *O*-GlcNAc is a post-translational protein modification, which consists of a single *N*-acetylglucosamine moiety attached via an *O*-β-glycosidic

linkage to serine and threonine residues[11, 12]. Cytosolic and nuclear *O*-GlcNAc glycosylation constitutes a dynamic process, which regulates the activity, localization or stability of the modified proteins[13]. In many respects, *O*-GlcNAc is similar to phosphorylation of proteins; for example, it can dynamically attach or remove *O*-GlcNAc in response to the changes in the cellular environment triggered by stress, hormones or nutrients[14]. Similar to protein phosphorylation, *O*-GlcNAcylation can influence protein function by regulating protein-protein interaction, protein stability, nuclear-cytoplasmic shuttling, and intrinsic protein activity[15]. The interplay between phosphorylation and *O*-GlcNAcylation has been implicated in the regulation of critical cellular processes.

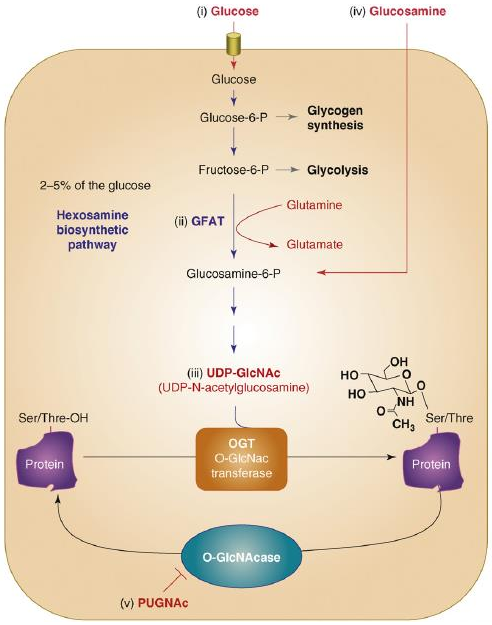

Figure 1.4 Hexosamine biosynthesis pathway

A small fraction of the glucose entering the cell feeds the hexosamine biosynthetic pathway (HBP) to produce UDP-GlcNAc, the substrate used by *O*-GlcNAc-transferase (OGT) to add N-acetyl glucosamine on serine or threonine residues of cytosolic or nuclear proteins.[13]

During short-term fasting, glucagon stimulates gluconeogenesis by enhancing the activity of the cyclic AMP-responsive element-binding protein (CREB). CREB is phosphorylated at Ser 133 by cAMP-dependent Ser/Thr kinase protein kinase A (PKA)[16]. CREB phosphorylation increases its interaction with CBP/p300[17, 18], which has been shown to promote gluconeogenic gene expression by acetylating nucleosomal histones[19, 20]. CREB directly enhances the expression of phosphoenolpyruvate carboxykinase 1 (PEPCK1), and glucose-6-phosphatase

(G6PC). CREB phosphorylation also promotes the expression of peroxisome proliferator-activated receptor-γ co-activator 1α (PGC1α), which is a critical co-activator for prolonged stimulation of gluconeogenic gene transcription[21].

O-GlcNAcylation of many gluconeogenic transcription factors and cofactors has been reported to promote glucose production in the liver. OGT can induce hepatic gluconeogenesis by *O*-GlcNAcylation of CRTC2, the co-activator of CREB. At basal levels, CRTCs are phosphorylated at the amino acid residues Ser 70 and Ser 171 by salt-inducible kinases (SIKs) and other members of the AMP-activated protein kinase (AMPK) family and are sequestered in the cytoplasm by 14-3-3 proteins[22]. In response to cAMP and calcium signals, CRTC2 is dephosphorylated and *O*-GlcNAcylated at the same site, leading to CRTC2 nucleus translocation and binding to CREB, thereby inducing gluconeogenesis[23].

On the other hand, during prolonged fasting, OGT primarily affects PGC1α-mediated expression of gluconeogenic genes. PGC1α acts as a co-activator for the glucocorticoid receptor, the hepatocyte nuclear factor 4 (HNF4), and FOXO1, which further stimulate the expression of gluconeogenic genes[21]. PGC-1α helps recruit OGT to *O*-GlcNAcylate and activate FOXO1[24], which further promotes hepatic glucose production. Therefore, OGT is also involved in glucocorticoid induction of gluconeogenesis[25]. Despite remarkable advances in the understanding of the role of *O*-GlcNAcylation in insulin signaling, how *O*-GlcNAcylation crosstalks with phosphorylation is not well known. Exploring the mechanistic and kinetic features of *O*-GlcNAcylation on key signaling proteins holds great promise for a better understanding of normal liver metabolism.

Uncontrolled gluconeogenesis is one of the hallmarks of diabetic liver and contributes to hyperglycemia. *O*-GlcNAcylation has been found on many gluconeogenic transcription factors and cofactors, including CRTC2, PGC-1α, and FOXO1. Global *O*-GlcNAcylation levels have been shown to be elevated in the liver of high fat diet-fed mice. Hepatic overexpression of OGA in these mice decreases *O*-GlcNAcylation of CRTC2, downregulates gluconeogenic gene expression, and attenuates hyperglycemia[21]. OGT *O*-GlcNAcylates and activates FOXO1 during prolonged fasting to stimulate gluconeogenesis. The levels of HCF-1 are elevated in the liver of high fat diet-fed and db/db mice, which is causally linked with uncontrolled gluconeogenesis and hyperglycemia.

Recent studies have indicated that *O*-GlcNAcylation modulates glycolysis by inhibiting

phosphofructokinase 1 (PFK1) activity and redirecting glucose flux into PPP. Overexpression of OGT or pharmacological inhibition of OGA in many cell lines leads to increased global *O*-GlcNAcylation, decreased glycolysis, and decreased ATP concentration. However, further studies should clarify whether *O*-GlcNAcylation inhibits glycolysis in the liver and whether *O*-GlcNAcylation contributes to the pathogenesis of insulin resistance. Small molecules that target *O*-GlcNAc signaling should be investigated as novel therapeutic agents for liver-related diseases.

1.1.5 Gluconeogenesis

Gluconeogenesis is the reverse process of glycolysis, which involves the conversion of non-carbohydrate molecules into glucose[26]. The non-carbohydrate molecules that are converted in this pathway include pyruvate, lactate, glycerol, alanine, and glutamine[26]. Although glycolysis and gluconeogenesis are not exactly the reverse of each other, both pathways share several enzymes and are reciprocally regulated within the same cell. The major differences between gluconeogenesis and glycolysis are at: (i) the conversion of pyruvate to phosphoenolpyruvate, (ii) the hydrolysis of fructose-1-6-biphosphate in fructose 6-phosphate, and (iii) the hydrolysis of glucose-6-phosphate in glucose. The first step of gluconeogenesis takes place in the mitochondria and consists in the carboxylation of pyruvate to oxaloacetate, at the expense of one ATP molecule by pyruvate carboxylase. Oxaloacetate can then be cleaved into phosphoenolpyruvate, by phosphoenolpyruvate carboxykinase (PEPCK) that is transported to the cytosol to follow the reversible glycolytic reversible steps until the formation of 1,3-bisphosphoglyerate, fueling the reaction mediated by glyceraldehyde 3-phosphate dehydrogenase. However, this reaction requires reducing equivalents at the level of NADH. As such, translocation of reducing equivalents from the mitochondria (where β-oxidation of fatty acid taks place leading to excess of these cofactors) is essential for gluconeogenesis. In this sense, mitochondrial oxaloacetate may be reduced to malate using the excess of mitochondrial NADH, which is then transported to the cytosol. Once in cytosolic, malate is re-oxidized to oxaloacetate, which, by the action of phosphoenolpyruvate carboxykinase, is simultaneously decarboxylated and phosphorylated to generate phosphoenolpyruvate at the expense of energy. Following these reactions, phosphoenolpyruvate is reversely converted to the upstream intermediates of the glycolytic pathway until the irreversible conversion of fructose-1-6-biphosphate into

fructose-6-phosphate. The phosphate ester at C1 is hydrolyzed by fructose-1-6-biphosphatase, thus yielding fructose 6-phosphate. After isomerization by phosphoglucose isomerase, the obtained glucose-6-phosphate is cleaved by endoplasmic reticulum-bounded glucose-6-phosphatase, which originates in glucose that is secreted to maintain the serum glucose levels. The ratio of mitochondrial transport of malate or phosphoenolpyruvate, or other source, to cytosol depends mainly on the availability of cytosolic NADH. This pathway is energetically expensive, being, therefore, replenished via fatty acid β-oxidation. Indeed, fatty acids are rapidly mobilized by the hydrolytic action of lipases from triglycerides. The fatty acid products undergo β-oxidation, whereas the glycerol produced is mainly used to replenish gluconeogenic precursors.

1.1.6 Carbohydrates as storage

Carbohydrates are typically stored as long polymers of glucose molecules with glycosidic bonds for structural support or for energy storage. However, the strong affinity of most carbohydrates for water makes storage of large quantities of carbohydrates inefficient due to the large molecular weight of the solvated water-carbohydrate complex. In most organisms, excess carbohydrates are regularly catabolized to form acetyl-CoA, which is a feed stock for the fatty acid synthesis pathway; fatty acids, triglycerides, and other lipids are commonly used for long-term energy storage. The hydrophobic character of lipids makes them a much more compact form of energy storage than hydrophilic carbohydrates. However, animals, including humans, lack the necessary enzymatic machinery and so do not synthesize glucose from lipids.

1.1.8 Metabolism and HBV

There are clinical associations between HBV infection and host metabolism since metabolic derangement exists in patients with HBV infection. From the molecular mechanism perspective, HBV infection influences the hepatic metabolc signaling pathway (Figure 1.5), including glucose, lipid, nucleic acid and bile acid metabolism, ultimately resulting in metabolic derangement. It is well known that glucose homeostasis is regulated by balancing the consumption and the uptake of glucose[27]. Glucose metabolism in hepatocytes can be divided broadly into two categories: anabolism and catabolism, including gluconeogenesis, glycolysis, aerobic oxidation

and PPP. Previous studies have provided some clues into the glucose metabolic alterations caused by HBV infection, including the up-regulation of PEPCK, G6Pase, and enzymes involved in glycolysis, PPP and TCA cycle[28].

The liver, the main organ for the synthesis and circulation of lipids (e.g., fatty acids, fats, phospholipids and cholesterol), oxidation of fatty acids and the production of ketone bodies, plays an important role in lipid metabolism[29]. A significant amount of basic research has indicated that HBV infection has an effect on fatty acid metabolism. Many, but not all, studies have shown that HBV can promote the synthesis and oxidation of fatty acids. HBV infection can induce the accumulation of lipids via three different regulatory mechanisms, including elevated expression of FABP1, up-regulation of LXR, SREBP1 and PPARγ and increased expression of *N*-acetylglucosaminyltransferase III. On the one hand, up-regulation of FABP1 would increase fatty acid binding and transport. On the other hand, induction of LXR-mediated SREBP1 and PPARγ would result in increased transcriptional activity of hepatic lipogenic genes (FAS, SCD, ACC) and adipogenic genes. In addition, elevation of *N*-acetylglucosaminyltransferase III would cause glycosylation and dysfunction of apolipoprotein B, finally leading to reduced secretion of very low-density lipoproteins (containing cholesterol and triglyceride).

Bile acid, mainly synthesized in the liver from cholesterol, plays a key role in the digestion and absorption of lipids[30]. The study of Yan et al[31] showed that the HBV pre-S1 lipopeptide efficiently blocked the uptake of bile salts by Na^+-taurocholate cotransporting polypeptide (NTCP), suggesting that HBV infection may limit the physiological function of NTCP. Moreover, reduced bile salts can promote compensatory bile acid synthesis to maintain its homeostasis[32, 33].

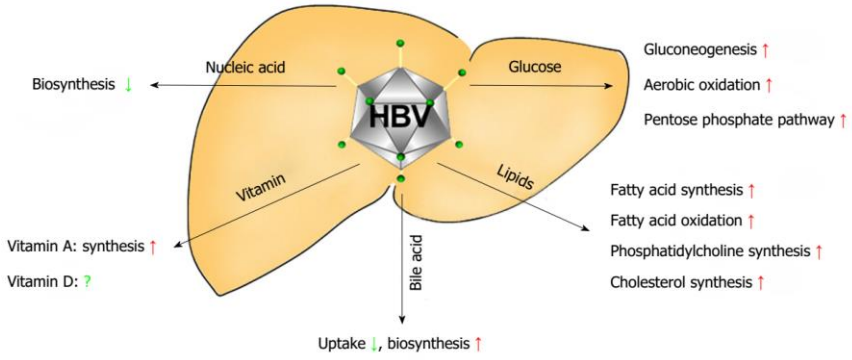

Figure 1.5 Changes in the hepatic metabolic signaling pathway induced by hepatitis B virus infection

Alterations in related signaling pathways (including glucose, lipids, nucleic acids, bile acids and

vitamins) following hepatitis B virus (HBV) infection are marked and highlighted. The influence of HBV infection on vitamin D metabolism is unclear.

It is well known that the main function of nucleotides is the biosynthesis of nucleic acids. Many studies have reported that DNA damage can cause abnormalities in nucleic acid metabolism[34]. HBV infection can decrease nucleic acid biosynthesis via HBx-induced DNA damage, which may result in hepatocarcinogenesis[35].

1.2 Hepatitis B virus

1.2.1 Molecular structure

HBV belongs to the hepadnavirus family[36]. It is an enveloped, partially double-stranded DNA virus with a length of 3.2 kb. It replicates through RNA intermediates and can be integrated into the host genome. Related viruses are found in woodchucks, ground squirrels, tree squirrels, Peking ducks, and herons. There are four overlapping open reading frames (ORFs) which encode seven proteins (pre-S1, pre-S2, S, pre-C, C, viral polymerase, HBx protein) and four regulatory elements (enhancer II/basal core promoter, preS promoter, preS2/S promoter, and enhancer I/X promoter) (Figure 1.6)[37].

Within the envelope is the viral nucleocapsid. The viral capsid contains a viral genome, a relaxed-circular (RC), partially duplex DNA of 3.2 kb, and a polymerase (also serving as a reverse transcriptase) that is responsible for the synthesis of viral DNA in infected cells and mRNA transcripts. Besides the virions particle, subviral particles, including 20-nm spheres and filaments are pleomorphic and exist in patient's serum. These two particles are not infectious and are composed of lipid and protein that form part of the surface of the virion, which is called the surface antigen (HBsAg). HBsAg is produced in excess during the life cycle of the virus.

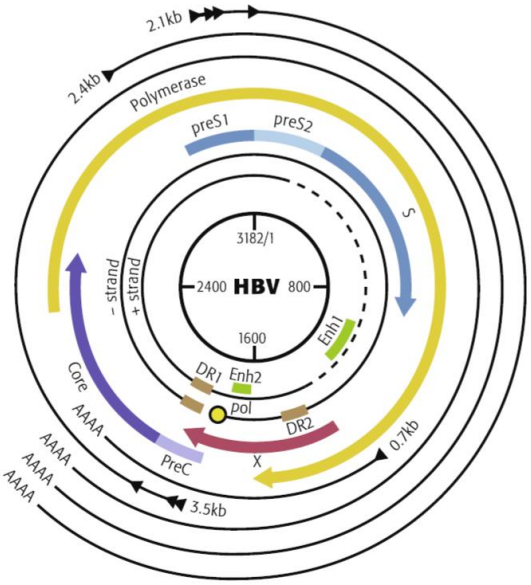

Figure 1.6 Hepatitis B virus (HBV) genome map

The genome consists of a circular, partially double-stranded DNA molecule 3.2 kb in length. During viral replication, the partially double-stranded genome, also named relaxed circular (RC) DNA, is repaired into covalently closed circular (ccc) DNA. cccDNA is a mini-chromosome that serves as the template for viral transcription, generating five major mRNAs that are 3.5-, 2.4-, 2.1-, and 0.7-kb in size. One 3.5 kb mRNA called pre-C mRNA serves as the template for translation of the HBeAg (pre-core protein), and one slightly shorter mRNA called pgRNA serves as the template for core and polymerase proteins, as well as the pre-genomic RNA used as a template during viral replication. The 2.4 kb transcript (pre-S1 mRNA) is used in the translation of the large surface antigen (L); the 2.1 kb transcripts (pre-S2 mRNAs) are used to produce the M and S surface antigens; and the 0.7 kb transcript is used in the production of the X protein.[37]

HBV contains a small, partially double-stranded genome that consists of a full-length negative strand and an incomplete positive strand (Figure 1.6). Its genome contains four promoters, two enhancer regions (Enh1, Enh2), and two direct repeats (DR1, DR2). During virus replication, the partially double-stranded DNA, also named relaxed circular (RC) DNA, is repaired into covalently closed circular (ccc) DNA, which serves as the template for viral transcription, generating mRNAs that are 3.5-, 2.4-, 2.1-, and 0.7-kb in size. One 3.5 kb mRNA called pre-C mRNA serves as the template for translation of the HBeAg (pre-core protein), and one slightly shorter mRNA called pgRNA serves as the template for core and polymerase proteins, as well as the pre-genomic RNA used as a template during viral replication. The 2.4 kb transcript (pre-S1 mRNA) is used in the translation of the large surface antigen (L), the 2.1 kb transcripts (pre-S2 mRNAs) are used to produce the M and S surface antigens, and the 0.7 kb transcript is used in the production of the X protein[38].

1.2.2 HBV life cycle

The HBV life cycle begins with the binding of HBV particles to hepatocytes through the interaction between cell surface receptors and viral envelope proteins (including HBsAg)[36]. Intranuclear HBV cccDNA is used as a template for transcription of viral RNA. HBV is one of the few known non-retroviral viruses that use reverse transcription as part of their replication process[39, 40]. Thus, the viral life cycle is special and complicated. As shown in Figure 1.7, the HBV life cycle includes six processes, like attachment, penetration, uncoating, replication, assembly and release. The detailed process is as follows:

The initial phase of HBV infection involves the attachment of mature virions to the host cell membrane, likely involving the pre-S domain of surface proteins. Na^+-taurocholate cotransporting polypeptide (NTCP) has been found and recognized as a specific receptor of HBV[41, 42]. There are two different pathways for HBV entry into the host cells: one is endocytosis followed by release of nucleocapsids from endocytic vesicles, and the other one is fusion of the viral envelope with the plasma membrane[43].

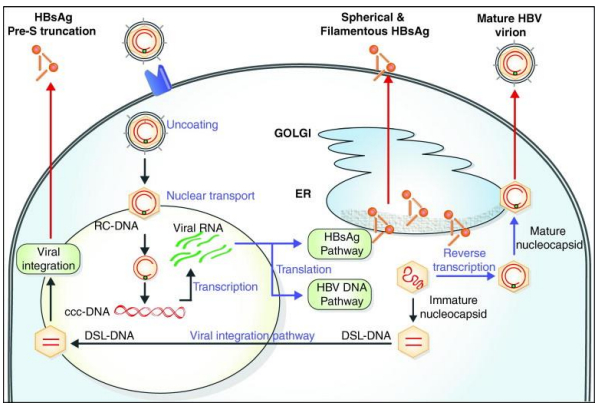

Figure 1.7 HBV life cycle

HBV enters hepatocytes through the specific receptor Na^+-taurocholate cotransporting polypeptide (NTCP), followed by uncoating, and nuclear transport of the rcDNA. The rcDNA is converted to cccDNA, which serves as the template for transcription of HBV mRNA. These RNAs are exported to the cytoplasm for protein translation. pgRNA is selectively packaged inside core particles, followed by P protein-mediated (-) strand DNA synthesis (reverse transcription), pgRNA degradation, and (+) strand DNA synthesis to generate rcDNA. Mature core particles are enveloped for release as virions, or transported to the nucleus to generate more cccDNA.[40]

Secondly, the viral membrane fuses with the host cell membrane and releases the DNA and core proteins into the cytoplasm[43]. Then, the nucleocapsid in cytoplasm

could be transported along with microtubules into the nucleus[44]. In this process, the partially double stranded viral DNA is dissociated from the core proteins, released into the nucleoplasm, repaired to full double stranded DNA, and transformed into covalently closed circular DNA (cccDNA), which serves as a template for transcription of four viral mRNAs[45, 46]. Then, viral mRNAs procees to replication. The largest transcript pgRNA is used to make the new copies of the genome and to make the capsid core protein and the viral DNA polymerase. In the nucleus, rcDNA could be repaired and form cccDNA by viral polymerase, combined with host cellular enzymes[47]. The cccDNA serves as a transcriptional template in the nucleus and utilizes the cellular transcriptional machinery to produce all viral RNAs[45]. The RNA transcripts are then transported to the cytoplasm and translate into associated proteins, while pgRNA is assembled with core protein and polymerase proteins to form the RNA-containing nucleocapsid in cytoplasm. Maturation of RNA-containing nucleocapsid includes synthesis of the (-) DNA strand, pgRNA degradation and synthesis of the (+) DNA strand by the different enzyme activities of viral polymerase[48].
Four viral transcripts, including 3.5 kb preC RNA and pgRNA, 2.4 and 2.1 kb preS/S mRNAs, and 0.7 kb HBx, undergo additional processing and go on to form progeny virions. The long mRNA is then transported back to the cytoplasm where the virion P protein synthesizes DNA via its reverse transcriptase activity[49, 50].
The last step is virions release. In this process, nucleocapsids can be directly bud into the endoplasmic reticulum (ER) or proximal Golgi membranes to acquire their glycoprotein envelope, and trigger new virions secretion, or they are re-imported into the nucleus to amplify the cccDNA pool[51]. This pathway is important for virus persistence in hepatocytes and also contributes to the relapse of viremia after stopping antiviral treatment in chronic HBV infected patients[45].

1.2.3 Modulation of HBV replication

HBV gene expression can be regulated during transcription or post-transcriptional processes. Therefore, HBV replication is regulated by many extracellular and intracellular factors such as specific hormones, inflammatory cytokines, intracellular signaling pathways and metabolic processes[52-55].
The HBV cccDNA plays a key role in the viral life cycle and permits the persistence of infection[45]. cccDNA accumulates in hepatocyte nuclei and forms a stable minichromosome organized as a template for the transcription of viral mRNAs. Thus,

HBV utilizes the cellular transcriptional machinery to produce all viral RNAs necessary for viral protein production and viral replication[56, 57]. Moreover, the acetylation status of cccDNA-bound histones is closely correlated with viremia levels, indicating that epigenetic mechanisms can regulate the transcriptional activity of the cccDNA[57].

Virus replication also relies on host cells. The ability of HBV replication mainly depends on the nature of the antiviral stimulus applied. Host cellular factors participate in HBV life cycle in almost every step from cccDNA formation, transcription, core particle formation and progeny secretion. The proliferation status of host cells also affects HBV replication[58, 59]. In addition, HBV replication can be controlled by multiple cellular transcription factors, in particular, several nuclear receptors like farnesoid X receptor α (FXRα), hepatocyte nuclear factor 4α (HNF4α), liver X receptor (LXR), retinoid X receptor α (RXRα), and peroxisome proliferator activated receptor α/γ (PPARα/γ)[60].

Moreover, there are other cell pathways that contribute to control HBV replication, such as host innate immunity[61]. As shown previously, type I IFNs, proinflammatory cytokines, and chemokines play essential roles in controlling HBV infection. IFNs elicit an anti-viral response by triggering the JAK-STAT signaling pathway, followed an increase in the expression levels of IFN-stimulated genes (ISGs), whose products exhibit antiviral effects[62]. At present, activation of innate immune response can act as a therapeutic approach for chronic hepatitis B infection.

Among the relevant intracellular pathways, the phosphatidylinositol 3-kinase (PI3K)/Akt signaling pathway is a major cellular pathway involved in regulating HBV infection[63, 64]. Guo et al. have reported that HBV replication could be inhibited by activation of the PI3K/Akt signal pathway[63]. This mechanism is likely in part responsible for the reduced HBV replication observed in tumor cells, which can show activation of the PI3K/Akt pathway. Moreover, Hepatitis B surface antigen (HBsAg) synthesis may also be regulated through the PI3K/Akt/mTOR signaling pathway[65].

HBV may also be regulated by metabolic processes, including autophagy[28, 66-68]. Autophagy is also known as one of the host defense responses against infections. However, it has been demonstrated that HBV induces autophagy and elicits this to facilitate its DNA replication. This process is mediated by the HBx protein, which binds to and activates class III phosphatidylinositol-3-kinase (PI3KC3), an enzyme important for autophagy initiation[69, 70]. There is also evidence showing that the small HBV surface protein is required to induce autophagy formation by triggering unfolded

protein responses[71].

1.2.4 HBV-associated liver diseases

According to the recent estimation of the World and Health Organisation (WHO), there are about 257 million people with chronic HBV infection worldwide. It is well established that chronic HBV infection leads to severe liver diseases and fibrosis, and may finally develop into liver cirrhosis and hepatocellular carcinoma (HCC)[72, 73]. Until now, HBV infection is still one of the most common chronic viral infection worldwide. HBV is primarily transmitted through parenteral routes, mucosal contact, or perinatal exposure. About 5% of adults with acute exposure to HBV develop chronic infections, and up to 90% of newborns exposed by vertical transmission may develop chronic HBV[74]. Acute HBV infection is self-limiting and may be self-cleaned in several months. Chronic infection with HBV is a major cause of HCC, a leading cause of cancer-related death[75]. The risk of HCC associated with HBV is significant and can exist without cirrhosis, resulting in a 20-fold increased risk of HCC in individuals with chronic infection[76]. In areas of high HBV endemicity, persons with cirrhosis have an approximately 16-fold higher risk of HCC than the inactive carriers, and a 3-fold higher risk for HCC than those with chronic hepatitis but without cirrhosis[77]. HBV DNA genome is able to integrate into the host chromosomal DNA, resulting in host genome rearrangements and instability, which lead to large inverted repeats, deletions and chromosomal translocations[78]. Although the tumorigenesis mechanism of HBV is still unclear, several factors have been found to be associated with a high risk of developing HCC in patients with chronic hepatitis B (CHB). For example, HBx seems to play a key role in the development of HCC[79-82]. HBx does not bind directly to host DNA, but acts on cellular promoters through protein-protein interactions and by regulating cytoplasmic signaling pathways. HBV exerts its carcinogenic potential through a multifactorial process, including both direct and indirect mechanisms that likely act synergistically[83]. In addition, the association between HCC and HBV recurrence after liver transplantation and the detection of cccDNA in HCC cells indicate the possibility of HBV replication in tumor cells. The latter may be a potential reservoir of HBV recurrence, especially in patients with recurrent HCC[84].

Vaccination can prevent HBV infection. The HBV vaccine can be administered as recombinant or plasma-derived HBsAg and is effective in preventing chronic HBV infection in over 95% of cases. According to data from a longitudinal cohort study,

vaccination can provide long-term immunity for more than 20 years[85]. Since the preventive vaccine was available in 1981, the implementation of universal vaccination of infants plays a key role in the sharp decline in prevalence[86]. Several serological markers of HBV infection, such as HBsAg and anti-HBs, HBeAg and anti-HBe, and anti-HBc IgM and IgG, have been used in clinical diagnosis. Currently, the treatments for patients with chronic HBV infection include interferon-α and nucleoside analogues. However, they are limited by low rates of sustained response, side effects, and the emergence of drug resistance[87]. The main obstacle in the cure of CHB is the inability to eradicate or inactivate cccDNA[45, 88]. Thus, it is essential to further investigate the complex host-HBV interaction and gain more thorough understanding of the mechanisms of HBV pathogenesis and identify potential new therapeutic targets.

1.3 Autophagy

1.3.1 The autophagy machinery

Macroautophagy (known as autophagy) is an evolutionarily ancient and highly conserved catabolic process, involving extensive degradation of cellular proteins and damaged organelles to provide macromolecular precursors for recycling or for fuel metabolic pathways[89-91]. The autophagy process is mediated by various autophagy-related (ATG) proteins and can be divided into at least five sequential steps: autophagy initiation, membrane nucleation and phagophore formation, phagophore expansion, fusion of the autophagosome (the fully enclosed phagophore) to a lysosome, and degradation of sequestered cargo in the autolysosome (Figure 1.8)[92]. Different ATG molecules are implicated in these steps[93]. Initiation begins with the activation of the ULK1 (also known as ATG1 in yeast) complex (ULK1-ATG13-FIP200), which activates a class III PI3K complex comprising VPS34, ATG14, UV radiation resistance-associated gene protein and activating molecule in BECN1-regulated autophagy protein 1, all of which are scaffolded by a putative tumor suppressor, Beclin 1[94]. The ATG5-ATG12 complex conjugates with ATG16 to expand the autophagosome membrane, and members of the LC3 (also known as ATG8 in yeast) are conjugated to the lipid phosphatidylethanolamine (PE) and recruited to the membrane. ATG4B, in conjunction with ATG7, conjugates LC3I and PE to form LC3II. This lipid-conjugated form of LC3 commonly serves as an autophagosome marker. Ultimately, the autophagosome fuses with the lysosome, the contents are degraded and macromolecular precursors are recycled or used to fuel metabolic pathways. The

adaptor protein sequestosome 1 (also known as p62), which targets specific substrates to autophagosomes, and LC3II are degraded along with other cargo proteins and can be used as a measure of autophagic flux[95].

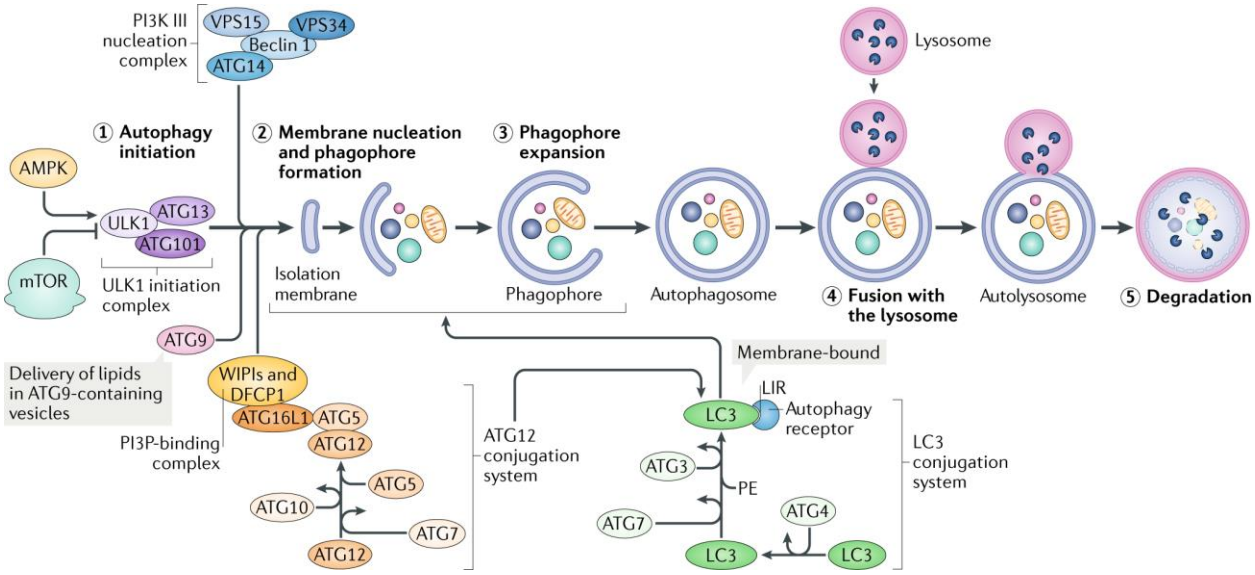

Figure 1.8 A schematic depicting the process and main regulatory machinery of autophagy

Autophagy is a multistep process that includes (1) initiation, (2) membrane nucleation and phagophore formation, (3) phagophore expansion, (4) fusion with the lysosome, and (5) degradation, which correspondingly are regulated by multiple proteins, referred to as autophagy- related proteins (ATGs). The conserved metabolic sensors and longevity determinants mTORC and AMP-activated kinase (AMPK) are the main regulators of autophagy, with mTORC acting as an inhibitor and AMPK as an activator.[92]

1.3.2 Main regulatory machinery of autophagy

Key upstream regulators of the autophagy process include the highly conserved nutrient sensors mTORC and AMP activated kinase (AMPK), which directly phosphorylate ULK1, a conserved kinase that serves as the key upstream initiator of autophagy (Figure 1.8). PKA directly activates mTORC1, inactivating both AMPK and autophagy. AMPK negatively regulates mTORCC1 either directly or by activating the TSC2 protein. Another important upstream factor is Akt/PKB, a negative regulator of the TSC1/2 complex.

Under growth factor deprivation or nutrient starvation, the activity of mTORC1 is inhibited by AMPK. The ULK1/2 complex is also directly activated by AMPK-mediated phosphorylation, resulting in the translocation of ULK1/2 complex to the membrane of endoplasmic reticulum (ER)[96-98]. In mammalian cells, ULK1 can be activated by both

AMPK-dependent (glucose starvation) and AMPK-independent (amino acid starvation) processes[96]. The ULK1/2-ATG13-RB1CC1 interaction is nutrient independent, forming a complex even in nutrient-rich conditions[99]. In this situation, mTORC1 phosphorylates and inhibits ULK1/2 and ATG13, disrupting the interaction between ULK1 and AMPK[96]. In contrast, under autophagy-inducing conditions, mTOR is released from the complex, resulting in activation of ULK1/2, which phosphorylates, and presumably activates, ATG13 and RB1CC1. AMBRA1 and BECN1, components of the autophagy-promoting PtdIns3K complexes, are also phosphorylated by ULK1. These modifications result in localization of the lipid kinase complex to the ER and its activation[100, 101].

Although mTORC was considered as a main regulatory machinery of autophagy, mTORC-independent pathways have been recently reported. Such as amino acid inhibits Raf-1-MEK1/2-ERK1/2 signaling cascade, thereby inhibiting autophagy[102] and JNK1 and DAPK phosphorylate and disrupt the interaction of anti-apoptotic proteins with Beclin 1, resulting in the activation of the Beclin 1-associated class III PtdIns3K complex and initiation of autophagy[103, 104].

1.3.3 Autophagy and HBV

Autophagy has been implicated in a number of cellular and developmental processes, including cell-growth control and programmed cell death[105]. Notably, the dysfunction of autophagy has been implicated in multiple diseases, including neurodegenerative diseases, muscle diseases, cancer, cardiac diseases, and infectious diseases. Autophagy can contribute to innate and adaptive immunity against intracellular microbial pathogens or their products[106, 107].

Most viruses, such as sindbis virus and vesicular stomatitis virus (VSV), seem to have evolved mechanisms to escape cellular clearance by autophagy[107-109]. Many viruses have developed counteracting mechanisms to escape autophagic degradation[110, 111]. For example, several herpesviruses, including herpes simplex virus type 1 (HSV-1), bovine herpesvirus type 1 (BHV-1), human cytomegalovirus (HCMV), and herpesvirus saimiri (HVS), can capably suppress autophagy. For HSV-1, the viral protein ICP34.5 interacts with Beclin-1 to inhibit autophagy induction[112, 113]. On the other hand, some DNA viruses including adenoviruses, human papillomavirus 16 (HPV16), human parvovirus B19 (HPV-B19) and HBV, activate portions of the autophagy pathway and employ this process to enhance viral replication[114, 115]. HBV induces early stages of

autophagy pathways in hepatocytes[71, 116, 117]. Thus, autophagy-induced cell death assists the final step of the adenovirus life cycle to release virus particles[118].

Previous studies have reported that HBV could be regulated by metabolic processes, including autophagy[28, 66-68]. HBV enhances and uses autophagy for its replication. However, the mechanisms responsible for autophagy induction as well as the step of HBV replication affected by autophagy are still controversial[119]. Upon viral infection, autophagy can be triggered by direct mechanisms like the recognition of viral element that promote autophagy protein expression, or by indirect mechanisms like virus triggered cellular stress. For example, during infection a large amount of viral proteins are synthesized and unfolded, and the misfolded proteins can activate ER stress response. HBV can use direct and indirect mechanisms to induce autophagy (Figure 1.9).

Different groups have shown that HBV expression is correlated with autophagy induction[71, 120]. HBV expression induces the formation of early phagosomes, whereas the rate of autophagic protein degradation is seemingly not increased. The exact steps impacted by autophagy are still unclear, but it seems that autophagy can either enhance HBV DNA replication or favor HBV envelopment. Sir et al. reported that the HBx protein interacts with PI3K to enhance autophagosome formation, which in turn activates viral DNA replication[69]. Moreover, the results of Liu et al. revealed that HBx impairs lysosome maturation by inhibiting lysosomal acidification without disturbing the autophagosome-lysosome fusion, which may be beneficial for HBV replication[121]. In addition, Li et al. reported that the small HBV surface protein triggers the unfolded protein responses and enhances the autophagic process without promoting protein degradation by the lysosomes, which is required for HBV envelopment but not for efficient HBV release[71]. Thus, cellular autophagy is closely related to HBV envelopment or its replication.

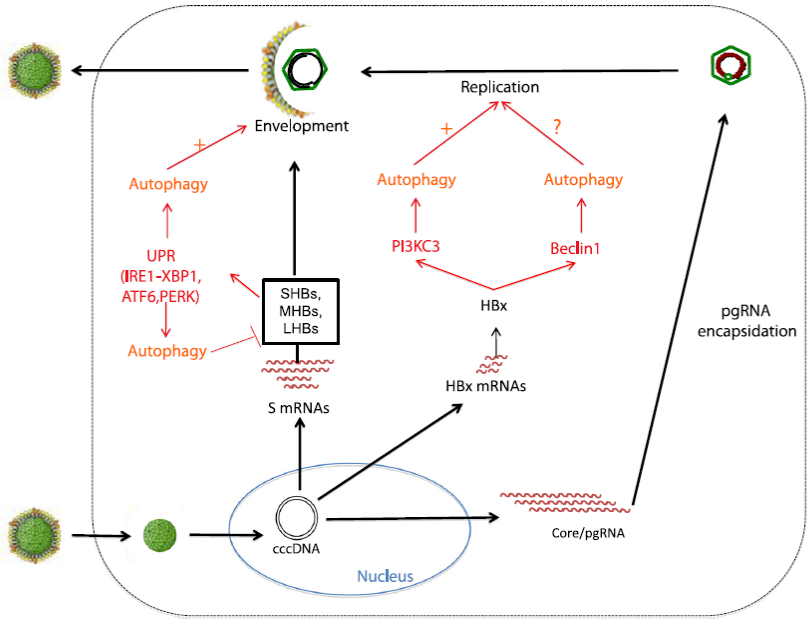

Figure 1.9 Autophagy is induced by HBV expression and enhances HBV replication.

HBV induces autophagy to favor its own replication. The exact steps impacted by autophagy are still unclear, but it seems that autophagy can either enhance HBV DNA replication or favor HBV envelopment. To date, different non-exclusive mechanisms for autophagy induction have been proposed. The regulatory protein HBx could directly activate autophagy through the induction of PI3KC3 activity or the up-regulation of beclin1 expression. Finally, the small envelope protein (SHBs) has been shown to induce autophagy via the establishment of ER stress that triggers the unfolded protein response (UPR) and autophagy. Interestingly, a study has reported that induction of UPR triggers autophagy-dependent degradation of three HBV envelope proteins. This mechanism seems to be in contradiction with the previous findings. It will be interesting to determine if this autophagy-dependent mechanism regulates the overall production of viral particles following autophagy induction.[122]

HBV can also induce autophagy indirectly via the induction of cellular stress[123, 124] (Figure 1.9). In searching for the mechanism leading to autophagy upon HBV expression, Li and collaborators found that the expression of HBV small surface protein (SHBs) induced ER stress and subsequently the activation of unfolded protein response (UPR) signaling pathways, such as PERK, ATF6 and IRE1[71]. They further demonstrated that the blockade of any of these three UPR signaling pathways blocked autophagy induction. Their study supports the idea that induction of ER stress by SHBs is the inducer of autophagy. Moreover, the authors observed an interaction between SHBs proteins and the autophagosome marker LC3, suggesting that this interaction could be involved in the enveloping process of HBV virions (Figure 1.9). How autophagy enhances viral envelope acquisition needs further investigation.

2. Aims of the study

Glucose is a ubiquitous energy source in biology. It is used as an energy source in most organisms, from bacteria to humans, through either various metabolic pathway including aerobic respiration and anaerobic respiration, or fermentation. Evidently, HBV infection interferes with most aspects of hepatic metabolic responses, including glucose, lipid, nucleic acid, bile acid and vitamin metabolism. Glucose and lipid metabolism are a particular focus due to the significant promotion of gluconeogenesis, glucose aerobic oxidation, the PPP, fatty acid synthesis or oxidation, phospholipid and cholesterol biosynthesis affected by HBV infection. Previous studies have reported that HBV replication induces systematic metabolic alterations in host cells. In recent years, it has been found that host metabolism has a significant impact on HBV replication. HBV infection upregulates the biosynthesis of hexosamine and phosphatidylcholine by activating GFAT1 and choline kinase alpha (CHKA) respectively. Importantly suppressing hexosamine biosynthesis and phosphatidylcholine biosynthesis can inhibit HBV replication and expression. In addition, HBV induces oxidative stress and stimulates central carbon metabolism and nucleotide synthesis. Thus, in this project, we asked two questions: whether the different glucose concentrations regulate HBV replication and what is the underlying molecular mechanism in this process?

To elucidate this study, we followed the subsequent steps:

1. Identified whether glucose could modulate HBV replication in primary human hepatocytes and hepatoma cells
2. Identified whether low glucose concentration modulate HBV replication through inducing autophagy
3. Identified the function of AMPK and Akt/mTOR in the regulation of HBV replication in response to glucose
4. Investigated whether inhibiting GLUTs by phloretin could modulate HBV replication by mimicking the culture condition at a low glucose concentration
5. Investigated whether 2-DG, an analogue of glucose, modulates HBV replication also through regulating AMPK and Akt/mTOR signaling pathway
6. Identified whether inhibition of *O*-GlcNAcylation plays an important role in modulating HBV replication
7. Identified whether inhibition of *O*-GlcNAcylation promotes HBV replication depending on induced autophagosome formation

8. Identified whether inhibition of *O*-GlcNAcylation promotes HBV replication by suppressing autophagic degradation
9. Identified whether inhibition of *O*-GlcNAcylation promotes HBV replication via inhibiting mTOR signaling pathway in hepatoma cells
10. Identified whether inhibition of *N*-glycosylation promotes HBV replication by suppressing autophagic degradation

3. Materials and methods

3.1 Materials

3.1.1 Plasmids

The HBV plasmid pSM2 was kindly provided by Prof. Hans Will as previously reported[125]. Plasmid GFP-LC3 was a gift from Prof. Jiming Zhang, Shanghai, China.

pGL3-HBV promoter report plasmids. The luciferase reporter plasmids containing HBV promoters were constructed by Dr. Xiaoyong Zhang[58]. The regions of HBV SP1 promoter (nt2224-2784), SP2 promoter (nt2814-3123), core promoter (nt1648-1853), and HBV X promoter (nt1237-1375) were amplified from pSM2 plasmid and inserted into pGL3-basic vector between Mlu I and Bgl II restriction sites (Promega, Madison, WI) (Figure 3.1, adopted from Promega), resulting in the luciferase reporter vectors pSP1, pSP2, pCP and pXP, respectively. The Renilla luciferase report plasmid was purchased from Clontech.

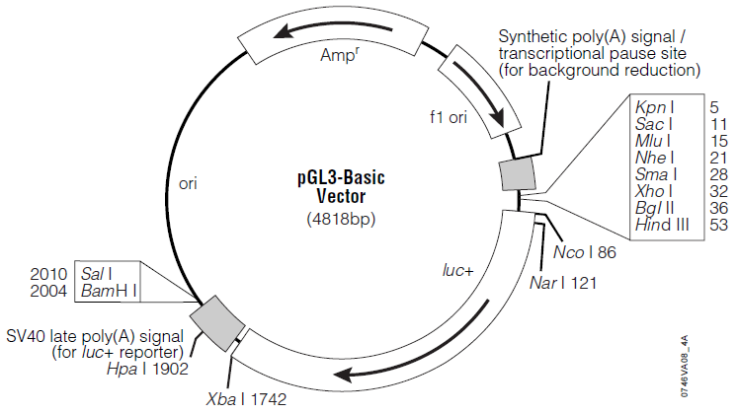

Figure 3.1 pGL3-basic vector circle map

3.1.2 Reagents

The list of the reagents used in the present study is shown as follows:

Name	Company
Glucose	Sigma-Aldrich
2-DG	Sigma-Aldrich
Phloretin	Sigma-Aldrich
AICAR	Selleck Chemicals
OSMI-1	Sigma-Aldrich
tunicamycin	Sigma-Aldrich

CQ	Sigma-Aldrich
3-MA	Sigma-Aldrich
MHY1485	Selleck Chemicals
Rapamycin	Sigma-Aldrich
Tunicamyicn	Sigma-Aldrich
Akti-1/2	Merck Millipore
RPMI 1640 Medium	Gibco
RPMI 1640 Medium, no glucose	Gibco
DMEM High Glucose medium	Gibco
DMEM, no glucose	Gibco
William’s Medium E	Biotech GmbH
Opti-MEM® I (1×) Reduced Serum Medium	Gibco
Trypsin-EDTA	PAA Laboratories
HEPES Buffer Solution	PAA Laboratories
FBS	PAA Laboratories
MEM Non-Essential Amino Acids	PAA Laboratories
G418	Merck Millipore
Penicillin/Stretomycin	PAA Laboratories
2-propanol	Roche
Tris	MP BioMedicals
Nonidet P-40	AppliChem
NaCl	MP BioMedicals
NaOH	AppliChem
EDTA solution (pH 8.0)	AppliChem
Tris buffer (pH7.4 / 8.0 / 8.8)	AppliChem
Hydrochloric Acid	Sigma-Aldrich
Chloroform	Sigma-Aldrich
Roti-phenol	Roche
Dimethyl sulfoxide (DMSO)	Sigma-Aldrich
DNAase I	Roche
D-PBS	Invitrogen
5× Green GoTaq™ Reaction Buffer	Promega
20× SSC Buffer	Invitrogen
Proteinase K	Qiagen

10% SDS	AppliChem
RNase A	Qiagen
$MgCl_2$	MP BioMedicals
Cocktail	ThermoFisher
Salmon Sperm DNA	Invitrogen
Sodium Acetate (3M, pH 5.5)	Ambion
4',6-Diamidino-2-phenylindole (DAPI)	Sigma-Aldrich
10× SDS-PAGE	Roche
10× TBE Buffer	Invitrogen
30% Acrylamide Solution	BIO-RAD
Glycin	MP BioMedicals
TEMED	Sigma-Aldrich
Alpha-P32 (dCTP)	Hartmann Analytic GmbH
Amersham ECL Western Blotting Reagent	GE Healthcare
Amersham™ Rapid-hyb Buffer	GE Healthcare
Amersham Protran 0.45 NC	GE Healthcare
EcoR I and Buffer	New England BioLab
Ethanol	AppliChem
peqGOLD protein marker Ⅳ(10-170kDa)	Peqlab
Illustra™ MicroSpin™ S-200 HR columns	GE Healthcare
Lipofectamine® 2000 Reagent	Invitrogen
NorthernMax®-Gly Sample Loading Dye	Thermofisher
Positively Chgd. Nylon transfer membrane	GE Healthcare
QIAprep Spin Miniprep Kit	Qiagen
QIAGEN Plasmid Midi Kit	Qiagen
QIAGEN Plasmid Maxi Kit	Qiagen
DNA Blood Mini Kit	Qiagen
Red lysis & Loading Buffer	Cell Signaling
QuantiFast SYBR Green RT-PCR kit	Qiagen
SmartLadder	Eurogentec
TRIzol® Reagent	Invitrogen
FUJI medical X-ray film (18×24)	FUJI FILM Corporation
Cell Counting Kit-8	Sigma-Aldrich

Lactate Colorimetric/Fluorometric Assay Kit	BioVision Inc
Sample Bag for BetaplateTM Maximum membranes Size 102*258mm	PerkinElmer
Tween 20	Biochemica
Yeast RNA	Ambion
protein A/G	Thermofisher

3.1.3 Buffers

The list of buffers used in the present study is shown as follows:

Name	**Component**
Lysis buffer for HBV EcDNA extraction	50 mM Tris pH 7.4 1 mM EDTA 1% Nonidet P-40
Denaturation buffer	1.5 M NaCl 0.5 M NaOH
Neutralization buffer	2.0 M NaCl 1.0 M Tris-base 2.5% hydrochloric acid
Wash buffer 1 for Southern blotting	2× SSC; 0.1% SDS
Wash buffer 2 for Southern blotting	0.1× SSC; 0.1% SDS
Lysis buffer for Immunoprecipitation	20 mM Tirs-HCl， pH 7.4; 150 mM NaCl; 10 mM EDTA; 1% NP-40; 1× cocktail
Wash buffer for Immunoprecipitation	10 mM Tirs-HCl， pH 7.4; 0.5 M NaCl; 5 mM EDTA; 0.5% NP-40;
12 % SDS Separation gel (10 ml)	3.3 ml ddH_2O 4.0 ml 30% acrylamide 2.5 ml 1.5M Tris pH 8.8 100 µl 10% SDS 100 µl 10% AP 4 µl TEMED
5% SDS Concentration gel (5 ml)	3.15 ml deionized water 720 µl 30 % acrylamide

	540 µl 1.0 M Tris pH 6.8 45 µl 10% SDS 25 µl 10% AP 5 µl TEMED
10× Transfer buffer (1 l)	142.6 g Glycin 30 g Tris-base
10× TBS	0.5 M Tris-HCl, pH 7.6 1.5 M NaCl

3.1.4 Instruments

The list of all the instruments used in the present study is shown as follows:

Name	Company
-20 °C Freezer	AEG, Germany
-80 °C Freezer	Thermo Forma, Germany
Amersham Hybond^{TM}-N^{+}	GE Healthcare, USA
BIO WIARD KOJAIR	BIO-FLOW Technik, Germany
Bio Imaging System	Syngene, UK
Bin DER	BIOTron Labortechnik GmbH, Germany
CAWOMAT 2000 IR	CAWO photochemisches Werk GmbH, Germany
Centrifuge Avanti J-26Xpi	Beckman Coulter, Germany
Centrifuge 5415 R	Eppendorf, Germany
Centrifuge: Ultracentrifuge Optima L-70K	Beckman Coulter, Germany
CO_2 incubator	Thermo, Germany
Cyclone Storage Phosphor Screen	Packard, USA
Hybidization Oven/Sharker	Amersham Pharmacia, USA
Model 785 Vacuum Blotter	BIO-RAD, USA
Mini Protein Tetra Cell	BIO-RAD, USA
Mini Trans-Blot Cell	BIO-RAD, USA
Rotor-Gene Q	Qiagen, Germany
TopCount.NXT^{TM}	Packard, UK
Vacuum Regulator	BIO-RAD, USA

3.1.5 siRNAs

The sequences of all siRNAs used in the present study are shown as follows:

Name	Product Name	Company	Target sequence
siR-C	Allstars Negative Control siRNA	Qiagen	Proprietary
siATG5	Hs_APG5L_6 FlexiTube siRNA	Qiagen	5'-AACCTTTGGCCTAAGAAGAAA-3'
siOGT	Hs_OGT_7 FlexiTube siRNA	Qiagen	5'-AAGATTAATGTTCTTCATAA-3'
siOGA	Hs_MGEA5_6 FlexiTube siRNA	Qiagen	5'-CAGCCTCTAGAATGGTAACAA-3'

3.1.6 Primers

The sequences of commercial used in the present study are shown as follows:

Name	Product Name	Company	Cat. No.
OGT	Hs_OGT_1_SG QuantiTect Primer Assay	Qiagen	QT00064631
OGA	Hs_MGEA5_1_SG QuantiTect Primer Assay	Qiagen	QT00085862
β-actin	Hs_ACTB_2_SG QuantiTect primer assay	Qiagen	QT01680476

The synthesized primer pairs were used as follows:

HBV RNA: 5'- CCGTCTGTGCCTTCTCATCT -3' (sense) and 5'-TAATCTCCTCCCCCAACTCC -3' (anti-sense).

HBV DNA primers: 5'-GTTGCCCGTTTGTCCTCTAATTC-3' (sense) and 5'-GGAGGGATACATAGAGGTTCCTT-3' (anti-sense).

3.1.7 Antibodies

Antibodies against the following proteins were used:

Name	Source	Company
Akt	Rabbit pAb	Cell Signaling
phospho-Akt	Rabbit pAb	Cell Signaling
mTOR	Rabbit pAb	Cell Signaling
phospho-mTOR	Rabbit mAb	Cell Signaling
O-GlcNAc	Rabbit pAb	Cell Signaling

RL2	Rabbit pAb	Santa Cruz Biotechnology
PGC1α	Rabbit pAb	Cell Signaling
ChREBP	Rabbit pAb	Abcam
CREB	Rabbit pAb	Cell Signaling
AMPK	Rabbit pAb	Cell Signaling
phospho-AMPK	Rabbit pAb	Cell Signaling
ULK1	Rabbit pAb	Cell Signaling
phospho- ULK1 S555	Rabbit pAb	Cell Signaling
anti-p62	Rabbit pAb	Abcam
anti-LC3	Rabbit pAb	Cell Signaling
anti-LC3	Mouse mAb	Cell Signaling
Anti-HBsAg	Horse hAb	Abcam
anti-β-actin	Mouse mAb	Sigma
p70S6 K	Rabbit pAb	Cell Signaling
phospho-p70S6 K	Rabbit mAb	Cell Signaling
IgG	Mouse mAb	Sigma
Albumin	Rabbit mAb	Cell Signaling

3.2 Methods

3.2.1 Plasmid extraction

The transformation of plasmids into *E.coli* strains (DH5α, Invitrogen) were performed according to manufacturer's instructions.

(1) Take competent cells out of -80 °C and thaw on ice (approximately 20-30 min).
(2) Remove agar plates (containing the appropriate antibiotic) from storage at 4 °C and let warm up to room temperature.
(3) Mix 1-5 μl of DNA (usually 10 pg-100 ng) into 20-50 μl of competent cells in a 1.5 ml microcentrifuge. Gently mix by flicking the bottom of the tube with your finger a few times.
(4) Incubate the competent cell/DNA mixture on ice for 20-30 min.
(5) Heat shock each transformation tube by placing the bottom 1/2 to 2/3 of the tube into a 42 °C water bath for 90-120 s.
(6) Put the tubes back on ice for 2 min.
(7) Add 300 μl LB or SOC media (without antibiotic) to the bacteria and grow in 37 °C shaking incubator for 45-60 min.

(8) Plate some or all of the transformation onto a 10 cm LB agar plate containing the appropriate antibiotic.

(9) Incubate plates at 37 °C overnight.

(10) Pick a single colony from a freshly streaked selective plate and inoculate a starter culture of 2-5 ml LB medium containing the appropriate selective antibiotic. Incubate for approx. 8 h at 37 °C with vigorous shaking (approx. 300 rpm).

(11) Dilute the starter culture 1/500 to 1/1000 into selective LB medium. For high-copy plasmids, inoculate 25 ml medium with 25-50 µl of starter culture. For low-copy plasmids, inoculate 100 ml medium with 250-500 µl of starter culture. Grow at 37 °C for 12-16 h with vigorous shaking (approx. 300 rpm)

(12) Harvest the bacterial cells by centrifugation at 6000 g for 15 min at 4 °C.

(13) Resuspend the bacterial pellet in 4 ml (high-copy plasmids) or 10 ml (low-copy plasmids) Buffer P1.

(14) Add 4 ml or 10 ml Buffer P2, mix thoroughly by vigorously inverting the sealed tube 4-6 times, and incubate at room temperature (15-25 °C) for 5 min.

(15) Add 4 ml or 10 ml of chilled Buffer P3, mix immediately and thoroughly by vigorously inverting 4-6 times, and incubate on ice for 15 min or 20 min.

(16) Centrifuge at 15, 000 g for 30 min at 4 °C. Remove supernatant containing plasmid DNA promptly. Recentrifuge the supernatant at 15,000 g for 15 min at 4 °C. Remove supernatant containing plasmid DNA promptly.

(17) Equilibrate a QIAGEN-tip 100 or QIAGEN-tip 500 by applying 4 ml or 10 ml Buffer QBT, and allow the column to empty by gravity flow.

(18) Apply the supernatant from step 16 to the QIAGEN-tip and allow it to enter the resin by gravity flow.

(19) Wash the QIAGEN-tip with 2 x 10 ml or 2 x 30 ml Buffer QC.

(20) Elute DNA with 5 ml Buffer QF.

(21) Precipitate DNA by adding 3.5 ml (0.7 volumes) room-temperature isopropanol to the eluted DNA. Mix and centrifuge immediately at 15,000 g for 30 min at 4°C. Carefully decant the supernatant.

(22) Wash DNA pellet with 2 ml room-temperature 70% ethanol, and centrifuge at 15,000 g for 10 min. Carefully decant the supernatant without disturbing the pellet.

(23) Air-dry the pellet for 5-10 min, and redissolve the DNA in 100 µl sterile water. DNA concentration was quantified by NanoDrop microvolume spectrophotometers.

(24) Finally, purified plasmid DNA was confirmed by restriction enzyme digestion.

3.2.2 Cell culture and transfection

The human hepatoma cell line HepG2.2.15, which harbors integrated dimers of the HBV genome (GenBank Accession Number: U95551) and shows a constantly detectable level of HBV replication, was cultured in RPMI-1640 medium (Gibco) with 10% fetal bovine serum (FBS), 100 U/ml penicillin, 100 μg/ml streptomycin (Gibco), 10% NEAA, 10% HEPES and 500 μg/ml G418 (Merck Millipore). Another human hepatoma cell line Huh7 was cultured in Dulbecco's Modified Eagle's Medium (DMEM, Gibco) supplemented with 10% FBS, 100 U/ml penicillin, 100 μg/ml streptomycin (Gibco), 10% NEAA and 10% HEPES. Primary human hepatocytes were kindly provided by Dr. Ruth Broering, University Hospital Essen, which were cultured in William E medium with 250 μl insulin, 2% DMSO and 125 μl hydrocortisone hemisuccinate. All cell cultures were incubated in a humidified atmosphere containing 5% CO_2 at 37 ºC.

The cultivation and viral infection of primary human hepatocytes are shown as follows:

(1) 2 days before HBV infection, separate the PHHs from patient and seed them into 12-well plate.

(2) 1 day before HBV infection, wash the cells with PBS one time. PHHs were incubated with 20 μl HBV viron (2×10^{10} copies/ml, 1:50) and 1 ml WM1 medium (WM2 medium + PEG 8000) at 37 °C for 24 h.

(3) At the end of incubation (0-day post HBV infection), wash the cells with PBS 3 times. Then PHHs were incubated with 1 ml WM2 medium.

(4) At 2, 4, 6, day post HBV infection, harvest the supernant, wash the cells with PBS 1 time, and change new medium with 1 ml WM2 medium.

(5) At 10-day post HBV infection, harvest the supernant to detect HBsAg and HBeAg, wash the cells with PBS 1 time, and change with no-glucose medium as for 48 h or for 72 h.

(6) At 13-day (72 h post treatment), collect the supernatant and cells for further detection.

Plasmids or siRNAs were transfected into cells at indicated concentrations using the Lipofectamine 2000 transfection reagent (Invitrogen) according to the manufacturer's instructions. The protocol of transfection used in this study is as

follows:

(1) 1 day before transfection, seed HepG2.2.15 cells/Huh7 cells into 6-well plate.

(2) At the day for transfection, dilute 1.5 μl of 20 μM siRNA into 250 μl Opti-MEM.

(3) Dilute 5 μl Lipo2000 into 250 μl Opti-MEM, incubate them at room temperature for 5 min.

(4) Add 250 μl Opti-MEM (diluted with Lipo2000) into 250 μl Opti-MEM (diluted with siRNA), incubate at room temperature for 20 min.

(5) Discard the old medium from 6-well plate, and wash with PBS once.

(6) Add 1 ml Opti-MEM® I (1×) Reduced Serum Medium into each well, and then add 500 μl Lipo2000-siRNA complex (from step 5) drop by drop.

(7) 4-6 hours later, change new medium with 2 ml 1640/DMEM medium with 2%FBS, then put the cells at 37 ºC in a humidified atmosphere.

3.2.3 RNA extraction

Total cellular RNA was extracted by using Trizol reagent (Invitrogen, Switzerland), followed by digestion with the DNase Set (Roche, Switzerland). The protocol of RNA extraction in detail is as follows:

(1) Collect the cells from 12-well plate with 500 μl Trizol reagent by pipetting the cells up and down several times.

(2) Incubate the homogenized sample for 5 min at room temperature to permit complete dissociation of the nucleoprotein complex.

(3) Add 100 μl chloroform, and shake tubes vigorously by hand for 15 s.

(4) Incubate at room temperature for 2-3 min. Centrifuge at 12,000 g at 4 °C for 15 min.

(5) Transfer the aqueous phase (about 250 μl) to a new 1.5 ml EP tube and add 250 μl isopropanol.

(6) Incubate at room temperature for 10 min. Centrifuge at 12,000 g at 4 °C for 10 min.

(7) Remove the supernatant from the tubes, and wash the RNA pellet with 100 μl 75% ethanol.

(8) Vortex the samples briefly, and centrifuge at 12,000 g at 4 °C for 5 min.

(9) Discard the supernatant, and air dry the RNA pellet for 5-10 min.

(10) Finally, elute the RNA into 50 μl RNase free water. Measure the concentration of RNA by NanoDrop microvolume spectrophotometers.

(11) The concentration of all samples is then diluted into 100 ng/μl by adding

RNase free water, and then store in -80 °C or for real-time RT-PCR.

3.2.4 Real-time RT-PCR

Quantitative real-time RT-PCR

The levels of relative mRNA expression in cells were determined by real-time RT-PCR analysis using commercial QuantiTect Primer Assays (Qiagen, Germany). HBV RNA levels in cells were also measured using real-time RT-PCR (Qiagen) with the primer pair: 5'-CCGTCTGTGCCTTCTCATCT-3' (forward) and 5'-TAATCTCCTCCCCCAAC TCC-3' (reverse). Finally, the ratio of mRNA levels was normalized to internal control beta-actin.

The protocol of real-time RT-PCR for RNA is as follows:

Quantification of the HBV RNA was performed by using QuantiFast SYBR Green RT-PCR kit (Qiagen).

Reaction mixture as follows:

Component	Volume (20 µl)
2× SYBR Green RT-PCR Master Mix	10 µl
10× primers	2 µl
QuantiFast RT mix	0.2 µl
Template RNA	1 µl
RNase-free water	6.8 µl

cycler conditions:

1) 50 °C, 10 min for reverse transcription
2) 95 °C, 5 min for initial activation of hotstar Taq DNA polymerase
3) 95 °C, 10 s for denaturation
4) 60 °C, 30 s for annealing and extension step

   40 cycles for DNA (step 3 to 4)

3.2.5 Analysis of HBV gene expression

Quantification of the levels of HBsAg and HBeAg in the supernatants

The levels of HBsAg and HBeAg in the culture medium were determined using the Architect System and the HBsAg and HBeAg CMIA kits (Abbott Laboratories, Germany) according to the manufacturer's instructions.

Quantification of HBV DNA levels

HBV progeny DNA was extracted from culture medium using the DNA Blood Mini Kit (Qiagen) and quantified by real-time polymerase chain reaction (PCR) (Invitrogen).

HBV DNA was extracted from intracellular core particles in hepatoma cell lines and detected by real-time PCR or Southern blotting analysis (mention below).

The protocol of quantitative real-time PCR for quantification of total HBV DNA levels is as follows:

Purification of HBV DNA from culture medium:

(1) Pipette 20 µl QIAGEN Protease into the bottom of a new 1.5 ml EP tube.

(2) Add 200 µl culture medium to the EP tube.

(3) Add 200 µl Buffer AL to the sample. Mix by pulse-vortexing for 15 s.

(4) Incubate at 56 °C for 10 min.

(5) Add 200 µl ethanol (96–100%) to the sample, and mix again by pulse-vortexing for 15 s.

(6) Carefully apply the mixture from step 5 to the QIAamp spin column without wetting the rim, close the cap, and centrifuge at 6,000 g for 1 min. Place the QIAamp spin column in a clean 2 ml collection tube, and discard the tube containing the filtrate.

(7) Carefully open the QIAamp spin column and add 500 µl Buffer AW1 without wetting the rim. Close the cap and centrifuge at 6,000 g for 1 min. Place the QIAamp spin column in a clean 2 ml collection tube, and discard the collection tube containing the filtrate.

(8) Carefully open the QIAamp spin column and add 500 µl Buffer AW2 without wetting the rim. Close the cap and centrifuge at full speed for 3 min.

(9) Place the QIAamp spin column in a new 2 ml collection tube and discard the collection tube with the filtrate. Centrifuge at full speed for 1 min.

(10) Place the QIAamp spin column in a clean 1.5 ml EP tube, and discard the collection tube containing the filtrate. Carefully open the QIAamp spin column and add 50 µl ddH_2O. Incubate at RT for 1 min, and then centrifuge at 6,000 g for 1 min.

(11) Store the samples at -20 °C or using as template for real-time PCR for detecting HBV progeny DNA directly.

Reaction mixture for real-time PCR:

Component	Volume (20 µl)
2× UDG mix	10 µl
Hope-forward prime	0.4 µl
Hope-reverse prime	0.4 µl
$MgCl_2$	0.8 µl
BSA	1 µl
Template	2 µl
Aqua	5.4 µl

cycler conditions:

(1) 95 °C, 15 s for denaturation
(2) 60 °C, 15 s for annealing
(3) 72 °C, 10 s for extension step
45 cycles (step 1 to 3)

3.2.6 Southern blotting analysis

HBV replicative intermediates from intracellular core particles were extracted from hepatoma cell lines and detected by Southern blotting, respectively. The encapsided HBV DNA in nucleocapsids was also detected by Southern blotting. However, HBV nucleocapsid in cell lysates was analyzed in a native agarose gel and then detected by Western blotting analysis.

The protocol of Southern blotting for detecting HBV replication is as follows:

EcDNA extraction:

(1) 3- or 4-days post-transfection wash the cells in 6-well plate with PBS 1 time.
(2) Add 800 µl iced lysis buffer and incubate on ice for 10 min.
(3) Collect the cell lysates into 2 ml EP tube, vortex vigorously for 15 s, and then incubate on ice for 10 min.
(4) Centrifuge at 13,200 rpm for 2 min.
(5) Transfer the supernatant to a new 2 ml EP tube, then add 8 µl of 1 M $MgCl_2$ and 8 µl of 10 mg/ml DNase I, mix gently, and incubate for 30 min at 37 °C.
(6) Shortly centrifuge, then add 40 µl of 0.5 M EDTA (pH 8.0) to a final concentration of 25 mM, mix by vortex.
(7) Shortly centrifuge, and add 80 µl 10% SDS, mix by vortex.

(8) Shortly centrifuge, and add 20 µl 20 mg/ml proteinase K.

(9) Incubate at 55 °C for 2 h.

(10) Add 900 µl Phenol/chloroform mix into the tube for extraction, vortex and static for 2 min, then centrifuge at 13,000 rpm at RT for 10 min.

(11) Suck up the first layer liquid and add 0.7 V of isopropanol, 0.1 V of 3 M NaAc (pH5.2) and 2 µl of 10 mg/ml yeast RNA, incubate over night at -20 °C.

(12) 13,200 rpm at 4 °C for 15 min, discard the supernatant carefully.

(13) Wash the pellet with 1 ml 75% ethanol, up and down 2 times gently without disrupt the whole pellet, centrifuge at 8,000 rpm at RT for 5 min. Discard the supernatant carefully, then air dry for 5-10 min.

(14) Dissolve the pellet in 15 µl TE buffer.

(15) Add 5 µl 5× green loading buffer, scrape on tube shelf and short centrifugate.

Run agarose gel:

(1) Prepare 1% agarose gel.

(2) Electrophoresis for 1.5 h at 50 V.

(3) Wash with ddH_2O one time, then denaturation for 30 min at RT with gentle agitation.

(4) Wash with ddH_2O one time, then neutralization for 30 min at RT with gentle agitation.

(5) Wash the agarose gels with ddH_2O one time, and then soak in 20× SSC.

(6) Transfer the membranes (from down to up including: white fiberboard, filter paper, Nylon membrane, green plastic membrane and the agarose gels), cover the cover. 13Hg for 2 h.

(7) Fix DNA on the membranes at 150 J/cm^2 2 times.

Hybridization probe preparation:

(1) Digest plasmid pSM2 (1 µg/µl) which contain HBV dimer by restriction enzyme EcoR I.

Component	Volume (100 µl)
EcoR I	1 µl
10× NEB 2	10 µl
pSM2	10 µl
Aqua	79 µl

(2) After digestion at 37 °C for 2 h, 25 μl 5× green loading buffer was added. Run 0.8% agarose gel at 130 V for 2 h to separate two bands (3.2 kb for HBV fragment and 2.7 kb for vector), and cut 3.2 kb band for agarose gel extraction.

(3) Agarose gel extraction to quantify the HBV fragment concentration and dilute into 25 ng/μl. The HBV fragments were put in -80 °C for long-term storage or used directly for Southern blotting hybridization.

Hybridization:

(1) Dilute 5 μl HBV DNA probe (5 ng/μl) into 41 μl TE in 1.5 ml tube.

(2) Mix and then denature at 95 °C for 5 min.

(3) Then snap cool the DNA by placing on ice for 5 min after denaturation.

(4) Prehybridize the membranes in 10 ml Rapid-Hyb buffer (Amersham) at 65 °C for 10-20 min.

(5) Centrifuge briefly the denatured DNA, and add into the reaction tube (GE Healthcare) which contains polymerase.

(6) Add 2 μl/reaction α-^{32}P dCTP into the reaction tube.

(7) Incubate at 37 °C for 10 min.

(8) Stop the reaction by adding 5 μl of 0.2 M EDTA.

(9) Loosen the cap of column 1/4 turn, snap off the bottom closure of the microspin columns, and centrifuge for 1 min at 3,000 rpm.

(10) Place the column in 1.5 ml tube with 100 μl of 10 mg/mL salmon sperm, and slowly apply the reaction sample to the resin.

(11) 3,000 rpm for 2 min.

(12) For use in hybridization, denature the labeled DNA by heating to 95 °C for 5 min, then snap cool on ice for 5 min.

(13) Add purified labeled DNA to the pre-hybridization solution by directly dropping into hybridization tube.

(14) Hybridize at 65 °C overnight.

(15) Wash the membranes with 50 ml wash buffer I (2× SSC + 0.1% SDS) at RT for 30 min 2 times.

(16) Wash the membranes with 50 ml wash buffer II (0.2× SSC + 0.1% SDS) at 65 °C for 30 min 2 times.

3.2.7 Western blotting analysis

Western blotting analysis was performed to detect the relative protein expression. Briefly, after transfection or treatment, cells were washed with phosphate-buffered saline and lysised with 1× lysis buffer (Cell Signaling Technology, USA). Protein samples were resolved by sodium dodecyl sulfate-polyacrylamide (SDS) gel electrophoresis and then electrotransferred to nitrocellulose membranes. The membranes were incubated with the indicated primary antibodies overnight at 4 °C after being blocked with 5% milk in 1× TBST. The membranes were washed with 1× TBST and incubated (as appropriate) with a secondary peroxidase-affiniPure Rabbit anti-mouse IgG antibody (Jackson ImmunoResearch West Grove, USA) or a peroxidase-affiniPure goat anti-rabbit IgG antibody (Jackson ImmunoResearch). Immunoreactive bands were visualized using an enhanced chemiluminescence system (GE Healthcare, UK).

The protocol of Western blotting in detail is as follows:

(1) Aspirate culture media from 12-well plate, wash the cells with PBS, and aspirate it.
(2) Lyses the cells by adding 100 µl of 1× red lysis buffer (Cell Signaling). Scrape off the cells from the plate immediately and transfer them to a new precool 1.5 ml centrifuge tube.
(3) Heat the samples at 95 ºC for 10 min; then cool on ice.
(4) Prepare four 12%-15% separate gel.
(5) Load protein samples into SDS-PAGE gel: 3 µl protein marker/well, 10 µl sample/well for purpose band, and 3 µl sample/well for beta-actin detection.
(6) Run at 90 V for 30 min firstly, and then change to 130 V for 1.5 h.
(7) Transfer to NC membrane, 250 mA for 1 h.
(8) Incubate the membranes in 5% milk at RT for 1 h.
(9) Wash the membranes with 1× TBST.
(10) Incubate the membranes in primary antibody (1:1000, by 0.25% milk in 1×TBST) at 4 ºC overnight with gentle agitation.
(11) Wash the membranes with 1× TBST for 10 min 3 times.
(12) Incubate the membranes in 5 ml HRP-conjugated secondary antibody (1:15000, by 0.25% milk in 1× TBST) at RT with gentle agitation for 1 h.
(13) Wash the membranes with 1× TBST for 10 min 3 times.
(14) Put the membrane in plastic wrap and add 600 µl ECL buffer/membrane, then

put into black-box for exposure.

3.2.8 Immunoprecipitation analysis

1. For adherent cells, harvest with trypsin-EDTA and then centrifuge at 3000 rpm for 5 min. For suspension cells, harvest by centrifuge at 3000 rpm for 5 min.

2. Wash cells by suspending the cell pellet with medium which contains FBS, centrifuge at 3000 rpm for 5 min. Use a pipette to carefully remove and discard the supernatant, leaving the cell pellet as dry as possible.

3. Add 770 µl lysate buffer （20 mM Tirs-HCl， pH 7.4; 150 mM NaCl; 10 mM EDTA; 1% NP-40） to the cells. Then add 32 µl 25×cocktail to the cell. Place the tube on a vibrating mixer in the cold room for 30 min at 4 ºC to completely break the cells. Centrifuge at 12,000 rpm for15 min at 4 ºC. Collect and transfer the supernatant to a new tube. This is the whole cell lysate (WCL).

4. Measure protein concentration by Bradford.

5. Prepare input aliquots, one for IP (usually ≥500 µg)*, one for direct western-blotting (“input sample”, usually 20-50 µg).

* Depending on the abundance of the protein to be Immuno-precipitated, ≥500 µg protein in input may be used for IP; for transfected 239T cells, usually 500 µg lysate is sufficient for IP the exogenously expressed protein.

6. Mix input aliquot and antibody or IgG (usually 2-4 µg is sufficient for 1000 µg input lysis, monoclonal antibody is highly recommended) together in a tube. Place IP mixture on a rotating mixer (slow rotating), and incubate for 4 h (non-Phosphorylated protein) at 4 ºC.

7. Wash protein-G agarose (20-30 µl per IP) with 1ml basic IP buffer. Repeat for twice.

8. Mix IP mixture and 80 µl protein-G agarose together in a tube, and incubate overnight at 4 ºC.

9. Spin the IP mixture for 12,000 rpm at 4 ºC for 1 min. Discard the supernatant. Wash the agarose with 1 ml basic IP buffer by inverting the tube several times to mix. Repeat washing at least twice, and use a gel loading tip (long tip) to completely remove the remaining basic IP buffer.

10. Mix the 1% SDS and 3× Red loading buffer (2:1), then add 30µl 1× Red loading buffer to the protein-G agarose, incubate the tube on ice for 5 min, followed by 5 min at 95 ºC. Mix on the vibrating mixer for 10s. Spin the tube, collect

the supernatant. This is the “IP sample”.

11. Then run the western blotting.

3.2.9 Luciferase reporter gene assay

The Dual-Glo luciferase reporter assay (Promega) was used to detect the firefly luciferase activity and the internal control Renilla luciferase activity. Four luciferase reporter plasmids pSP1 (nt 2224-2784), pSP2 (nt 2814-3123), pCP (nt 1648-1853), and pXP (nt 1237-1375), based on pGL3 basic were constructed with HBV promoters previously and used in the assay as described[58].The protocol of Dual-Glo luciferase reporter assay is as follows:

(1) 48 h post transfection, discard the culture medium, wash the cells with PBS once, and remove it.
(2) Add 50 μl PBS for each well.
(3) Add 50 μl Dual-Glo luciferase Reagent to each well.
(4) Punch the cells with tip into 96-well black plate from 48-well plate.
(5) Cap the plate and measure the firefly luminescence.
(6) Add 50 μl Dual-Glo stop reagent to each well and wait for at least 10 min then measure Renilla luminescence.
(7) Calculate the ratio of firefly to Renilla.

3.2.10 Immunofluorescence staining and quantification

Immunofluorescence staining was performed as described previously[120]. Briefly, HepG2.2.15 cells were grown on coverslips and cultured with different concentrations of glucose as indicated in each experiment. After 48 h, the cells were washed with PBS, fixed in 4% paraformaldehyde, and permeabilized with 0.1% Triton X-100. The cells were incubated with anti-LC3B and anti-HBsAg primary antibodies and then stained with Alexa Fluor 488-(Jackson ImmunoResearch, 111-545-003) conjugated Goat anti-Rabbit IgG (H+L) or Alexa Fluor 574-(Jackson ImmunoResearch) conjugated Goat anti-Horse IgG (H+L). The nuclei were stained with 4’,6-diamidino-2-phenylindole (DAPI), and the distribution of LC3B protein was visualized with an LSM 710 microscope (Zeiss, Jena, Germany) with a Plan-Apochromat 63×/1.40 oil Iris M27 objective. Moreover, Huh7 cells were grown on cover slips and cotransfected with the plasmid GFP-LC3, or siRNAs. After transfection for 48 h, cells were fixed in 4% paraformaldehyde for 10 min, and

permeabilized with 0.1% Triton X-100 for 10 min. The nuclei were stained with 4', 6-Diamidino-2-phenylindole (DAPI), and the distribution of the GFP-tagged LC3 protein was visualized with an LSM 710 microscope (Zeiss, Jena, Germany) with a Plan-Apochromat 63×/1.40 oil Iris M27 objective. In addition, Huh7 cells were grown on cover slips and trasfected with the plasmid GFP-mCherry-LC3, 6 h post transfection, cells were treated with OSMI-1 or TM for 48 h. Then, cells were fixed in 4% paraformaldehyde for 10 min, and permeabilized with 0.1% Triton X-100 for 10 min. The nuclei were stained with 4', 6-Diamidino-2-phenylindole (DAPI), and the distribution of the GFP-mCherry-tagged LC3 protein was visualized with an LSM 710 microscope (Zeiss, Jena, Germany) with a Plan-Apochromat 63×/1.40 oil Iris M27 objective. Images were acquired by ZEN acquisition software (2012; Carl Zeiss) and analyzed by ImageJ software. The number of LC3B puncta in cells was quantified as described previously[126].

The protocol of immunofluorescence staining in detail is as follows:

(1) Fix the cells with 200 μl 4% formaldehyde, incubate at RT for 10 min.
(2) Wash the cells with 200 μl PBS for 5 min 3 times.
(3) Incubate with 200 μl 0.1% Triton X-100 at RT for 10 min.
(4) Wash the cells with 200 μl PBS for 5 min 3 times.
(5) Block with 150 μl 5% FBS in PBS, at RT for 30 min.
(6) Wash the cells with 200 μl PBS for 5 min 3 times.
(7) Incubate with 150 μl primary-antibody (1:200) at RT for 1 h.
(8) Wash the cells with 200 μl PBS for 5 min 3 times.
(9) Incubate with 150 μl second-antibody (1:200) with FITC-labeled at RT for 1 h.
(10) Incubate with 150 μl DAPI (1:1000) at RT for 10-15 min.
(11) Wash the cells with 200 μl PBS for 5 min 3 times.
(12) Add 1 drop fluorescent mounting medium (Dako) onto the slide. Cover with glass lip and seal with nail polish.

3.2.11 Cell proliferation assay

Cell proliferation was determined by a Cell Counting Kit-8 Assay kit (Sigma-Aldrich, 96992) according to the manufacturer's protocol. The protocol of CCK8 in detail is as follows:

(1) Inoculate cells (about 1× 10^4/well in 100 μl medium) in a 96-well plate. Pre-incubate the plate in a humidified incubator at 37 °C and with 5% CO_2.
(2) 24 h later, treated the cell with indicated small chemical reagents for 6, 12, 24, 48,

and 72 h.

(3) Add 10 µl of the CCK8 solution to each well of the plate. Note: Be careful not to introduce bubbles to the wells, as they interfere with the O.D. reading.
(4) Incubate the plate for 1 h in the incubator at 37 °C and with 5% CO_2.
(5) Measure the O.D. absorbance at 450 nm using a microplate reader.

3.2.12 Lactate assay

Accumulation of lactate in the culture medium was determined using a Lactate Colorimetric/Fluorometric Assay Kit (BioVision Inc, K607), according to the manufacturer's protocol. After centrifugation (3,500 rpm, 15 min, 4 °C), cell culture medium was stored at -20°C. Samples were diluted in assay buffer and mixed with lactate reaction mixture for 30 min. The optical density of the mixture in each well was measured at 577 nm on a microplate reader (Molecular Devices, Sunnyvale, CA). The lactate concentration was calculated from a standard curve and normalized against cell numbers.

3.2.13 Statistical analysis

Data are presented as mean ± SEM. Statistical analyses were performed using Graph Pad Prism software version 7 (La Jolla, CA, USA). Analysis of variance with two-tailed Student's t test or by one-way ANOVA with a Tukey posttest was used to determine significant differences. Differences were considered statistically significant when $p<0.05$. All experiments were repeated independently at least three times.

4. Results

4.1 Low glucose concentration enhances HBV progeny secretion, replication and transcription in hepatocytes

4.1.1 Low glucose concentration enhances HBV progeny secretion and replication in HepG2.2.15 cells

Given glucose as one of the most important metabolic substrates in living organisms, we asked whether and how external glucose supply regulates HBV replication. Under the standard condition, HepG2.2.15 cells with stable HBV replication were grown in complete RPMI-1640 medium with 10 mM glucose. We first examined how the glucose concentration in the culture medium affected HBV replication and gene expression. HepG2.2.15 cells were cultured with different glucose concentrations (5, 10, and 25 mM). HBV RIs were prepared on day 4 and subjected to Southern blotting analysis. The amount of HBV RIs decreased significantly with increasing glucose concentrations (Figure 4.1, A). The levels of encapsidated and secreted HBV DNA (in HBV virions) were determined using real-time PCR. Consistently, a low glucose concentration of 5 mM in the cell culture medium led to increased levels of both intracellular and secreted HBV DNA (Figure 4.1, B). The levels of intracellular and secreted HBsAg and HBeAg were measured by CMIA. The levels of intracellular and secreted HBsAg but not secreted HBeAg were substantially higher under the low glucose condition (Figure 4.1, C).

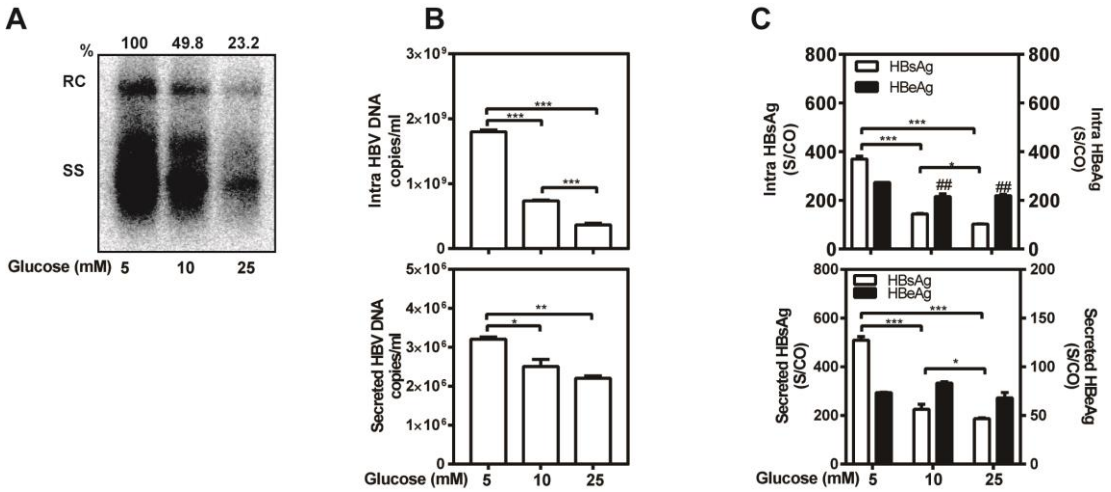

Figure 4.1 Low glucose concentration enhances HBV replication and progeny secretion in HepG2.2.15 cells

HepG2.2.15 cells were cultured with different glucose concentrations (5, 10, and 25 mM) and harvested after 72 h. (A) Encapsidated HBV replicative intermediates (RIs) were detected by Southern blotting. (B) The levels of intracellular and secretion HBV DNA were determined by real time PCR. (C)

HBsAg and HBeAg in supernatant were quantified by chemiluminescence immunoassay (CMIA). S/CO = signal to cutoff ration; RC = relaxed circular DNA; SS = single-stranded DNA. *p<0.05; **, ## p<0.01; ***p<0.001; ns, not significant.

4.1.2 Low glucose concentration enhances HBV transcription

To explain the changes in HBV replication activity at different glucose concentrations, the effects of glucose concentrations on HBV gene expression were judged by determining the levels of HBV RNAs using real time RT-PCR and the HBV promoter activity using luciferase reporter assays. The levels of HBV RNAs were highest at the glucose concentration of 5 mM, compared with those at higher glucose concentrations (10 and 25 mM) (Figure 4.2, A). However, HBV RNAs levels changed less than 2-fold among the different glucose concentrations in the cell cultures. The luciferase reporter assays clearly showed that single HBV promoter activity dropped slightly (Figure 4.2, B), though the levels of some specific transcription factors, such as PGC1α, CREB, and ChREBP, were strongly reduced at the higher glucose concentrations (Figure 4.2, C). These results suggest that the glucose concentration modulates HBV transcription. Nevertheless, the regulation at the level of transcription was apparently not the only mechanism to determine the changed magnitude of HBV replication at different glucose concentrations.

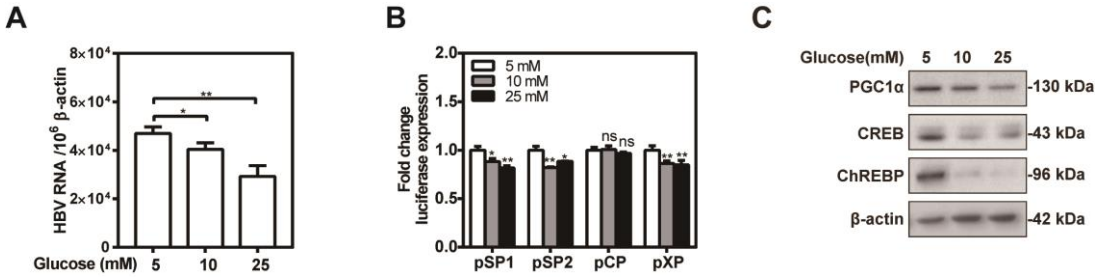

Figure 4.2 Low glucose concentration enhances HBV transcrition in HepG2.2.15 cells

(A) HepG2.2.15 cells were cultured with different glucose concentrations (5, 10, and 25 mM) and harvested after 72 h. HBV RNA levels in HepG2.2.15 cells were analyzed by RT-PCR. (B) HepG2.2.15 cells were co-transfected with pGL3, pSP1, pSP2, pCP, pXP and Renilla, 6 h post-transfection, cultured with different glucose concentrations (5, 10, and 25 mM) for 48 h. Dual-Glo luciferase report assay was performed to measure the firefly and Renilla luciferase activities. The results were calculated by fold change and normalized to the control samples. (C) HepG2.2.15 cells were cultured with different glucose concentrations (5, 10, and 25 mM) and harvested after 72 h. PGC1α, ChREBP and CREB expression were analyzed by western blotting, and beta-actin was used as a loading control. *p<0.05; **p<0.01; ***p<0.001; ns, not significant.

4.1.3 Different concentration of glucose in medium did not affect cell proliferation

Low glucose concentration may cause insufficient nutrition of cells. Therefore, we added pyruvate as a supplement at different glucose concentrations in the culture medium. Nevertheless, adding pyruvate did not affect HBV replication at low glucose concentration (Figure 4.3, A). Next, cell proliferation was measured using a CCK8 assay at indicated time points from 6 to 72 h after cultured in different glucose concentrations. These glucose concentrations did not affect cell proliferation of HepG2.2.15 cells at any indicated time point (Figure 4.3, B).

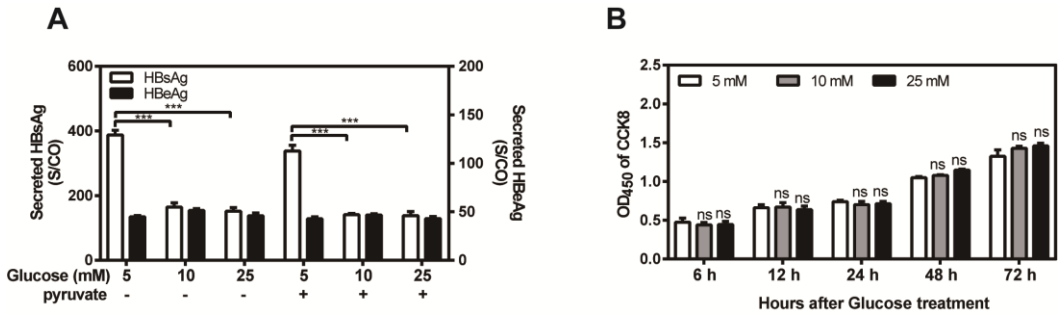

Figure 4.3 Different concentration of glucose in medium did not affect cell proliferation

(A) HepG2.2.15 cells were cultured with different concentration of glucose (5, 10, and 25 mM) combined with 1 mM pyruvate for 48 h. HBsAg and HBeAg secretion in supernatant were detected by CMIA. (B) Cell proliferation was measured by CCK8 assay at 6, 12, 24, 48, and 72 h after cultured with different concentration of glucose (5, 10, and 25 mM). *p<0.05; **p<0.01; ***p<0.001; ns, not significant.

4.1.4 Low glucose concentration enhances HBV progeny secretion and replication in primary human hepatoma cells

Finally, PHHs were infected with HBV and cultured at glucose concentrations of 5 and 10 mM up to 10 days post-infection. HBV infection in PHHs was determined by measuring levels of HBsAg and HBeAg in the culture supernatants. At low glucose concentration, the HBsAg but not HBeAg levels were markedly increased in the culture supernatants (Figure 4.4, A), consistent with the findings in HepG2.2.15 cells. To assess the differentiation status of cultured PHHs during the course of infection and treatment, we examined the expression level of albumin by western blotting. There was almost no change in the expression level of albumin during the experiments (Figure 4.4, B), suggesting that PHHs maintained the differentiated status. In fact, HBsAg and HBeAg production usually increases during the time frame up to 12 days [127], indicating that PHHs fully support HBV replication.

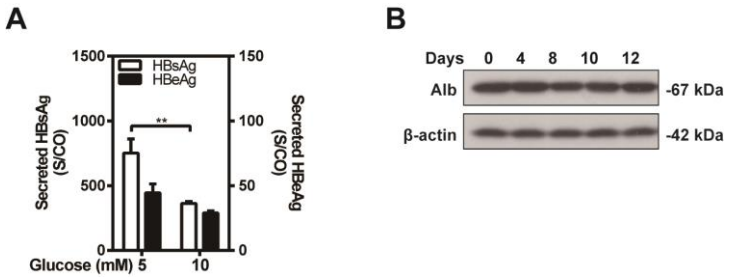

Figure 4.4 Low glucose concentration enhances HBV progeny secretion and replication in primary human hepatoma cells

PHHs were infected with HBV virions (multiplicity of infection (MOI)=30). 10 days post-infection, PHHs were cultured in DMEM medium with the indicated glucose concentrations (5, and 10 mM) and harvested after 48 h. (A) The HBsAg and HBeAg levels in the culture supernatants were determined as described above. (B) PHHs were infected with HBV virions (multiplicity of infection (MOI)=30). The cell lysates were collected at the indicated time points. The expression of albumin was detected by western blotting using beta-actin as a loading control. *p <0.05; **p <0.01.

Collectively, the data suggest that low glucose concentration enhances HBV replication in hepatoma cells and PHHs. However, the changes in HBV transcription do not fully explain the difference on HBV replication activity at low and high glucose concentrations. Other cellular mechanisms may participate in the modulation of HBV replication.

4.2 Enhanced HBV replication at low glucose concentration is dependent on increasing autophagic flux

4.2.1 Low glucose concentration increases autophagic flux

AMPK is active at low glucose concentrations and interacts with ULK1, subsequently phosphorylating ULK1 at amino acid residue Ser 555, thereby initiating autophagy [96]. Furthermore, the Akt/mTOR pathway is inhibited at low glucose concentrations [128, 129]. In addition, previous studies reported that the Akt/mTOR pathway is negatively associated with HBV replication [126, 130, 131]. Therefore, we proposed that glucose modulated HBV replication through the AMPK- and Akt/mTOR/ULK1-induced autophagy. The levels of LC3 at the indicated glucose concentrations were measured using IF staining and western blotting analysis. At low glucose concentration (5 mM), the numbers of endogenous LC3-positive autophagic puncta as well as HBsAg expression (Figure 4.5, A), and the expression levels of LC3-II and p62 (Figure 4.5, B) were markedly higher than those at higher glucose concentrations in HepG2.2.15 cells. In an additional experiment, HepG2.2.15 cells were cultured at three indicated glucose concentrations with or without CQ, an inhibitor of autolysosomal cargo

degradation. The 5 mM glucose further permitted LC3-II accumulation (Figure 4.5, C), suggesting a stronger autophagic flux at the low glucose concentration.

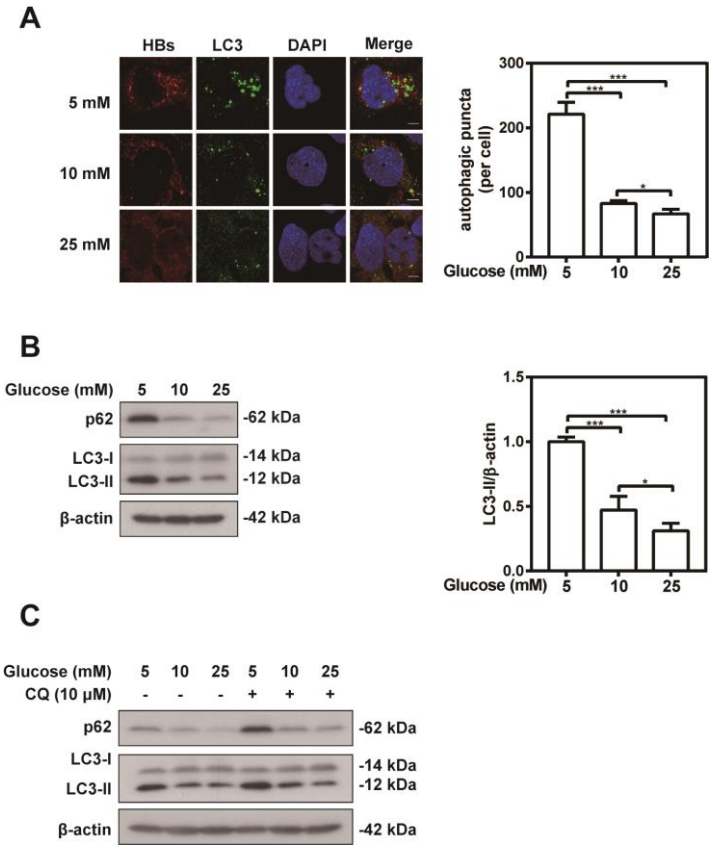

Figure 4.5 Low glucose concentration incrases autophagasome formation

(A) HepG2.2.15 cells were cultured with different glucose concentrations (5, 10, and 25 mM) and harvested after 48 h. The cells were fixed, and incubated with a primary rabbit anti-LC3B and horse anti-HBsAg antibodies, and then stained with an Alexa Fluor 488-conjugated anti-rabbit and Alexa Fluor 594-conjugated anti-horse secondary antibody IgG, respectively. The distribution of LC3 was imaged by immunofluorescence microscopy. Scale bar, 5 μm. (B) HepG2.2.15 cells were cultured with different glucose concentrations (5, 10, and 25 mM) and harvested after 48 h. LC3 and p62 expression were analyzed by western blotting, and beta-actin was used as a loading control. (C) HepG2.2.15 cells were cultured with different concentration of glucose (5, 10, and 25 mM) for 24 h. After that, treated the cells with 10 μM chloroquine (CQ) for 24 h. LC3 and p62 expression were analyzed by western blotting, using beta-actin as a loading control. *p<0.05; **p<0.01; ***p<0.001; ns, not significant.

4.2.2 Low glucose concentration enhances HBV replication through increasing autophagic flux

To further investigate the involvement of autophagy in the modulation of HBV replication at different glucose concentrations, the autophagy-related gene ATG5 was silenced and HBV replication, intracellular HBsAg and HBeAg levels, and HBsAg and

HBeAg levels in the supernatants were measured. ATG5 silencing decreased the LC3-II levels in HepG2.2.15 cells at all three indicated glucose concentrations used for cell culture (Figure 4.6, A). Furthermore, HBV IRs, intracellular HBV DNA levels, intracellular HBsAg levels, and HBsAg levels in the supernatants were also lower at all used glucose concentrations (Figure 4.6, B). In summary, low glucose concentration increases autophagic flux which is associated with enhanced HBV replication.

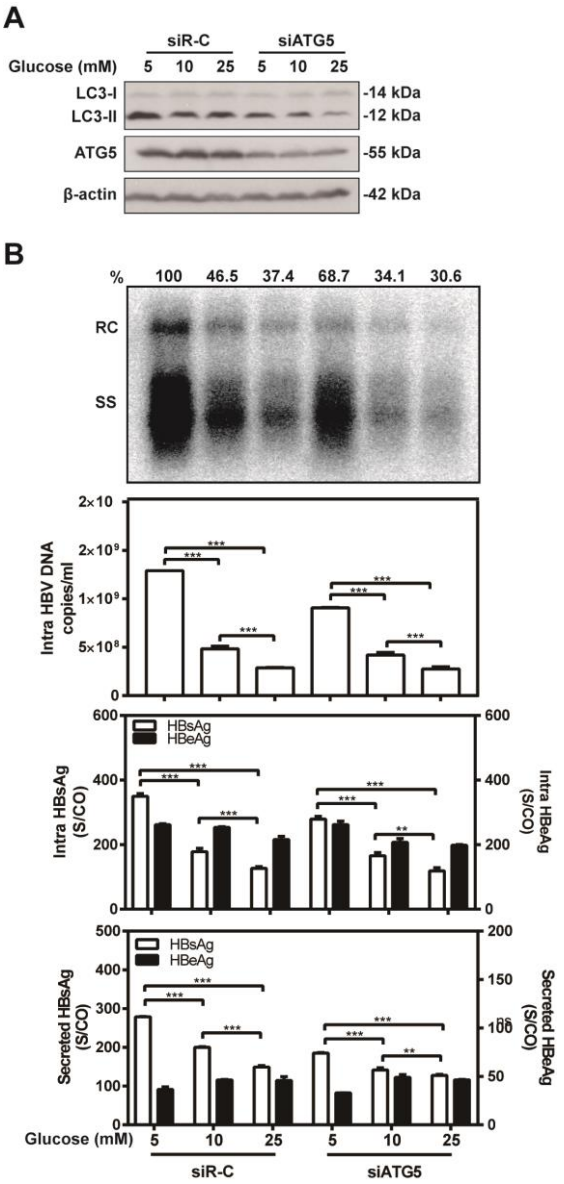

Figure 4.6 Low glucose concentration enhances HBV replication through incrasing autophagic flux

(A) HepG2.2.15 cells were transfected with specific small interfering RNAs against ATG5 mRNA, or a control siRNA (siR-C) at 40 nM, 24 h post-transfection, cultured with different glucose concentrations (5, 10, and 25 mM) and harvested after 48 h. LC3 and p62 expression were analyzed by western blotting,

and beta-actin was used as a loading control. (B) HepG2.2.15 cells were transfected with specific small interfering RNAs against ATG5 mRNA, or a control siRNA (siR-C) at 40 nM, 24 h post-transfection, cultured with different glucose concentrations (5, 10, and 25 mM) and harvested after 72 h. HBV RIs in cells were isolated and detected by Southern blotting. The levels of intracellular HBV DNA were detected by qRT-PCR. The levels of intracellular HBsAg and HBeAg, and that in supernatants were determined as described above. S/CO = signal to cutoff ration; RC = relaxed circular DNA; SS = single-stranded DNA. *p<0.05; **p<0.01; ***p<0.001; ns, not significant.

4.3 Glucose changes HBV replication through regulating AMPK-Akt/mTOR-dependent autophagy

4.3.1 Low glucose concentration incrases AMPK activity, but decreases Akt/mTOR avtivities

Next, we examined in detail how glucose concentration modulates cellular signaling pathways and thereby regulates HBV replication. Previous studies established that autophagy is regulated by the AMPK and mTOR signaling pathways [96, 132-134]. Therefore, we tested whether changed glucose concentrations regulated AMPK, Akt, and mTOR activities in host cells. HepG2.2.15 cells were cultured with the indicated glucose concentrations (5, 10, and 25 mM) for 48 h. The expression of total AMPK, Akt, mTOR, and p70S6K proteins, and its phosphorylated forms were detected using western blotting. While AMPK and ULK1 were significantly activated, Akt, mTOR, and p70S6K were inactivated at 5 mM glucose, respectively, according to the relative level of their phosphorylated forms (Figure 4.7). Due to long-term experiments, the total levels of these proteins vary with the trend of phosphorylated forms. Therefore, the AMPK pathway was activated, whereas the Akt/mTOR pathway was inhibited at the low glucose concentration.

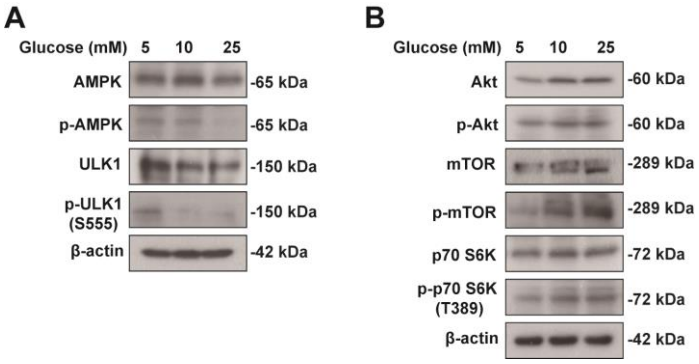

Figure 4.7 Low glucose concentration incrases AMPK activity, but decreases Akt/mTOR avtivities

(A, B) HepG2.2.15 cells were cultured with different glucose concentrations (5, 10, and 25 mM) and

harvested after 48 h. Western blotting analysis was performed to detect the total or phosphorylated levels of the AMPK, ULK1, mTOR, AKT and p70 S6K, using beta-actin as a loading control.

In addition, PHHs were infected with HBV and cultured with indicated glucose concentration (5, and 10 mM) up to 10 days post-infection. HBV infection in PHHs was determined by measuring levels of HBsAg and HBeAg in the culture supernatants. Consistently with the previous results in HepG2.2.15 cells, the levels of phosphorylated AMPK and ULK1 as well as LC3-II in PHHs were elevated after lower glucose concentration were used to culture the cells (Figure 4.8).

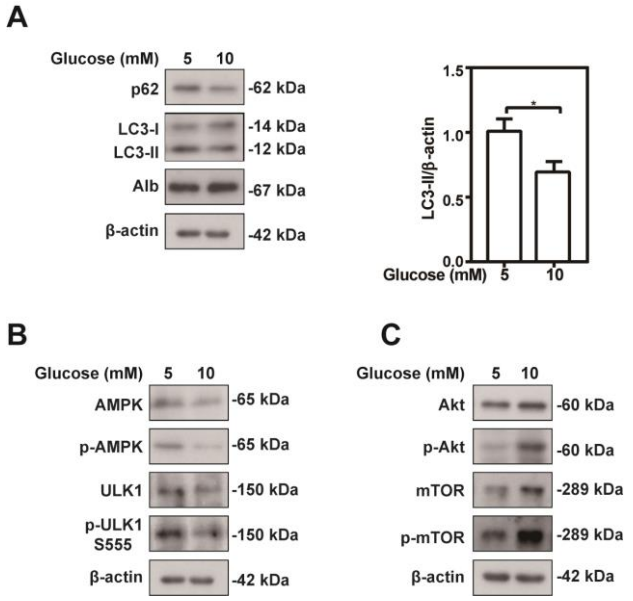

Figure 4.8 Low concentration of glucose induced AMPK-, Akt/mTOR-autophagy axis in PHHs

PHHs infected with HBV virions (multiplicity of infection (MOI)=30), 10 days post-infection, PHHs were cultured with different glucose concentrations (5, and 10 mM) and harvested after 48 h. (A) LC3 and p62 expression were analyzed by western blotting, and beta-actin was used as a loading control. (B) Western blotting analysis was performed to detect the total or phosphorylated levels of the AMPK and ULK1, using beta-actin as a loading control. (C) The total or phosphorylated levels of the Akt and mTOR were analyzed by western blotting, and beta-actin was used as a loading control. *p<0.05; **p<0.01; ***p<0.001; ns, not significant.

4.3.2 AMPK activation plays a positive role in HBV replication

To confirm the function of AMPK in regulation of HBV replication, the HepG2.2.15 cells were treated with an AMPK agonist AICAR for 72 h and the HBV DNA levels in cells and supernatants were analyzed by Southern blotting hybridization and real-time PCR, respectively. The levels of intracellular HBsAg and secreted HBsAg in the supernatant were markedly increased after AICAR treatment (Figure 4.9, A). And the levels of intracellular and secreted HBV DNA were significantly higher in

AICAR-treated cells compared with control cells (Figure 4.9 B), indicating that AMPK activity positively regulates HBV replication and virion production. Western blotting analysis showed notably increased levels of phosphorylated AMPK and ULK1 and LC3-II after AICAR treatment in HepG2.2.15 cells (Figure 4.9, C). Thus, AMPK played a key role in promoting autophagy and thereby increasing HBV replication.

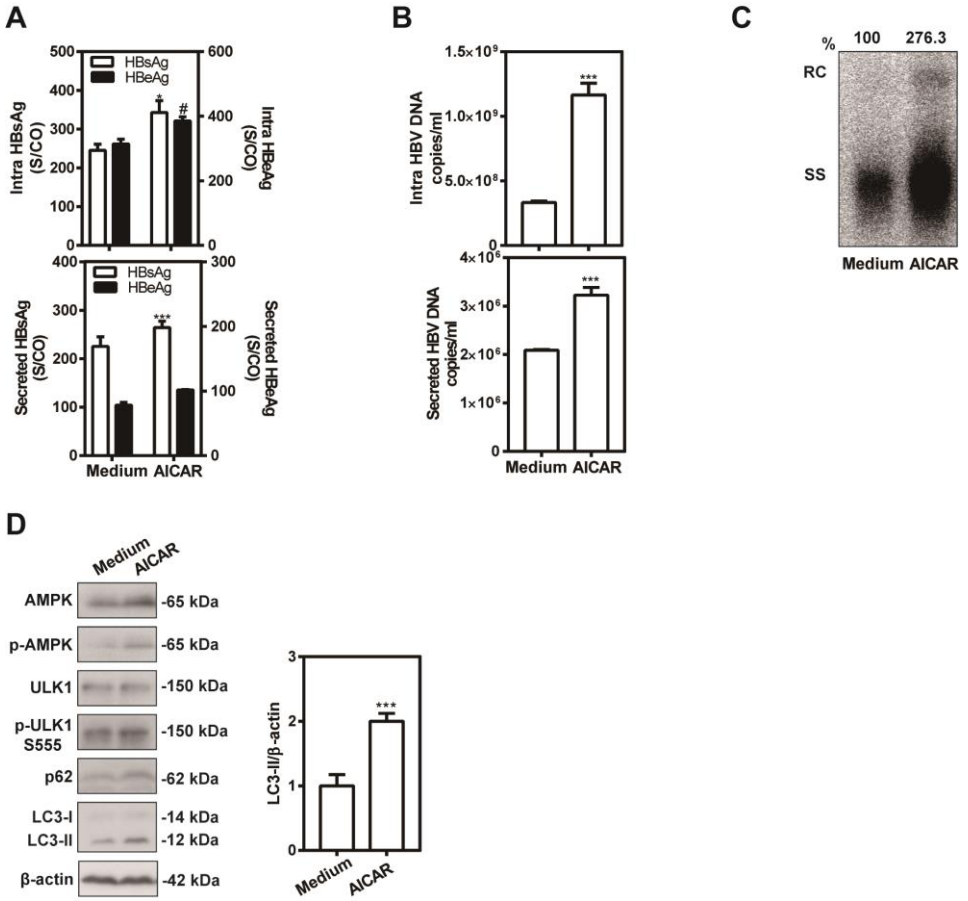

Figure 4.9 AMPK activation plays a positive role in HBV replication in HepG2.2.15 cells

(A-C) HepG2.2.15 cells were treated with AICAR for 72 h. (A) HBsAg and HBeAg in supernatant were determined as above described. (B) The levels of HBV DNA in culture supernatants and in intracellular were determined by qRT-PCR. (C) HBV RIS were detected by Southern blotting. (C) HepG2.2.15 cells were treated with AICAR for 48 h. (D) HepG2.2.15 cells were treated with AICAR for 48 h.Total and phosphorylated AMPK, LC3, and p62 expression were analyzed by western blotting, and beta-actin was used as a loading control. S/CO = signal to cutoff ration; RC = relaxed circular DNA; SS = single-stranded DNA. *p<0.05; **p<0.01; ***p<0.001; ns, not significant.

In addition, PHHs were infected with HBV and treated with AICAR up to 10 days post-infection. HBV infection in PHHs was determined by measuring levels of HBsAg and HBeAg in the culture supernatants. After AICAR treatment, the HBsAg but not HBeAg levels in the culture supernatants were slightly higher (Figure 4.10, A).

Consistently with the previous results obtained in HepG2.2.15 cells. The levels of phosphorylated AMPK and ULK1, and LC3-II in PHHs were elevated after AICAR treatment (Figure 4.10, B).

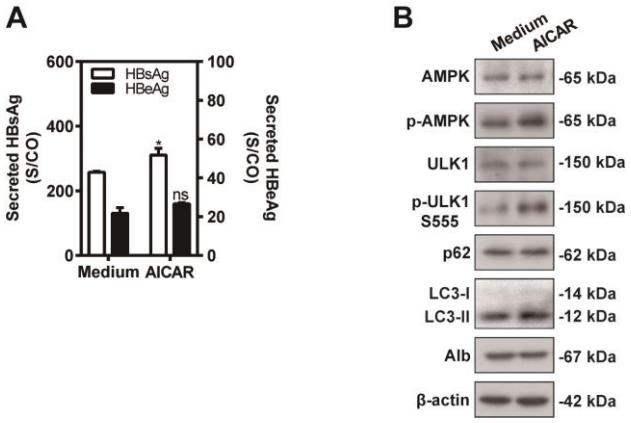

Figure 4.10 AMPK activation plays a positive role in HBV replication in PHHs

PHHs were infected with HBV virions (MOI=30). 10 days post-infection, PHHs were treated with AICAR (0.1 mM) and harvested after 48 h. (A) The HBsAg and HBeAg levels in the culture supernatants were determined as described above. (B) Western blotting analysis was used to determine the levels of AMPK, p-AMPK, LC3, and p62 in the lysates of PHHs, using beta-actin as a loading control. *p,# <0.05; **p <0.01; ***p <0.001; ns, not significant.

4.3.3 AMPK activation promotes HBV replication regardless the glucose concentration

To further confirm whether the positive role of AMPK in regulation of HBV replication is depended on the glucose concentration, we cultured the HepG2.2.15 cells with different concentration of glucose, and then treated with AICAR (an AMPK agonist) for 48 h. The levels of secreted HBsAg and HBeAg in the cell culture supernatants were measured using CMIA. And levels of intracellular and secreted HBV DNA (in HBV virions) were determined using real-time PCR. As depicted in Figure 4.11, the levels of secretion and intracellular HBV DNA were significantly increased in AICAR-treated cells regardless the glucose concentration, suggesting that AMPK activity positively regulated HBV production.

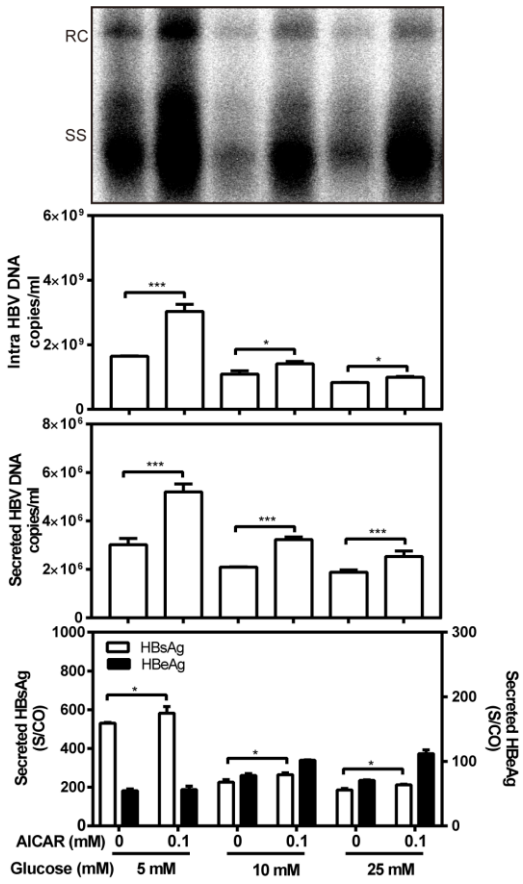

Figure 4.11 AMPK activation promotes HBV replication regardless the glucose concentration

HepG2.2.15 cells were treated with AICAR under different concentration of glucose conditions for 48 h. HBsAg and HBeAg in supernatant were determined as above described. The levels of HBV DNA in culture supernatants and in intracellular were determined by real-time PCR. HBV RIS were detected by Southern blotting. S/CO = signal to cutoff ration; RC = relaxed circular DNA; SS = single-stranded DNA. *p<0.05; **p<0.01; ***p<0.001; ns, not significant.

Collectively, the data suggest that AMPK positively regulated autophagy and thereby increased HBV replication in hepatoma cells and PHHs.

4.3.4 Low glucose concentration enhances HBV replication through inactivating Akt/mTOR signaling pathway

We also investigated the involvement of the Akt/mTOR pathway in HBV replication at different glucose concentrations. HepG2.2.15 cells were grown in the presence of Akti 1/2 or rapamycin in cultures with the indicated glucose concentrations for 72 h. The intracellular HBV DNA levels, intracellular HBsAg and HBeAg levels, and HBV proteins levels in the supernatants were markedly higher in the presence of Akti 1/2 or rapamycin than in the mock control, especially if higher glucose concentrations were used (Figure 4.12, A). The expression levels of LC3-II and p62 in HepG2.2.15 cells

were higher after Akti 1/2 or rapamycin treatment (Figure 4.12, B).

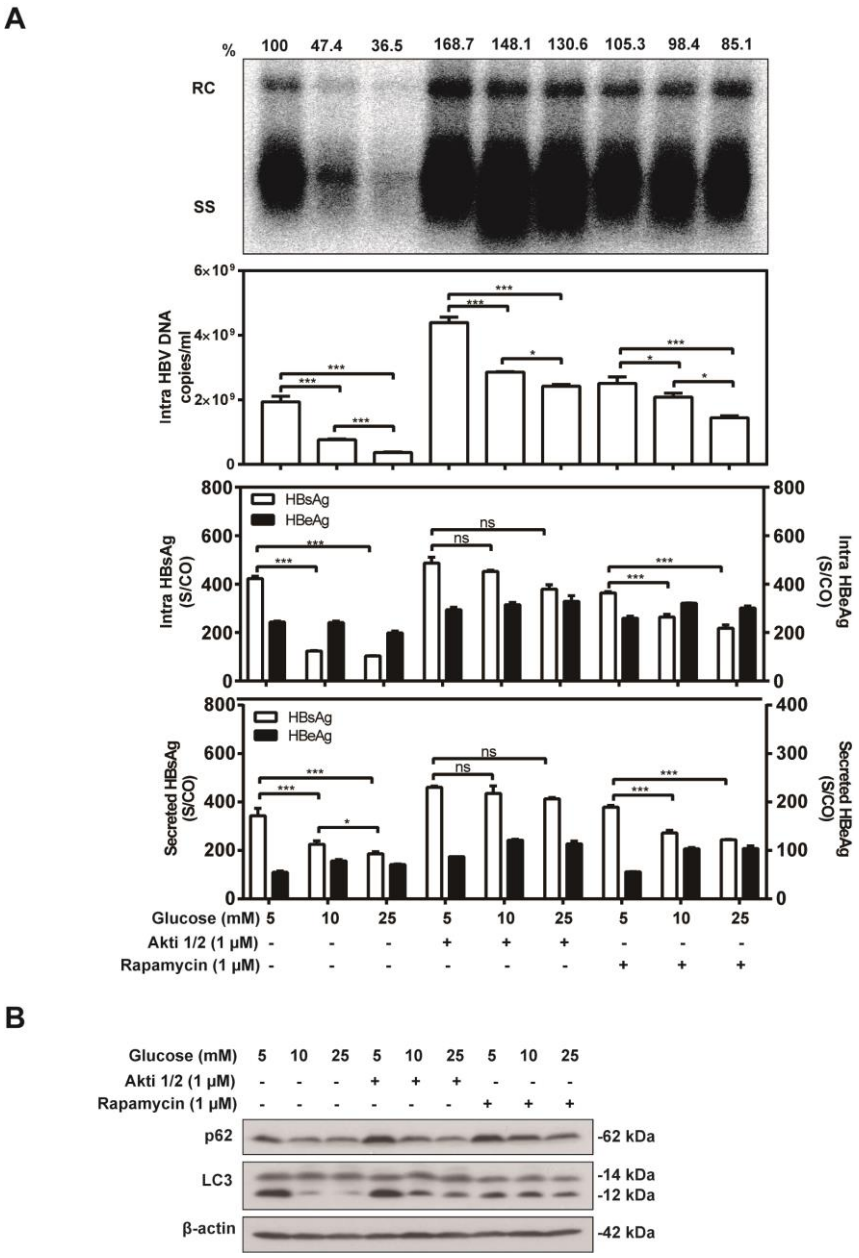

Figure 4.12 Low glucose concentration enhances HBV replication through inactivating Akt/mTOR signaling pathway

(A) HepG2.2.15 cells were cultured with different glucose concentrations (5, 10, and 25 mM), supplement with or without inhibitor Akti 1/2 (1 μM) or rapamycin (1 μM) for 72 h. HBV RIs in cells were isolated and detected by Southern blotting. The levels of HBV DNA in intracellular were determined by qRT-PCR. The levels of HBsAg and HBeAg in intracellular and in supernatants were determined as described above. (B) HepG2.2.15 cells were cultured with different glucose concentrations (5, 10, and 25 mM) supplement with or without inhibitor Akti 1/2 (1 μM) or rapamycin (1 μM) for 48 h. LC3 and p62 expression were analyzed by western blotting, using beta-actin as a loading control. S/CO = signal to cutoff ration; RC = relaxed circular DNA; SS = single-stranded DNA. *p<0.05; **p<0.01; ***p<0.001; ns, not significant.

Taken together, these findings show that low glucose concentration in the medium activates the AMPK pathway, but inhibits the Akt/mTOR signaling pathway to induce autophagy, thereby upregulating HBV replication.

4.4 GLUTs inhibitor phloretin enhances HBV replication by upregulating AMPK-Akt/mTOR-induced autophagy

Glucose is uptaken by GLUTs into cells. Phloretin is a well-known inhibitor of GLUTs and reduce the rate of glucose transport into host cells[135]. We assumed that phloretin may modulate HBV replication by mimicking the culture conditions at low glucose concentration. HepG2.2.15 cells were grown under the standard condition and treated with phloretin at 20 and 50 μM for 72 h. Phloretin treatment at 50 μM markedly increased the levels of intracellular and secreted HBV DNA, and HBsAg in the cell culture supernatants (Figure 4.13, A). Consistently, the secreted HBV DNA levels in the supernatants increased after 50 μM phloretin treatment (Figure 4.13, B). Furthermore, phloretin at 50 μM increased the levels of intracellular HBV DNA and HBV RIs in HepG2.2.15 cells (Figure 4.13, B and C). Real-time RT-PCR analysis showed that phloretin treatment also enhanced HBV RNA transcription in HepG2.2.15 cells (Figure 4.13, D).

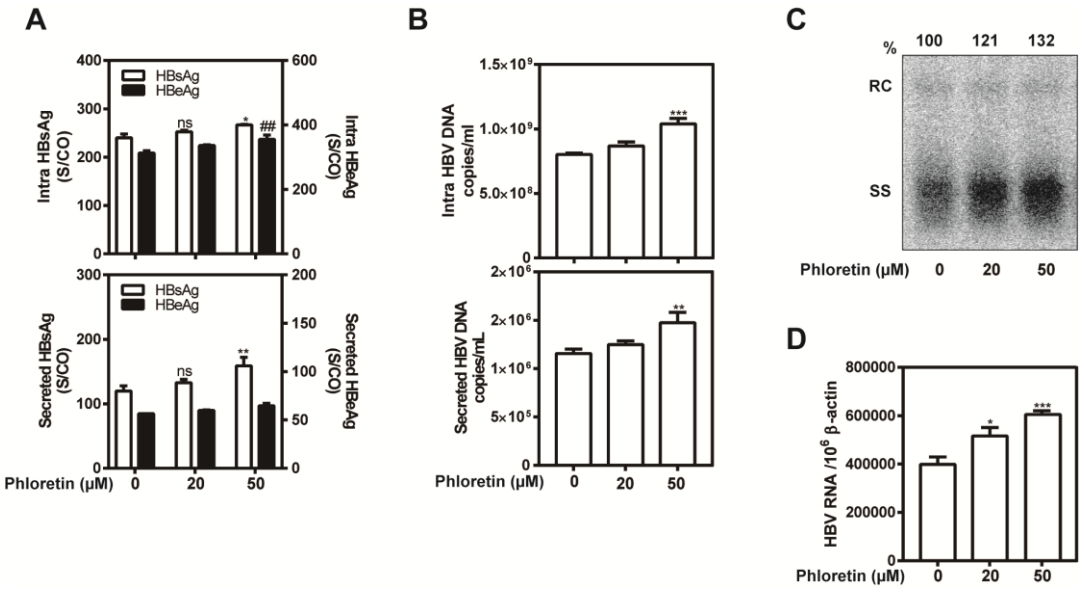

Figure 4.13 GLUTs inhibitor phloretin enhances HBV replication and transcription

HepG2.2.15 cells were treated with 20 or 50 μM phloretin and harvested after 72 h. (A) HBsAg and HBeAg secretion in the supernatants was determined as described above. (B) The levels of intracellular and secreted HBV DNA in the supernatants were detected by real-time PCR. (C) HBV RIs in cells were isolated and detected by Southern blotting. (D) HBV RNA levels in HepG2.2.15 cells were

analyzed by real-time RT-PCR. S/CO = signal to cutoff ration; RC = relaxed circular DNA; SS = single-stranded DNA. *p<0.05; **p<0.01; ***p<0.001; ns, not significant.

Next, we examined whether phloretin enhanced HBV replication by regulating AMPK and Akt/mTOR, as observed in cells cultured at the low glucose concentration. The cellular levels of total AMPK, Akt, and mTOR, and their phosphorylated forms, were determined using western blotting. Phloretin treatment elevated the levels of AMPK phosphorylation and reduced Akt/mTOR phosphorylation (Figure 4.14), proven that phloretin activated AMPK but inhibited Akt/mTOR. Furthermore, phloretin treatment increased the expression of p62 and LC3-II in HepG2.2.15 cells.

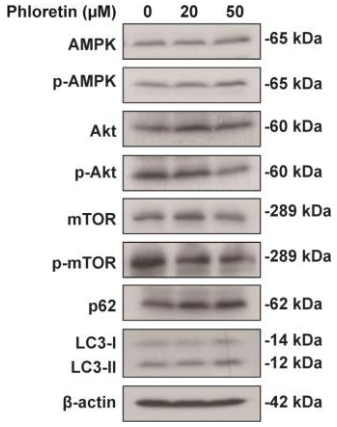

Figure 4.14 Phloretin activates AMPK, and inactivates mTOR signaling in HepG2.2.15 cells
HepG2.2.15 cells were treated with 20 or 50 μM phloretin and harvested after 48 h. Western blotting analysis was performed to detect the levels of total or phosphorylated AMPK, Akt, and mTOR. LC3, and p62 levels were analyzed by western blotting, using beta-actin as a loading control.

Similarly, the phloretin treatment led to slightly enhanced HBsAg production in PHHs. PHHs were infected with HBV and treated with phloretin at 20 or 50 μM up to 10 days post-infection. After phloretin treatment, the HBsAg but not HBeAg levels were slightly increased in the culture supernatants (Figure 4.15, A). Consistently, the levels of phosphorylated AMPK and ULK1 and LC3-II in PHHs were elevated after phloretin treatment, while decreased levels of phosphorylated Akt and mTOR were detected (Figure 4.15, B). Thus, phloretin treatment upregulates AMPK-Akt/mTOR-induced autophagy in hepatoma cells and PHHs.

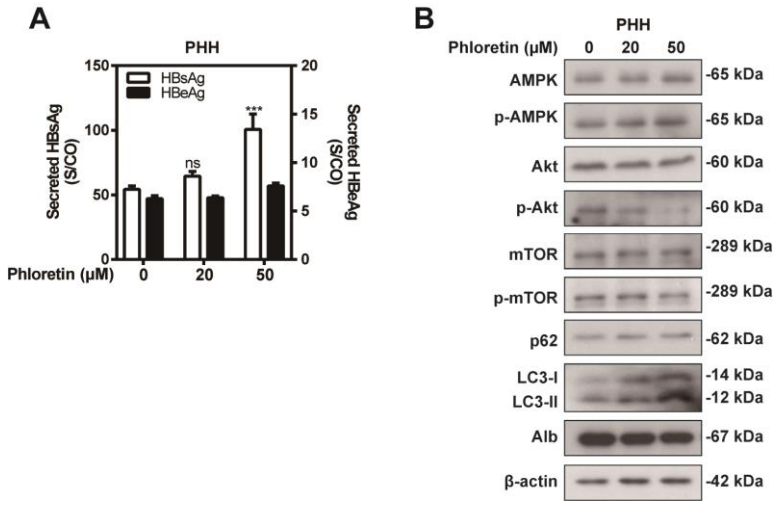

Figure 4.15 Phloretin promotes HBV replication and activates AMPK, and inactivates mTOR signaling in PHHs

PHHs were infected with HBV virions (MOI=30). 10 days post-infection, PHHs were treated with phloretin (20, and 50 μM) and harvested after 48 h. (A) The HBsAg and HBeAg levels in the culture supernatants were determined as described above. (B) Western blotting analysis was performed to detect the levels of total or phosphorylated AMPK, Akt, and mTOR, and LC3 and p62, using beta-actin as a loading control. *p <0.05; **p <0.01; ***p <0.001; ns, not significant.

In addition, phloretin slightly enhanced glycolysis, as indicated by increased lactate production in the culture medium (Figure 4.16, A). Finally, the presence of pyruvate did not alter the effect of phloretin on the production of HBsAg and HBeAg (Figure 4.16, B). The proliferation of HepG2.2.15 cells was measured using the CCK8 assay, and the results confirmed that phloretin treatment did not affect cell proliferation at any indicated time point (Figure 4.16, C).

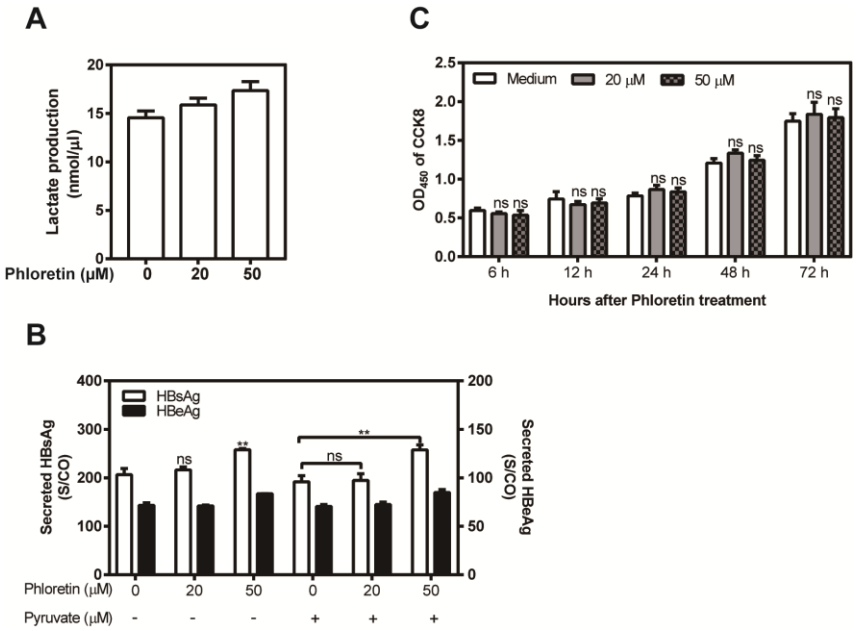

Figure 4.16 Phloretin slightly enhanced glycolysis in HepG2.2.15 cells

(A) HepG2.2.15 cells were treated with 20 or 50 μM phloretin and harvested after 72 h. Lactate production was measured by a Lactate Colorimetric/Fluorometric Assay kit, according to the manufacturer's instructions. (B) HepG2.2.15 cells were treated with 20 or 50 μM phloretin in combination with 1 mM pyruvate and harvested after 72 h. HBsAg and HBeAg secretion in the supernatant were determined as described above. (C) Cell proliferation was measured by the CCK8 assay at 6, 12, 24, 48, and 72 h after treatment with phloretin (20, and 50 μM). S/CO = signal to cutoff ratio; *p <0.05; **p <0.01; ***p <0.001; ns, not significant.

Taken these data together, phloretin treatment enhances HBV replication, upregulates AMPK/mTOR-ULK1-autophagy, and increases glycolysis in hepatoma cells.

4.5 2-DG inhibits HBV replication through upregulating Akt/mTOR signaling pathway

4.5.1 2-DG inhibits HBV progeny secretion and replication

2-DG, an analogue of glucose, is best known as an inhibitor of glycolysis and blocks the cellular HK enzymes [136]. We addressed the question whether blocking of glycolysis affects HBV replication. Therefore, we treated the HepG2.2.15 cells with 2-DG for 72 h. As shows in the Figure 4.17A, 2-DG treatment significantly decreased glycolysis in HepG2.2.15 cells. Interestingly, 2-DG markedly decreased the levels of intracellular HBV RIs, extracellular HBV DNA, and intracellular HBsAg, and secreted HBsAg in the supernatants in a dose-dependent manner in HepG2.2.15 cells (Figure 4.17, B). HBV RNA levels were detected by real-time RT-PCR. We found that 2-DG

obviously inhibits HBV RNA transcription (Figure 4.17, C). Consistent with our previous results, adding pyruvate simultaneously did not change the 2-DG-mediated inhibition of HBsAg expression in HepG2.2.15 cells (Figure 4.17, D). These data suggest that treatment with 2-DG inhibits glycolysis and HBV replication and gene expression in HepG2.2.15 cells in a dose-dependent manner.

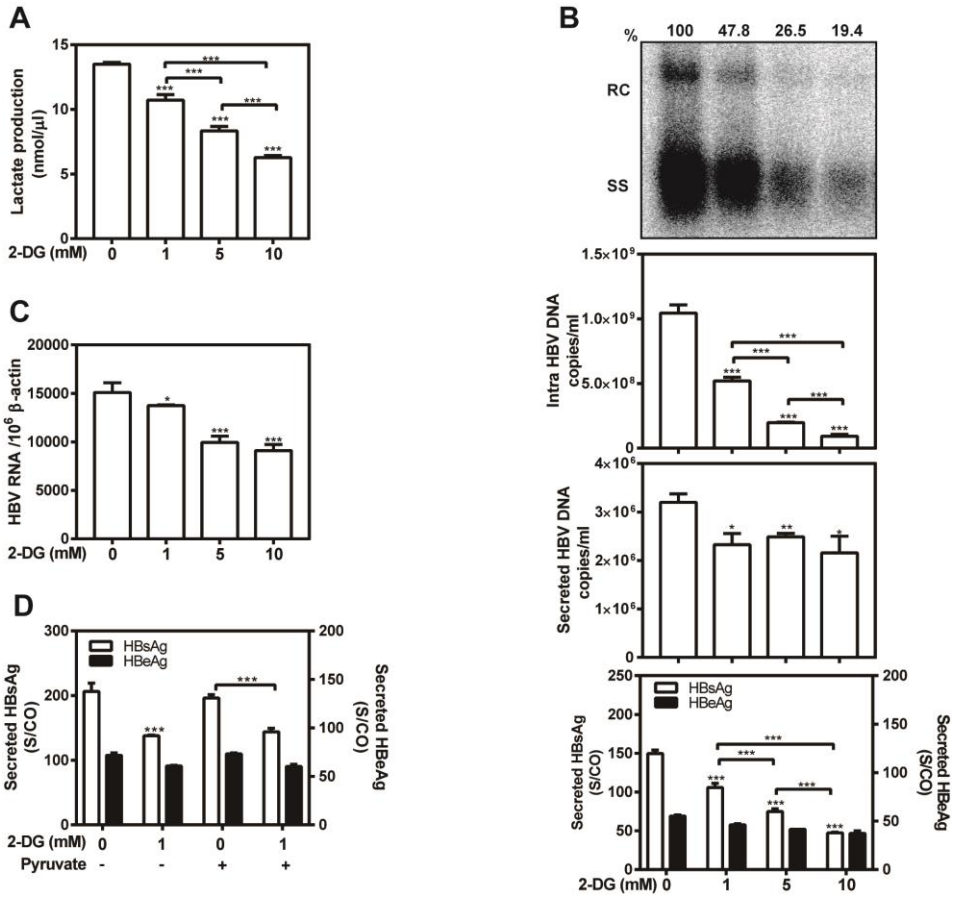

Figure 4.17 2-DG decreases HBV replication and gene expression

(A-C) HepG2.2.15 cells were treated with 2-DG (1, 5, and 10 mM) and harvested after 72 h. (A) Lactate production was measured by a Lactate Colorimetric/Fluorometric Assay kit, according to the manufacturer's instructions. (B) HBsAg and HBeAg secretion in the supernatant were detected as described above. The levels of intracellular and secreted HBV DNA were measured by real-time PCR. HBV RIs in cells were isolated and detected by Southern blotting. (C) HBV RNA levels in HepG2.2.15 cells were analyzed by real-time RT-PCR. (D) HepG2.2.15 cells were treated with 2-DG in combination with 1 mM pyruvate and harvested after 72 h. HBsAg and HBeAg secretion in the supernatants were determined as described above. S/CO = signal to cutoff ration; RC = relaxed circular DNA; SS = single-stranded DNA. *p <0.05; **p <0.01; ***p <0.001; ns, not significant.

4.5.2 2-DG treatment leads to AMPK and Akt/mTOR phosphorylation

It has been reported that 2-DG treatment results in an increase in intracellular AMP/ATP ratio, thereby activating AMPK. Consistently, the level of phosphorylated

AMPKα subunit (Thr172) increased, when hepatoma cells were treated with 2-DG (1, 5, and 10 mM) for 48 h (Figure 4.18). However, the levels of phosphorylated Akt (Ser473), which is required for Akt to activate its downstream targets, was enhanced, as well as mTOR phosphorylation and p70 S6K expression (Figure 4.18). 2-DG also promoted the p62 and LC3-II expression in HepG2.2.15 cells, consistent with results of previous reports [137, 138].

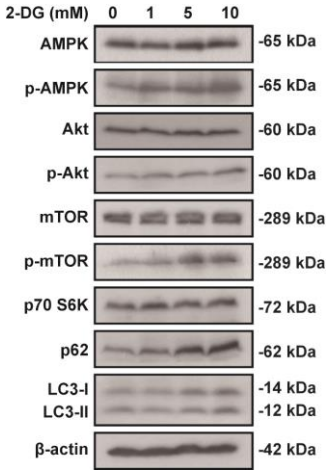

Figure 4.18 2-DG treatment leads to AMPK and Akt/mTOR phosphorylation

HepG2.2.15 cells were treated with 2-DG (1, 5, and 10 mM) and harvested after 48 h. Western blotting analysis was performed to detect the levels of total or phosphorylated AMPK, AKT, and mTOR. LC3 and p62 expression were also analyzed by western blotting, using beta-actin as a loading control.

Then, we asked whether the Akt/mTOR pathway participated in the regulation of HBV replication in the presence of 2-DG. Akt and mTOR were blocked using the inhibitors Akti 1/2 and rapamycin after 2-DG treatment, respectively. Both inhibitors abrogated the suppressive effect of 2-DG on HBV replication (Figure 4.19), suggesting an involvement of Akt/mTOR signaling pathway in the regulation of HBV replication in the presence of 2-DG.

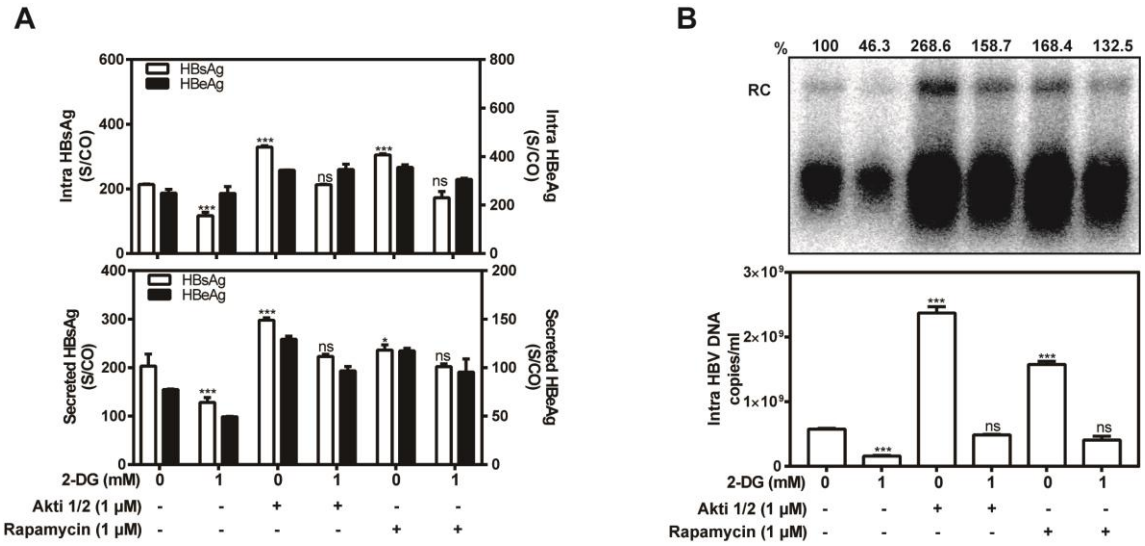

Figure 4.19 2-DG inhibits HBV replication through activating Akt/mTOR signaling pathway

HepG2.2.15 cells were cultured with 2-DG (1, 5, and 10 mM) with or without inhibitor Akti 1/2 (1 μM) or rapamycin (1 μM) for 72 h. (A) The levels of intracellular HBsAg and HBeAg, and that secretion in the supernatants were determined as described above. (B) The levels of intracellular HBV DNA were measured by real time RT-PCR. HBV RIs in cells were isolated and detected by Southern blotting. S/CO = signal to cutoff ration; RC = relaxed circular DNA; SS = single-stranded DNA. *p <0.05; **p <0.01; ***p <0.001; ns, not significant.

4.5.3 2-DG inhibits HBV replication regardless glucose concentration

We further examined whether the suppressive effect of 2-DG on HBV was dependent on the glucose concentration in the culture medium. HepG2.2.15 cells were grown in the medium with the indicated glucose concentrations (5, 10, and 25 mM), and then treated with 2-DG (1 mM). Treatment with 2-DG markedly decreased the levels of HBV RIs and secreted HBsAg in the supernatants in HepG2.2.15 cells regardless of the glucose concentrations used (Figure 4.20, A). The expression levels of total Akt, and its phosphorylated form significantly increased in HepG2.2.15 cells regardless of the glucose concentration (Figure 4.20, B). Thus, the effect of 2-DG on HBV replication and gene expression, as well as Akt phosphorylation was dominant over glucose.

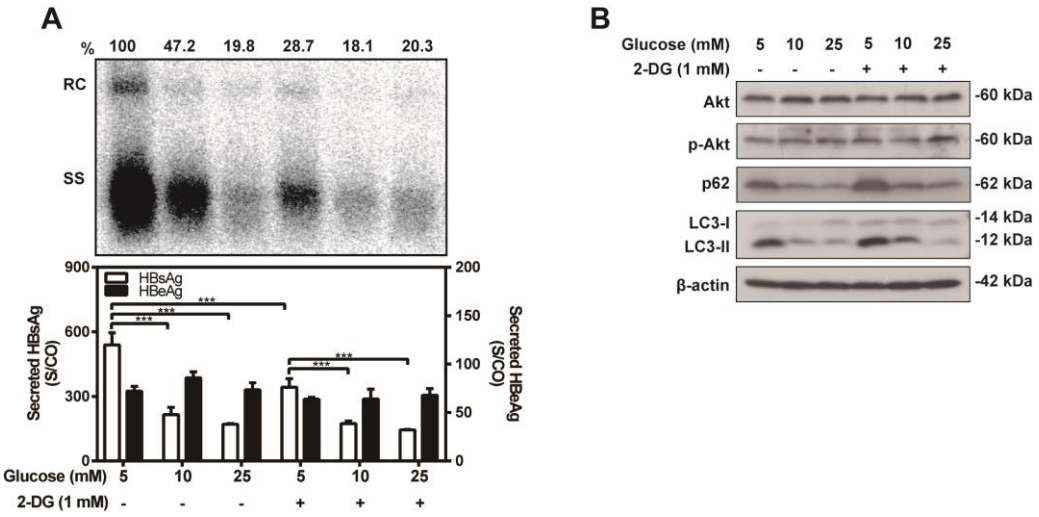

Figure 4.20 2-DG inhibits HBV replication regardless glucose concentration

(A, B) HepG2.2.15 cells were cultured with different glucose concentrations (5, 10, and 25 mM), then treated with 1 mM 2-DG, and harvested after 72 h. HBV RIs in cells were isolated and detected by Southern blotting. HBsAg and HBeAg secretion in the supernatants were detected as described above. (D) The levels of total and phosphorylated Akt, LC3, and p62 were analyzed by western blotting, using beta-actin as a loading control. S/CO = signal to cutoff ration; RC = relaxed circular DNA; SS = single-stranded DNA. *p <0.05; **p <0.01; ***p <0.001; ns, not significant.

In addition, 2-DG has a similar inhibitory effect on HBV infection in PHHs. PHHs were infected with HBV and treated with 2-DG (1, 5, and 10 mM) up to 10 days post-infection. After 2-DG treatment, the HBsAg and HBeAg levels in the culture supernatants were markedly decreased in a dose-dependent manner (Figure 4.21, A). Consistently, the levels of phosphorylated Akt, mTOR, AMPK and ULK1 in PHHs were increased after 2-DG treatment (Figure 4.21, B).

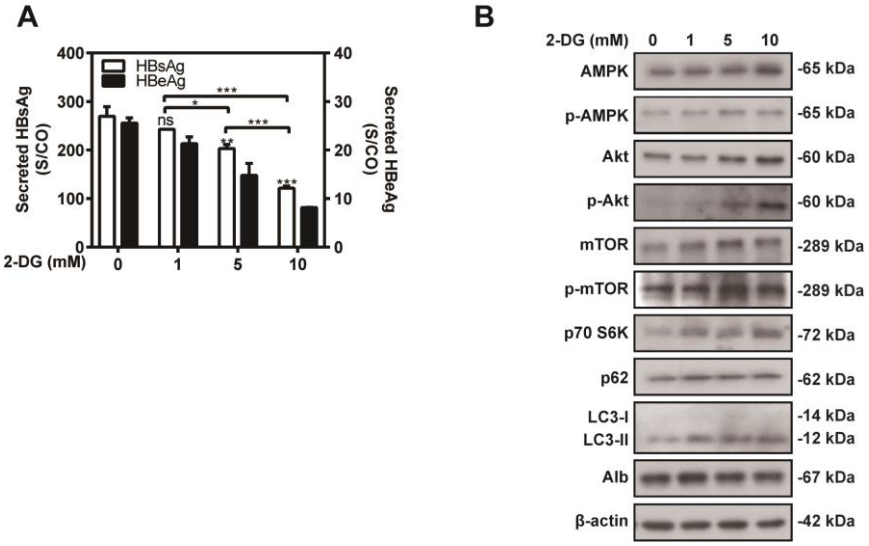

Figure 4.21 2-DG decreases HBV replication and gene expression by upregulating the

Akt/mTOR signaling pathway in PHHs.

PHHs were infected with HBV virions (MOI=30). 10 days post-infection, PHHs were treated with 2-DG (1, 5, and 10 mM) and harvested after 48 h. (A) The HBsAg and HBeAg levels in the culture supernatants were determined as described above. (B) Western blotting analysis was performed to detect the levels of total or phosphorylated AMPK, Akt, and mTOR, LC3, and p62, using beta-actin as a loading control. *p <0.05; **p <0.01; ***p <0.001; ns, not significant.

The upregulated AMPK and Akt/mTOR phosphorylation by 2-DG may explain decreased HBV replication and gene expression under these culture conditions. Due to the complexity of the functions controlled by these pathways, other mechanisms may also contribute to HBV suppression and need to be considered in future study.

4.6 Decreasing the levels of *O*-GlcNAcylation promotes HBV replication by suppressing autophagic degradation and inhibiting mTOR signaling

Many intracellular proteins are *O*-GlcNAylated in the presence of glucose. Therefore, *O*-GlcNAcylation has been thought to function as a nutrient sensor to regulate many cellular processes in cells[139]. To test whether and how disruption of *O*-GlcNAcylation affects HBV replication, small chemical inhibitor OSMI-1 and small interfering RNAs were used.

4.6.1 Inhibition of *O*-GlcNAcylation promotes HBV replication

It is well-known that protein *O*-GlcNAcylation is modulated by two enzymes: the transfer of GlcNAc to serine or threonine residues on proteins is catalyzed by *O*-GlcNAc transferase (OGT), while its removal is catalyzed by *O*-GlcNAcase (OGA). The small chemical inhibitor molecule OSMI-1, an inhibitor of OGT, which reduces the level of *O*-GlcNAcylation, was added into the culture medium to examine its effect on HBV replication. Western blotting analysis demonstrated an obviously decreased levels of *O*-GlcNAcylation by OSMI-1 in HepG2.2.15 cells (Figure 4.22, A). Then, the effects of OSMI-1 on HBV gene expression were analyzed by measuring the levels of intracellular and secreted HBsAg and HBeAg, HBV DNA in the supernatants, and intracellular HBV replicative intermediates (RIs). The levels of secreted HBsAg and HBeAg in the cell culture supernatants were detected by CMIA. The levels of intracellular and secreted HBsAg but not HBeAg, in the supernatants obviously increased after OSMI-1 treatment of HepG2.2.15 cells (Figure 4.22, B). HBV replicative intermediates (HBV RIs) were prepared at day 4 and analyzed by Southern

blotting. The levels of intracellular and secreted HBV DNA were determined by real-time RT-PCR. Consistently, OSMI-1 led to higher levels of intracellular and secreted HBV DNA. The amount of HBV RIs increased significantly after OSMI-1 in HepG2.2.15 cells (Figure 4.22, B). Furthermore, HBV RNA levels were not affected by OSMI-1 treatment (Figure 4.22, C), meaning that OSMI-1 did not affect HBV transcript. These results suggest that inhibition of OGT activity positively regulated HBV production in HepG2.2.15 cells.

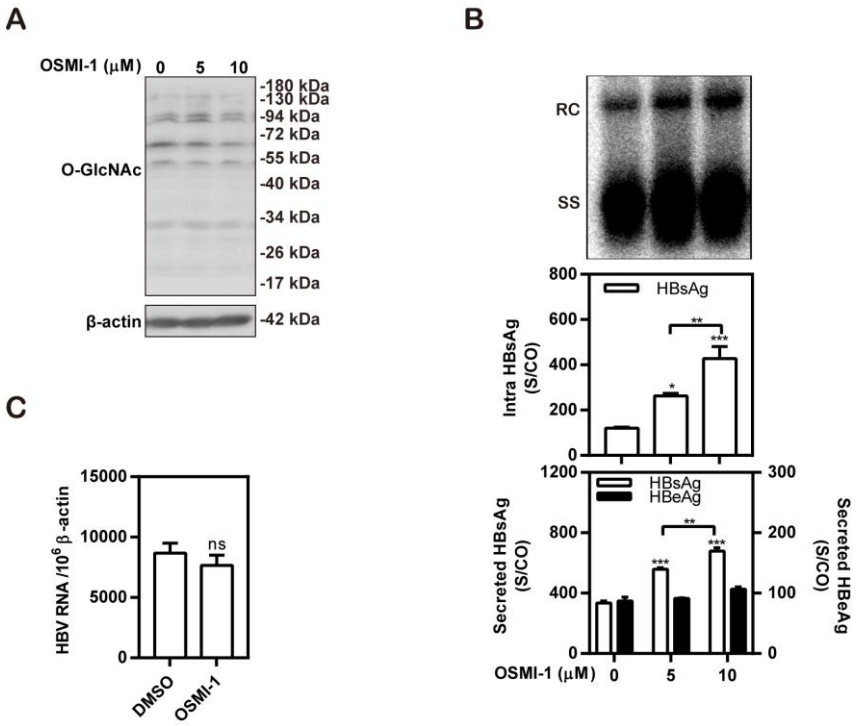

Figure 4.22 Inhibition of *O*-GlcNAcylation promotes HBV replication in HepG2.2.15 cells

(A) HepG2.2.15 cells were treated with 10 μM of the small inhibitor OSMI-1 for 48 h. The global *O*-GlcNAcylation expression levels were analyzed by western blotting, and beta-actin was used as a loading control. (B and C) HepG2.2.15 cells were treated with 10 μM OSMI-1 for 72 h. (B) Analysis of secreted HBsAg and HBeAg from the supernatants and those intracellularly was performed as described above. The levels of intracellular HBV DNA were measured by RT-PCR. The amount of HBV RIs was detected by Southern blotting. (C) HBV RNA levels were detected by RT-PCR. S/CO = signal to cutoff ration; RC = relaxed circular DNA; SS = single-stranded DNA. *p <0.05; **p <0.01; ***p <0.001; ns, not significant.

In addition, PHHs were infected with HBV and treated with OSMI-1 up to 10 days post-infection. Western blotting analysis demonstrated decreased levels of *O*-GlcNAcylation by OSMI-1 in PHHs (Figure 4.23, A). HBV infection in PHHs was determined by measuring levels of HBsAg and HBeAg in the culture supernatants. After OSMI-1 treatment, HBsAg but not HBeAg levels were significantly increased

(Figure 4.23, B), consistently with the previous results in HepG2.2.15 cells.

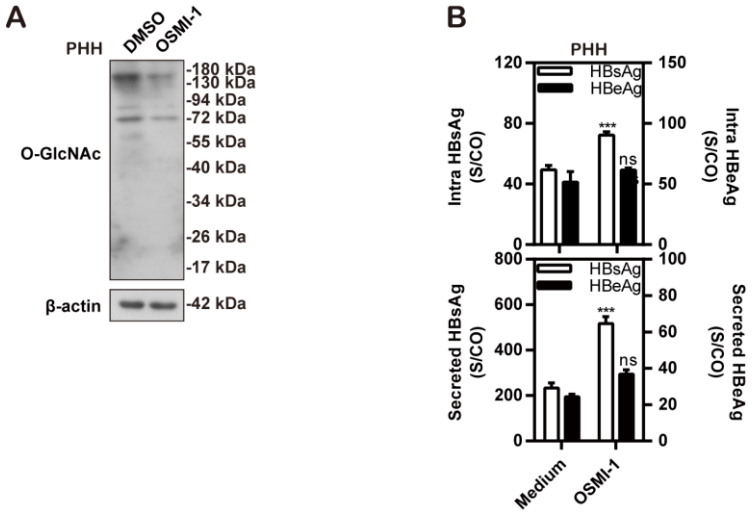

Figure 4.23 Inhibition of *O*-GlcNAcylation promotes HBV replication in PHHs

PHHs were infected with HBV virions (MOI=30). 10 days post-infection, PHHs were treated with 10 μM OSMI-1 and harvested after 48 h. (A) Western blotting analysis was performed to detect the levels of global *O*-GlcNAcylation, using beta-actin as a loading control. (B) The levels of intracellular HBsAg and HBeAg and that in the culture supernatants were determined as described above. *p <0.05; **p <0.01; ***p <0.001; ns, not significant.

Collectively, these data suggest that OSMI-1 positively regulated HBV replication in hepatoma cells and PHHs.

4.6.2 Silencing OGT promotes HBV replication in hepatoma cells

Next, to further verify the role of OGT in HBV replication, Huh7 cells were cotransfected with siOGT or siR-C (negative control siRNA) and HBV expression plasmid pSM2 for 72 h. At first, we detected the global levels of *O*-GlcNAcylation after silencing OGT by western blotting. The results showed that silencing OGT significantly decreased the global levels of *O*-GlcNAcylation in Huh7 cells (Figure 4.24, A). Then, the levels of HBsAg and HBeAg in the supernatants were detected by CMIA. HBV RIs were prepared at 72 h post-transfection and analyzed by Southern blotting. Consistent with the effect of OSMI-1, the results showed that silencing of OGT obviously increased the levels of secreted HBsAg, but not HBeAg (Figure 4.24, B). Moreover, Southern blotting confirmed that silencing OGT significantly increased HBV replication in Huh7 cells (Figure 4.24, B). In addition, OGT silencing enhanced HBV replication and HBsAg expression in Huh7 cells in a dose-dependent manner (Figure 4.24, C). However, silencing of OGA, which enhances the global levels of

O-GlcNAcylation (Figure 4.24, A), obviously decreased the levels of secreted HBsAg and HBV RIs (Figure 4.24, B).

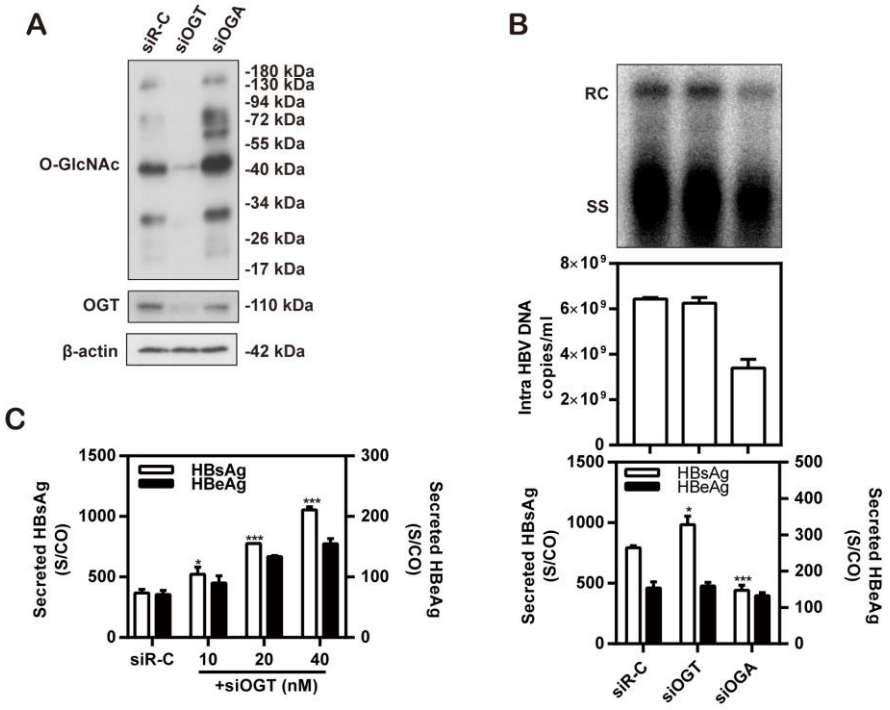

Figure 4.24 Silencing OGT promotes HBV replication in Huh7 cells

(A and B) Huh7 cells were cotransfected with HBV plasmid pSM2 and siOGT, siOGA or si-control (siR-C) at 40 nM for 72 h. (A) Western blotting analysis was performed to detect the global levels of *O*-GlcNAcylation after silencing OGT, and beta-actin was used as a loading control. (B) The HBsAg and HBeAg levels in the culture supernatants were determined as described above. HBV RIs in cells were isolated and detected by Southern blotting. (C) Huh7 cells were transfected with different doses of siOGT (at 0, 10, 20, or 40 nM) or siR-C (40 nM), and harvested after 72 h. Analysis of secreted HBsAg and HBeAg in the culture supernatants was performed as previously described. RC = relaxed circular DNA; S/CO = signal to cutoff ratio; SS = single stranded DNA. *p <0.05; **p <0.01; ***p <0.001; ns, not significant.

Then, we examined the consequences of silencing of OGT on HBV replication in HepG2.2.15 cells with stable HBV production. The cells were transfected with specific siOGT and harvested after 72 h. Western blotting results showed that OGT silencing significantly decreased the global levels of *O*-GlcNAcylation in HepG2.2.15 cells (Figure 4.25, A). In concordance with the results of HBsAg in Huh7 cells, the CMIA results showed that the levels of HBsAg in the supernatant obviously increased after OGT silencing in HepG2.2.15 cells (Figure 4.25, B). Furthermore, Southern blotting confirmed that OGT silencing significantly enhanced HBV replication (Figure 4.25, B). In addition, OGT silencing enhanced HBV replication and HBsAg expression in

HepG2.2.15 cells in a dose-dependent manner (Figure 4.25, C). On the other hand, silencing of OGA enhanced the global levels of *O*-GlcNAcylation (Figure 4.25, A), and obviously decreased the levels of secreted HBsAg in the supernatants, and intracellular HBV RIs (Figure 4.25,B and C) in HepG2.2.15 cells.

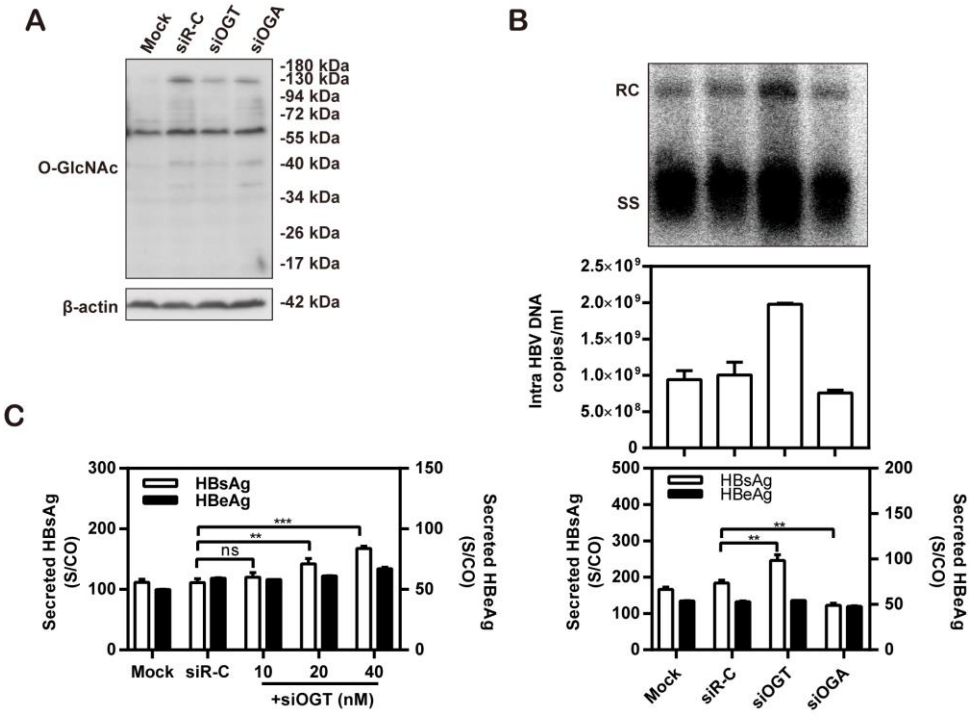

Figure 4.25 Silencing OGT promotes HBV replication in HepG2.2.15 cells

(A-C) HepG2.2.15 cells were transfected with siOGT or si-control (siR-C) at 40 nM for 72 h. (A) Western blotting analysis was performed to detect the global levels of *O*-GlcNAcylation after silencing OGT using beta-actin as a loading control. (B) HBsAg and HBeAg levels in the culture supernatants were determined as described above. HBV RIs in cells were isolated and detected by Southern blotting. (C) HepG2.2.15 cells were transfected with different doses of siOGT (at 0, 10, 20, or 40 nM) or siR-C (40 nM) and harvested after 72 h. Analysis of secreted HBsAg and HBeAg in the culture supernatants was performed as previously described. RC = relaxed circular DNA; S/CO = signal to cutoff ratio; SS = single stranded DNA. *p <0.05; **p <0.01; ***p <0.001; ns, not significant.

Taken together, these data demonstrate that silencing of OGT increases the amount of secreted HBsAg in the supernatants, as well as the levels of secreted HBV DNA and intracellular HBV replication in hepatoma cells.

4.6.3 Inhibition of OGT promotes HBV replication depending on induced autophagosome formation

Accumulation of misfolded proteins and disruption of calcium storage in the ER cause ER stress, which initiates UPR. It has been reported that disruption of *O*-GlcNAc

signaling can induce ER stress[140-142]. Previously, ER stress and UPR were found to regulate HBV replication through inducing autophagy[71]. Thus, this mechanism may explain our findings that disruption of *O*-GlcNAcylation signaling by the inhibitor of OGT or silencing of OGT promotes HBV replication. We addressed the hypothesis whether disruption of *O*-GlcNAcylation signaling enhances cellular autophagy, thereby increasing HBV replication. The levels of LC3 in HepG2.2.15 cells after treatment with different small inhibitors involved in the disruption of *O*-GlcNAcylation were measured using IF staining and western blotting analysis. The numbers of endogenous LC3-positive autophagic puncta (Figure 4.26, A), and the levels of LC3-II and p62 (Figure 4.26, B), were markedly increased in OSMI-1 treatment cells, suggesting a stronger autophagosome formation after inhibition of *O*-GlcNAcylation by OSMI-1.

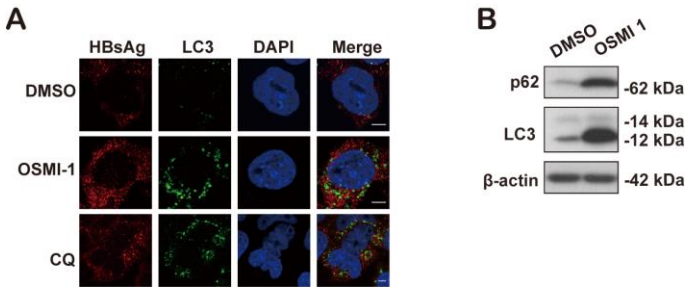

Figure 4.26 Inhibition of *O*-GlcNAcylation by OSMI-1 increases autophagosome formation

(A) HepG2.2.15 cells were treated with 10 μM OSMI-1, and harvested after 48 h. The cells were fixed, incubated with rabbit anti-LC3B and horse anti-HBsAg primary antibody, followed by staining with Alexa Fluor 488-conjugated anti-rabbit secondary antibody IgG and Alexa Fluor 594-conjugated anti-horse secondary antibody IgG. Finally, the cells were visualized by a fluorescence microscope. Scale bar, 5 μm. (B) HepG2.2.15 cells were treated with 10 μM OSMI-1, and harvested after 48 h. LC3 and p62 expression were analyzed by western blotting, and beta-actin was used as a loading control. *p<0.05; **p<0.01; ***p<0.001; ns, not significant.

To further confirm the role of autophagy in the regulation of HBV replication following OSMI-1 treatment, we treated the cells with OSMI-1 and autophagy inhibitors, such as CQ and 3-MA. Then, HBsAg and HBeAg production in the supernatants were measured. CQ did not block the promoting effect of OSMI-1, while 3-MA obviously suppressed the promoting effect of OSMI-1, because the levels of intracellular and secreted HBsAg were significantly inhibited after treatment with OSMI-1 and 3-MA, (Figure 4.27, A). Furthermore, the autophagy-associated gene ATG5 was silenced prior to treatment with OSMI-1. Intracellular HBV DNA levels, and HBsAg levels in the

culture supernatants were also decreased after silencing ATG5 (Figure 4.27, B). In summary, OSMI-1 increases autophagosome formation, which is associated with enhanced HBV replication.

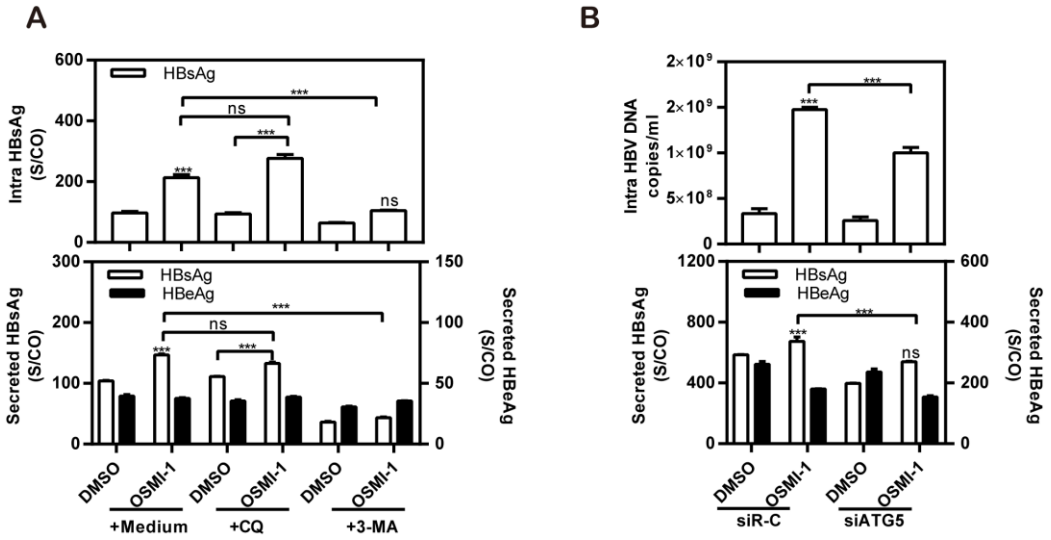

Figure 4.27 Inhibition of *O*-GlcNAcylation by OSMI-1 enhances HBV replication through increasing autophagosome formation

(A) HepG2.2.15 cells were treated with OSMI-1, with or without autophagy inhibitors CQ or 3-MA, and harvested after 72 h. (B) HepG2.2.15 cells were transfected with siATG or siR-C, then treated with 10 μM OSMI-1, and harvested after 72 h. HBsAg and HBeAg levels in the culture supernatants and those in the intracellular were determined as described above. Intracellular HBV DNA levels were isolated and detected by RT-PCR. *p<0.05; **p<0.01; ***p<0.001; ns, not significant.

4.6.4 Inhibition of OGT promotes HBV replication by suppressing autophagic degradation

In view of the increase in the number of LC3 puncta and the level of p62 autophagy cargo, inhibition of OGT appeared to increase the number of autophagosomes by blocking autophagy degradation. Therefore, we suspected that inhibition of OGT can inhibit autophagic degradation. To assess whether inhibition of OGT decreases autophagic degradation, HepG2.2.15 cells were treated with these inhibitors for 48 h, and then incubated with DQ Red BSA for 30 min. The fluorescent signal of DQ Red BSA resulting from autolysosomal proteolysis decreased with OSMI-1 or BADGP treatment, but was increased in cells treated with Earle's balanced salt solution (EBSS) (Figure 4.28, A).

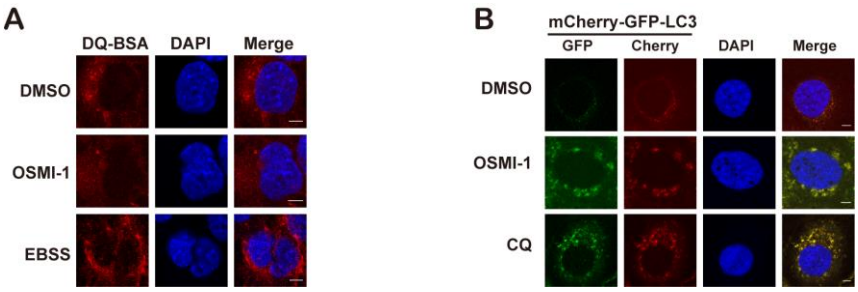

Figure 4.28 Inhibition of OGT by OSMI1 suppresses autophagic degradation

(A) HepG2.2.15 cells were treated with 10 μM OSMI-1, and harvested after 48 h. Then, cells were incubated with 10 mg/ml DQ Red BSA for 30 min. The accumulating fluorescent signal of DQ Red BSA was analyzed by confocal microscopy. Cells treated with Earle's balanced salt solution (EBSS) for 2 h were used as a positive control. (B) Huh7 cells were transfected with mCherry-GFP-LC3 plasmid. 6 h post transfection, cells were treated with 10 μM OSMI-1. Cells cultured with 10 μM CQ for 24 h were used as positive controls. The expression of mCherry and GFP was imaged by confocal microscopy. Scale bars, 5 μm.

To strengthen the evidence that inhibition of OGT by OSMI-1 influences autophagic degradation, Huh7 cells were transfected with a plasmid expressing mCherry-GFP-LC3 and then treated with 10 μM OSMI-1 or 10 μM CQ for 48 h. CQ inhibits acidification of the lysosomal compartment and prevents degradation of the cargo in the lysosome. Like CQ treatment, OSMI-1 led to an accumulation of LC3 puncta with strong expression of both GFP and mCherry, indicating incomplete autophagy and reduced cargo degradation in autophagosomes (Figure 4.28, B). These results consistently demonstrated that OSMI-1 treatment increases the number of autophagosomes by blocking autophagic degradation.

It has been reported that there are two ways to block autophagy degradation, one is by changing the lysosomal proteolytic activity, and the other one is by inhibiting autophagosome-lysosomal fusion. Therefore, it is necessary to distinguish between these two ways of action. Firstly, we measured lysosomal enzyme activity by staining lysosomes with fluorescent dyes to determine changes in lysosomal function during autophagy. HepG2.2.15 cells were treated with 10 μM OSMI-1 for 48 h or EBSS for 2 h, and then stained with 100 nM LysoTracker Red for 1 h. There was no change in the fluorescence intensity of LysoTracker staining in cells treated with OSMI-1 (Figure 4.29), indicating that OSMI-1 has no effect on lysosomal enzyme activity.

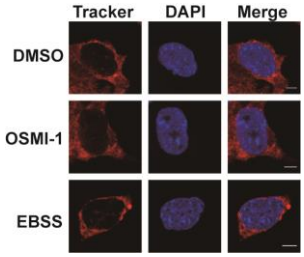

Figure 4.29 OSMI-1 has no effect on lysosomal enzyme activity in HepG2.2.15 cells

HepG2.2.15 cells were treated with 10 μM OSMI-1 for 24 h. The cells were stained with 100 nM LysoTracker Red for 1 h. Cells treated with EBSS for 2 h were used as a positive control. The fluorescence intensity of LysoTracker Red was analyzed by confocal microscopy. Scale bar, 5 μm.

Presumably, OSMI-1 treatment may block lysosomal degradation by preventing autophagosome-lysosomal fusion. The colocalization of LC3 and LAMP1 (lysosomal associated membrane protein 1), a lysosome marker, was analyzed by confocal microscopy. Co-localization of LC3 and LAMP1 was markedly decreased upon OSMI-1 treatment in HepG2.2.15 cells (Figure 4.30, A). It has been reported that there is a direct interaction between HBsAg and LC3, and thus the colocalization of HBsAg and LAMP1 was further analyzed by confocal microscopy in HepG2.2.15 cells. Colocalization of HBsAg and LAMP1 was decreased upon OSMI-1 treatment (Figure 4.30, B).

Collectively, these findings indicate that inhibition of OGT by OSMI-1 interfered with autophagosome-lysosome fusion and promoted HBV replication and HBsAg expression.

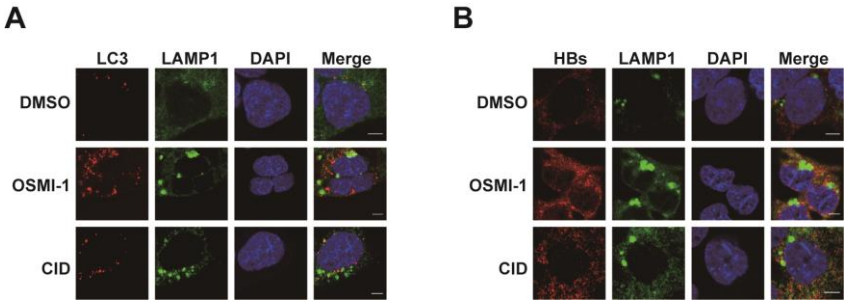

Figure 4.30 OSMI-1 suppresses autophagic degradation mediated by blocking the autophagosome-lysosomal fusion

HepG2.2.15 cells were treated with 10 μM OSMI-1 for 48 h. CID1067700 (CID) was used as a positive control. The cells were fixed, and perforated for 10 min. Then, the cells were incubated with rabbit anti-LAMP1 and mouse anti-LC3B (A) or horse anti-HBsAg (B) antibodies for 1 h, and stained with Alexa Fluor 488-conjugated anti-rabbit and Alexa Fluor 594-conjugated anti-mouse (A) or Alexa Fluor 594-conjugated anti-horse (B) secondary antibody IgG, respectively. Colocalization of LAMP1 and LC3 or HBsAg was imaged by confocal microscopy. Scale bar, 5 μm.

4.6.5 Silencing OGT enhances HBV replication via increasing autophagosome formation in hepatoma cells

To further determine the exact mechanism of OGT affecting HBV formation, we analyzed the effect of silencing OGT on the accumulation of LC3-II. We observed that silencing of OGT increased the number of LC3 puncta by immunofluorescence microscopy in Huh7 cells (Figure 4.31, A). Western blotting analysis of cellular lysates confirmed that silencing of OGT elevated the levels of autophagic cargo LC3-II and p62 by specific siOGT compared to the levels observed with siRNA control (Figure 4.31, B) in Huh7 cells. Similar to the findings in Huh7 cells, OGT silencing elevated the number of LC3 puncta and the levels of autophagic cargo LC3-II and p62 (Figure 4.32).

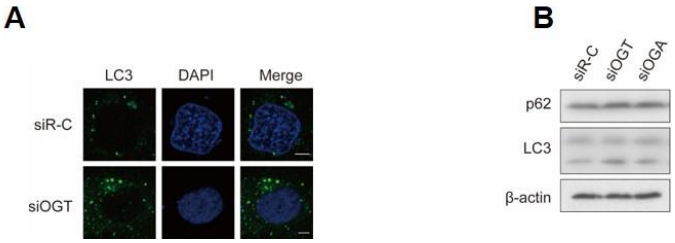

Figure 4.31 Silencing OGT increases autophagosome formation in Huh7 cells

(A) Huh7 cells were cotransfected with siOGT or siR-C and HBV expression plasmid pSM2, and harvested after 48 h. The cells were fixed, incubated with primary antibody rabbit anti-LC3B, followed by staining with Alexa Fluor 488-conjugated anti-rabbit secondary antibody IgG. Finally, the cells were imaged by a fluorescence microscope. Scale bar, 5 μm. (B) Huh7 cells were co-transfected with siOGT or siR-C and HBV expression plasmid pSM2, and harvested after 48 h. LC3 and p62 expression were analyzed by western blotting, and beta-actin was used as a loading control. *p<0.05; **p<0.01; ***p<0.001; ns, not significant.

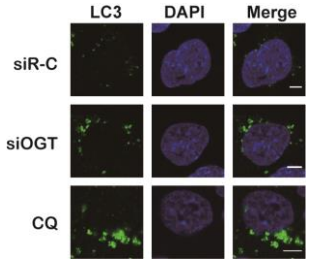

Figure 4.32 Silencing OGT increases autophagosome formation in HepG2.2.15 cells

(A) HepG2.2.15 cells were transfected with siOGT or siR-C, and harvested after 48 h. The cells were fixed, incubated with primary antibody rabbit anti-LC3B, followed by staining with Alexa Fluor 488-conjugated anti-rabbit secondary antibody IgG. Finally, the cells were imaged by a fluorescen microscope. Scale bar, 5 μm. (B) HepG2.2.15 cells were transfected with siOGT or siR-C, and harvested after 48 h. LC3 and p62 expression was analyzed by western blotting, and beta-actin was used as a loading control. *p<0.05; **p<0.01; ***p<0.001; ns, not significant.

To further confirm the involvement of autophagy in the regulation of HBV replication after silencing, the autophagy-related gene *ATG5* and *OGT* were co-silenced in HepG2.2.15 cells. After that, HBV replication, and HBsAg and HBeAg production were measured. ATG5 and OGT co-silencing decreased LC3-II levels compared to those in OGT silenced cells (Figure 4.33, A). Furthermore, HBV RIs, intracellular HBV DNA levels, and HBsAg levels in the culture supernatants were also decreased after silencing ATG5 (Figure 4.33, B). Similar to the findings in HepG2.2.15 cells, co-silencing ATG5 could block the promoting effect of silencing of OGT in transiently transfected Huh7 cells (Figure 4.34).

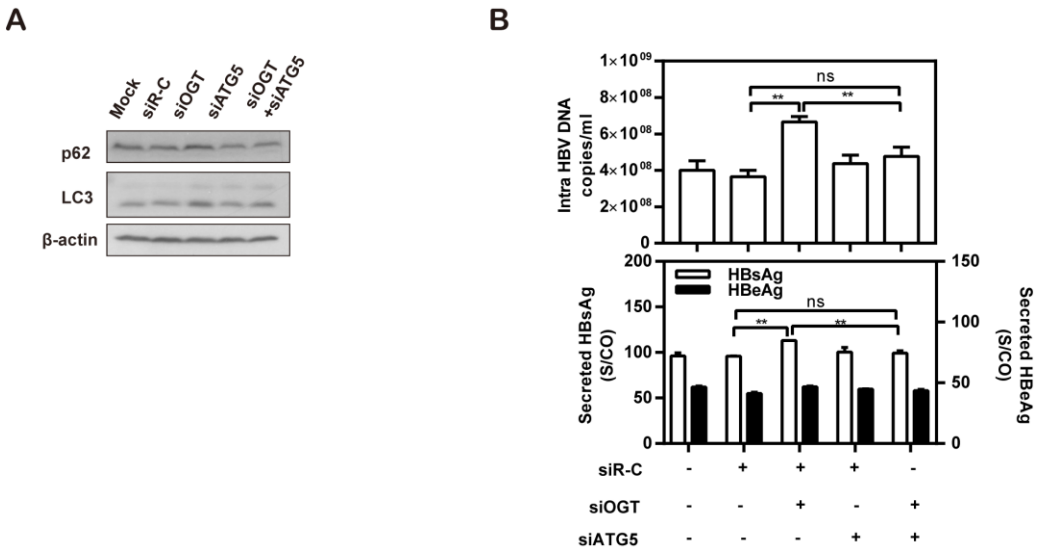

Figure 4.33 Co-silencing ATG5 and OGT block the promoting effect of OGT silencing in HepG2.2.15 cells

HepG2.2.15 cells were co-transfected with siATG5, siOGT or siR-C, and harvested after 72 h. (A) LC3 and p62 expression were analyzed by western blotting, and beta-actin was used as a loading control. (B) HBsAg and HBeAg levels in the culture supernatants were determined as described above. HBV RIs in cells were isolated and detected by Southern blotting. RC = relaxed circular DNA; S/CO = signal to cutoff ratio; SS = single stranded DNA. *p<0.05; **p<0.01; ***p<0.001; ns, not significant.

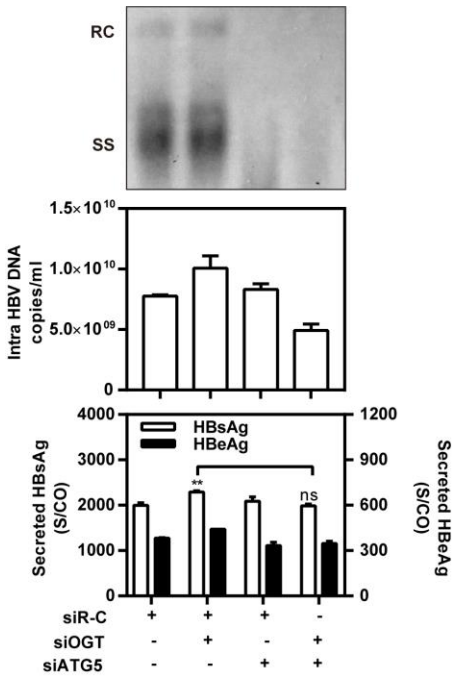

Figure 4.34 Co-silencing ATG5 and OGT block the promoting effect of OGT silencing in Huh7 cells

Huh7 cells were co-transfected with siATG5, siOGT or siR-C, and HBV expression plasmid pSM2, and harvested after 72 h. (A) LC3 and p62 expression were analyzed by western blotting, and beta-actin was used as a loading control. (B) The HBsAg and HBeAg levels in the culture supernatants were determined as described above. HBV RIs in cells were isolated and detected by Southern blotting. RC = relaxed circular DNA; S/CO = signal to cutoff ratio; SS = single stranded DNA. *p<0.05; **p<0.01; ***p<0.001; ns, not significant.

In summary, these data demonstrate that silencing of OGT promotes HBV production by increasing autophagosome formation.

4.6.6 Silencing OGT enhances HBV replication via decreasing autophagic degradation in hepatoma cells

Given the increase in the number of LC3 puncta and the level of p62 autophagy cargo, OGT silencing increases the number of autophagosomes likely via inhibiting autophagic degradation. To identify whether OGT silencing affects autophagic degradation, Huh7 cells were transfected with siOGT for 48 h, and then stained with DQ Red BSA for 30 min. The fluorescent signal of DQ Red BSA produced by autolysosomal proteolysis decreased with OGT silencing, but increased in positive cells treated with Earle Balanced Salt Solution (EBSS) (Figure 4.35, A). To strengthen the evidence that OGT silencing affects autophagic degradation, Huh7 cells were cotransfected with a plasmid expressing mCherry-GFP-LC3 and siOGT or siR-C for

48 h. OGT silencing led to an accumulation of LC3 puncta with strong expression of both GFP and mCherry, indicating incomplete autophagy and reduced cargo degradation in autophagosomes (Figure 4.35, B). These results consistently demonstrated that OGT silencing increases the number of autophagosomes via inhibiting autophagic degradation.

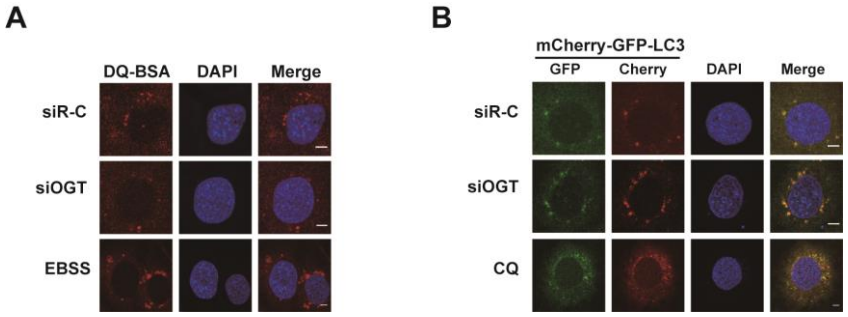

Figure 4.35 Silencing OGT decreases autophagic degradation in hepatoma cells

(A) Huh7 cells were cotransfected with mCherry-GFP-LC3 plasmid and siOGT or siR-C for 48 h, followed by incubation with 10 mg/ml DQ Red BSA for 30 min. The accumulating fluorescent signal of DQ Red BSA was analyzed by confocal microscopy. Cells treated with Earle's balanced salt solution (EBSS) for 2 h were used as a positive control. (B) Huh7 cells were cotransfected with mCherry-GFP-LC3 plasmid and siOGT or siR-C for 48 h. Cells cultured with 10 μM CQ for 24 h were used as positive controls. The expression of mCherry and GFP was imaged by confocal microscopy. Scale bars, 5 μm.

4.6.7 Inhibition of OGT promotes HBV replication via inhibiting the mTOR signaling pathway in hepatoma cells

To date, thousands of *O*-GlcNAcylated proteins with a wide range of functions have been identified, including kinases and phosphatases, most of which are also phosphoproteins[143]. In fact, *O*-GlcNAcylation and phosphorylation can modulate each other at the same or adjacent sites[144]. Previous studies have reported that the initiation of autophagy can be regulated by the Akt/mTOR signaling pathway[98, 126]. In the present study, we observed that OSMI-1 decreased the levels of phosphorylation of Akt (Ser473), which is required for Akt to activate its downstream targets, but did not affect the total levels of Akt (Figure 4.36, A). In addition, OSMI-1 decreased the expression of mTOR as well as its downstream kinase p70 S6K in HepG2.2.15 cells. However, OSMI-1 treatment significantly increased the phosphorylated levels of ULK1 on Ser 555 residues, which is important for triggering autophagy. This indicated that OSMI-1 may trigger autophagy and autophagosome formation through inhibiting mTORC1 signaling. Based on these findings, we suspect that OSMI-1 inhibits the

level of O-GlcNAc of Akt, which is required for Akt to activate its downstream targets. To confirm this hypothesis, HepG2.2.15 cells were treated with OSMI-1 for 24 h. The results of immunoprecipitation showed that Akt and mTOR were *O*-GlcNAcylation, and OSMI-1 reduced the level of *O*-GlcNAc of Akt and mTOR in hepatoma cells (Figure 4.36, B).

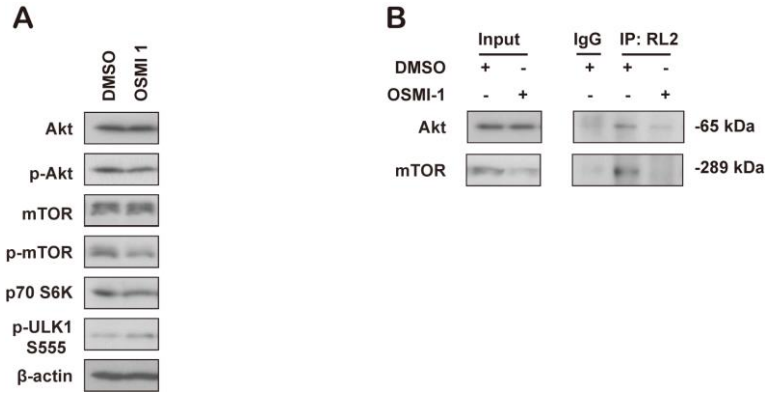

Figure 4.36 Inhibition of OGT inhibits mTOR signaling pathway by decreasing Akt/mTOR *O*-GlcNAcylation in hepatoma cells

(A) HepG2.2.15 cells were treated with 10 μM OSMI-1 for 48 h. Western blotting analysis was performed to detect the levels of total or phosphorylated AKT, mTOR, and p70 S6K. Beta-actin was used as a loading control. (B) HepG2.2.15 cells were treated with 10 μM OSMI-1 for 24 h. Immunoprecipitation was used to detect the levels of *O*-GlcNAcylation.

Based on the above findings, promoting HBV replication by OSMI-1 treatment could be dependent on autophagy induction by mTORC1-dependent signaling. To prove this hypothesis, HepG2.2.15 cells were treated with OSMI-1 with or without MHY1485 (a mTOR activator) for 72 h. The CMIA and real time PCR results revealed that MHY1485 suppressed HBsAg production and intracellular HBV DNA levels in OSMI-1-treated cells (Figure 4.37). These data indicate that OSMI-1 promotes HBV production by triggering autophagy signaling, leading to autophagosome formation.

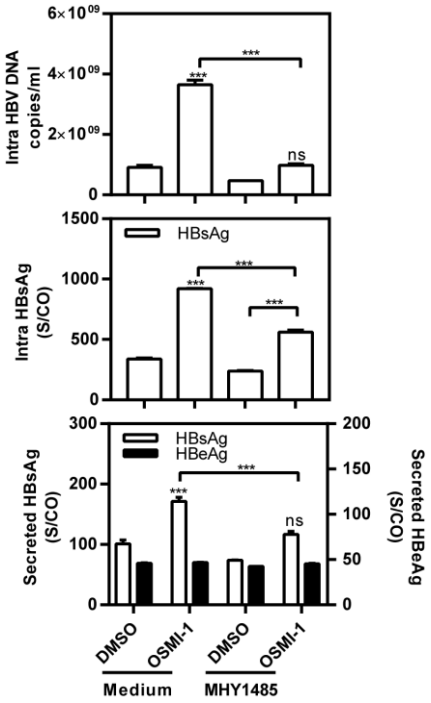

Figure 4.37 MHY1485 blocks the promoting HBV replication by OSMI-1 in HepG2.2.15 cells

HepG2.2.15 cells were treated with 10 μM OSMI-1 with or without the mTOR activator MHY1485 (1 μM) for 72 h. The levels of intracellular HBV DNA were determined by real-time PCR. The HBsAg and HBeAg secretion levels in the supernatants and those in the intracellular were determined as described above. *p <0.05; **p <0.01; ***p <0.001; ns, not significant.

In addition, promoting HBV replication by silencing OGT may also be dependent on triggering autophagy by mTOR1-dependent signaling. To confirm this conjecture, HepG2.2.15 cells were transfected with siOGT or siR-C, 6 h post transfection, followed by treatment with MHY1485 for 72 h. The levels of intracellular HBV DNA were prepared and analyzed by RT-PCR. We found that MHY1485 obviously suppressed intracellular HBV DNA levels in OGT silenced cells (Figure 4.38). The HBsAg and HBeAg in the supernatants were detected by CMIA. MHY1485 markedly inhibited HBsAg production in OGT silenced cells. Consistent with HepG2.2.15 cells, MH1485 also blocked the promoting effect on HBV replication by silencing OGT in Huh7 cells (Figure 4.39). In conclusion, promoting HBV replication by silencing OGT also relies on inducing autophagy by mTORC1-dependent signaling in HepG2.2.15 cells with stable HBV production.

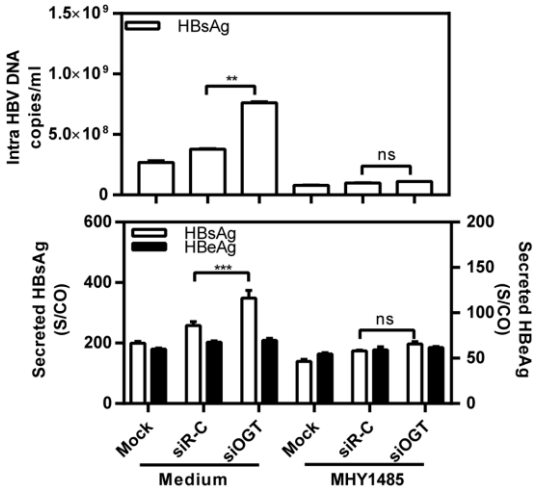

Figure 4.38 MHY1485 blocks the promoting HBV replication by silencing of OGT in HepG2.2.15 cells

HepG2.2.15 cells were transfected with siOGT or siR-C, and 6 h post-transfection, cells were treated with or without the mTOR activator MHY1485 (1 μM) for 72 h. The levels of intracellular HBV DNA were determined by real-time PCR. The HBsAg and HBeAg secretion levels in the supernatants were determined as described above. *p <0.05; **p <0.01; ***p <0.001; ns, not significant.

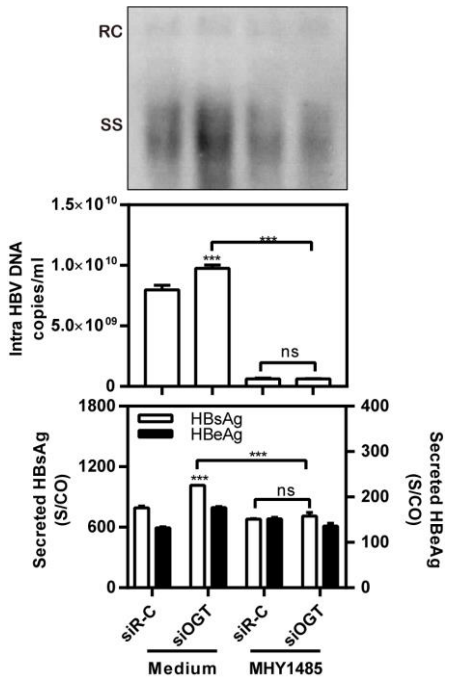

Figure 4.39 MHY1485 blocks the promoting effect on HBV replication by silencing of OGT in Hhu7 cells

Huh7 cells were transfected with siOGT or siR-C, 6 h post-transfection, treated with or without the mTOR activator MHY1485 (1 μM) for 72 h. Encapsidated HBV RIs were detected by Southern blotting. The levels of intracellular HBV DNA were determined by real-time PCR. The HBsAg and HBeAg secretion levels in the supernatants were determined as described above. S/CO = signal to cutoff ratio;

SS = single stranded DNA. *p <0.05; **p <0.01; ***p <0.001; ns, not significant.

4.7 Decreasing the levels of *N*-glycosylation by TM promotes HBV replication by suppressing autophagic degradation

4.7.1 Inhibition of *N*-glycosylation by TM promotes HBV replication

N-glycosylation, *N*-linked glycosylation, is the attachment of an oligosaccharide, a carbohydrate consisting of several sugar molecules to a nitrogen atom (the amide nitrogen of an asparagine (Asn) residue of a protein), which is catalyzed by *N*-acetylglucosamine transferases. Hepatitis B virus has three specific glycoproteins (L, M and S), derived from the alternating translation of the same ORF. All three glycoproteins share a common *N*-glycosylation site in the S domain, while M has an additional *N*-glycosylation site at its amino terminus[145, 146]. Changes in *N*-glycosylation are associated with different diseases, including rheumatoid arthritis, type 1 diabetes, and cancer[147-151]. However, the effect of altering *N*-linked glycosylation on HBV replication remains unknown. We addressed the question whether inhibition of *N*-glycosylation affects HBV replication. Tunicamycin (TM) is a *N*-glycosylation inhibitor, which blocks the formation of protein *N*-glycosidic linkages by inhibiting the transfer of *N*-acetylglucosamine 1-phosphate to dolichol monophosphate. To test the effect of inhibition of *N*-glycosylation on HBV replication, HepG2.2.15 cells were treated with tunicamycin (0.1, and 0.2 μM) for 72 h. The levels of intracellular and secreted HBsAg but not HBeAg, in the supernatants obviously increased after TM treatment in HepG2.2.15 cells (Figure 4.40, A). Consistently, TM led to higher levels of intracellular HBV DNA (Figure 4.40, B). These results suggest that TM positively regulated HBV production in HepG2.2.15 cells.

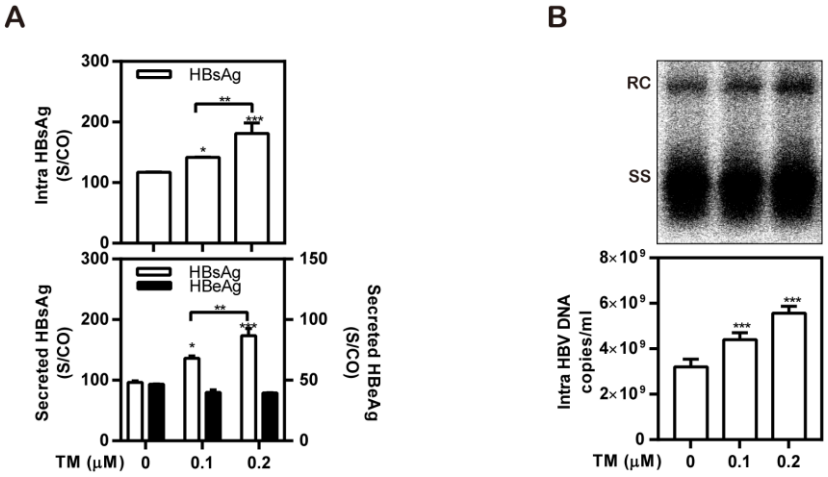

Figure 4.40 TM promotes HBV replication in HepG2.2.15 cells

HepG2.2.15 cells were treated with TM (0.1, and 0.2 μM) for 72 h. (A) The HBsAg and HBeAg levels in

the culture supernatants and intracellular HBsAg and HBeAg from cell lysates were quantified by CMIA. (B)The levels of intracellular HBV DNA were determined by real-time PCR. *p <0.05; **p <0.01; ***p <0.001; ns, not significant.

We examined the effects of TM on HBV production in other cell models, including primary human hepatoma cells infected with HBV virons (MOI=30) (Figure 4.41, A), and Huh7 cells transfected with HBV plasmids pSM2 (Figure 4.41, B). Consistently, TM significantly increased HBsAg, but not HBeAg production, in these cell models.

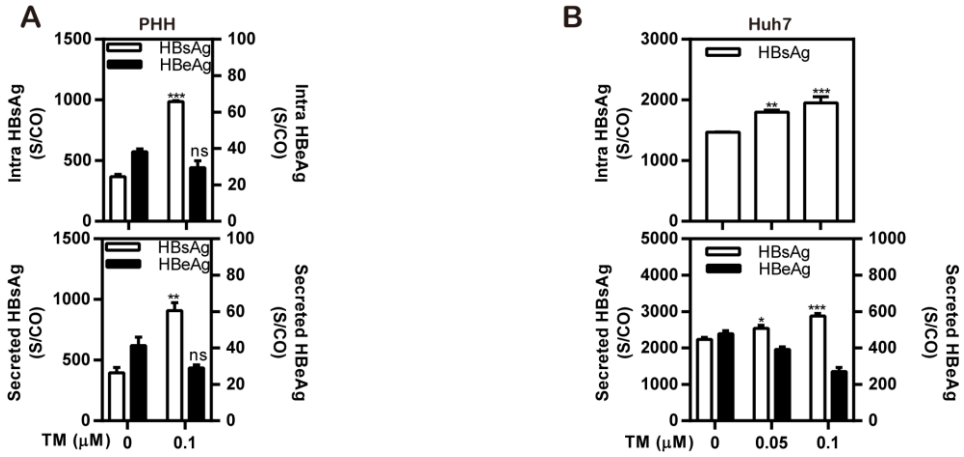

Figure 4.41 TM promotes HBV replication in other cell models

(A) PHHs were infected with HBV virions (multiplicity of infection (MOI)=30). 10 days post-infection, PHHs were treated with TM and harvested after 48 h. (B) Huh7 cells were transfected with pSM2 plasmid, and 6 h post-transfection, cells were treated with TM and harvested after 48 h. The levels of intracellular HBsAg and HBeAg and those in the culture supernatants were determined as described above. *p <0.05; **p <0.01; ***p <0.001; ns, not significant.

4.7.2 Inhibition of *N*-glycosylation by TM promotes HBV replication through increasing autophagosome formation

Next, we assumed that TM may modulate HBV replication by mimicking the mechanism of OSMI-1. *N*-glycosylation may have the same effect on cellular signaling pathways as *O*-GlcNAcylation. The levels of LC3 in HepG2.2.15 cells after treated with TM were measured using IF staining and western blotting analysis. The numbers of endogenous LC3-positive autophagic puncta (Figure 4.42, A), and the levels of LC3-II and p62 (Figure 4.42, B), were markedly increased after TM treatment, suggesting a stronger autophagosome formation after inhibition of *N*-glycosylation by TM.

To further confirm the role of autophagy in the regulation of HBV replication following

TM treatment, we treated the cells with TM and autophagy inhibitors, such as CQ and 3-MA. Then, intracellular HBV replication, and the HBsAg and HBeAg production in the supernatants were measured. CQ did not block the promoting effect of TM, while 3-MA obviously suppresses the promotion effect of TM, because the levels of intracellular and secreted HBsAg were significantly inhibited after treated with TM and 3-MA, (Figure 4.42, C). In summary, TM increases autophagosome formation, which is associated with enhanced HBV replication.

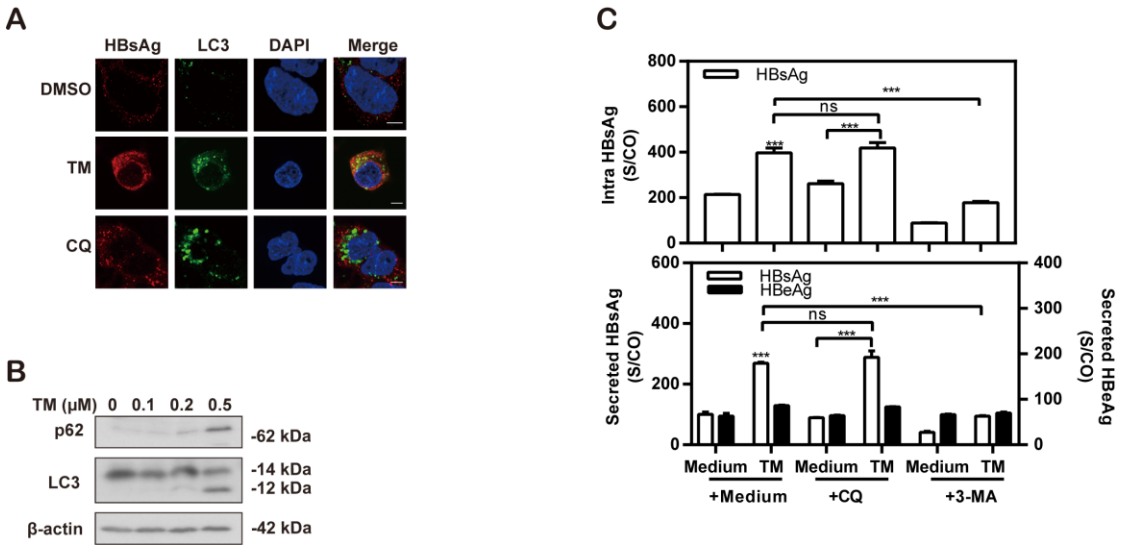

Figure 4.42 TM promotes HBV replication by increasing autophagosome formation in HepG2.2.15 cells

(A) HepG2.2.15 cells were treated with TM (0.2 μM) and harvested after 48 h. The cells were fixed, and incubated with a primary rabbit anti-LC3B and horse anti-HBsAg antibodies, and then stained with an Alexa Fluor 488-conjugated anti-rabbit and Alexa Fluor 594-conjugated anti-horse secondary antibody IgG, respectively. The distribution of LC3 was imaged by immunofluorescence microscopy. Scale bar, 5 μm. (B) HepG2.2.15 cells were treated with TM (0.2 μM) and harvested after 48 h. The LC3 and p62 expression levels were analyzed by western blotting, using beta-actin as a loading control. (C) HepG2.2.15 cells were treated with TM (0.2 μM), with or without CQ or 3-MA, and harvested after 48 h. The levels of intracellular HBsAg and HBeAg and those in the culture supernatants were determined as described above. *p <0.05; **p <0.01; ***p <0.001; ns, not significant.

4.7.3 Inhibition of *N*-glycosylation by TM promotes HBV replication by suppressing autophagic degradation

Since CQ did not further promote viral replication, and the number of LC3 puncta and the level of p62 autophagy cargo increased, inhibition of *N*-glycosylation appeared to increase the number of autophagosomes by blocking autophagy degradation. Therefore, we suspected that TM can inhibit autophagic degradation. To assess

whether TM decreases autophagic degradation, HepG2.2.15 cells were treated with TM for 48 h, and then incubated with DQ Red BSA for 30 min. The fluorescent signal of DQ Red BSA resulting from autolysosomal proteolysis decreased with TM treatment, but increased in cells treated with Earle's balanced salt solution (EBSS) (Figure 4.43, A).

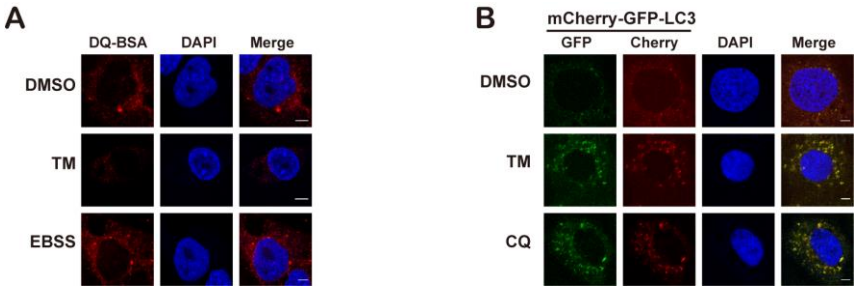

Figure 4.43 TM suppresses autophagic degradation in HepG2.2.15 cells

(A) HepG2.2.15 cells were treated with 0.2 μM TM, and harvested after 48 h. Then, the cells were incubated with 10 mg/ml DQ Red BSA for 30 min. The accumulating fluorescent signal of DQ Red BSA was analyzed by confocal microscopy. Cells treated with Earle's balanced salt solution (EBSS) for 2 h were used as a positive control. (B) Huh7 cells were transfected with mCherry-GFP-LC3 plasmid. 6 h post transfection, cells were treated with 0.2 μM TM. Cells cultured with 10 μM CQ for 24 h were used as positive controls. The expression of mCherry and GFP was imaged by confocal microscopy. Scale bars, 5 μm.

To further investigate how TM blocks autophagic degradation, Huh7 cells were transfected with a plasmid expressing mCherry-GFP-LC3 and then treated with 0.2 μM TM or 10 μM CQ for 48 h. CQ inhibits acidification of the lysosomal compartment and prevents degradation of the cargo in the lysosome. Like CQ treatment, TM led to an accumulation of LC3 puncta with strong expression of both GFP and mCherry, indicating incomplete autophagy and reduced cargo degradation in autophagosomes (Figure 4.43, B). These results consistently demonstrated that TM treatment increases the number of autophagosomes by blocking autophagic degradation, consistent with the results obtained after OSMI-1 treatment.

Then, we tested which pathways were changed to prevent autophagy degradation, either to alter lysosomal proteolytic activity or to inhibit autophagosome-lysosomal fusion. Firstly, we measured lysosomal enzyme activity by staining lysosomes with fluorescent dyes to determine changes in lysosomal function during autophagy. HepG2.2.15 cells were treated with 0.2 μM TM for 48 h or EBSS for 2 h, and then stained with 100 nM LysoTracker Red for 1 h. There was no change in the

fluorescence intensity of LysoTracker staining in cells treated with TM (Figure 4.44), indicating that TM has no effect on lysosomal enzyme activity.

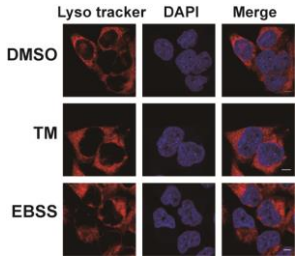

Figure 4.44 TM has no effect on lysosomal enzyme activity in HepG2.2.15 cells

HepG2.2.15 cells were treated with 5 mM TM for 24 h. The cells were stained with 100 nM LysoTracker Red for 1 h. Cells treated with EBSS for 2 h were used as a positive control. The fluorescence intensity of LysoTracker Red was analyzed by confocal microscopy. Scale bar, 5 μm.

After that, we suggested that TM treatment may block lysosomal degradation by preventing autophagosome-lysosomal fusion. To confirm this idea, the colocalization of LC3 and LAMP1 (lysosomal associated membrane protein 1), a lysosome marker, was analyzed by confocal microscopy. Co-localization of LC3 and LAMP1 was markedly decreased upon TM treatment in HepG2.2.15 cells (Figure 4.45, A). Consistently, colocalization of HBsAg and LAMP1 was also decreased after TM treatment (Figure 4.45, B).

Collectively, these findings indicate that TM interfered with autophagosome-lysosome fusion and promoted HBV replication and HBsAg expression.

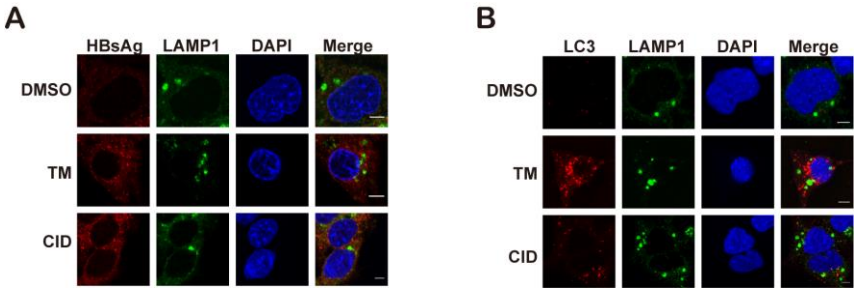

Figure 4.45 TM suppresses autophagic degradation mediated by blocking the autophagosome-lysosomal fusion

HepG2.2.15 cells were treated with 0.2 μM TM for 48 h. CID1067700 (CID) was used as a positive control. The cells were fixed, and perforated for 10 min. Then, the cells were incubated with rabbit anti-LAMP1 and mouse anti-LC3B (A) or horse anti-HBsAg (B) antibodies for 1 h, and stained with Alexa Fluor 488-conjugated anti-rabbit and Alexa Fluor 594-conjugated anti-mouse (A) or Alexa Fluor 594-conjugated anti-horse (B) secondary antibody IgG, respectively. Colocalization of LAMP1 and LC3 or HBsAg was imaged by confocal microscopy. Scale bar, 5 μm.

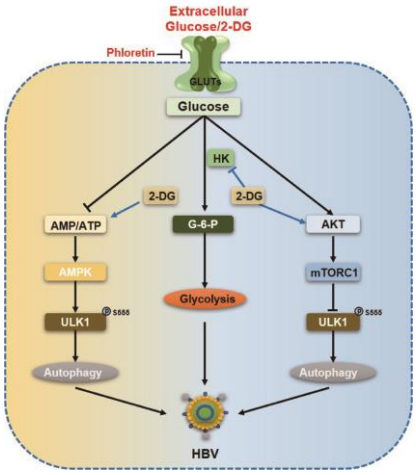

Figure 4.46 A model of regulation of HBV replication by glucose and 2-DG

Glucose and 2-DG are transported into the cell through GLUTs. After entry, low glucose concentration increases the AMPK activity to induce autophagy, thereby promoting HBV replication. In concordance, GLUTs inhibition by phloretin also induces HBV replication through upregulating AMPK-mTOR-ULK1-induced autophagy. However, 2-DG inhibits HBV replication via inhibiting glycolysis and upregulating the Akt/mTOR signaling pathway.

5. Discussion

In the present study, we found that the different glucose concentration supply in the medium were able to regulate HBV replication in hepatoma cells. Low glucose concentration obviously activates the AMPK activity, but inactivates the Akt/mTOR activity, thereby inducing autophagy to promote HBV replication. When autophagy-related gene ATG5 was silenced, HBsAg levels in culture supernatants, intracellular HBV DNA levels and HBV RIs were decreased at the different glucose concentrations. Blocking the activity of Akt or mTOR by small chemical inhibitors obviously abolished the decreasing effect of the low glucose concentration on HBV replication. Furthermore, inhibition of GLUTs by phloretin also enhances HBV replication, upregulates AMPK/mTOR-ULK1-autophagy, and increases glycolysis. Interestingly, 2-DG inhibits HBV progeny secretion and replication through inhibiting glycolysis and activating Akt/mTOR signaling pathway. Based on these data, we conclude that the low glucose concentrations enhanced HBV replication via increasing the autophagosome formation.

5.1 Low glucose concentration promotes HBV replication through upregulating AMPK-, Akt/mTOR-ULK1 induced autophagy

Viruses depend on the supply of energy and building blocks for their replication[152, 153]. Indeed, various metabolic pathways are essential for efficient viral replication. Here, we found that HBV replication was significantly influenced by the glucose concentration in the medium and by glucose uptake via GLUTs at the step of transcription and via AMPK-Akt/mTOR-ULK1-induced autophagy. However, its analogue 2-DG suppressed HBV replication by inhibiting the glycolytic pathway and activating the Akt/mTOR signaling pathway despite the increased AMPK and autophagic activity (Figure 4.46).

Defining the cellular metabolic processes related to viral infection may reveal new therapeutic targets and contribute to the development of safe and effective therapies against viral infections[154]. HBV is thought to be a “metabolovirus”[155] and its transcription is largely dependent on hepatic metabolic controls[156, 157] and cellular transcription factors[158-160]. Previous studies in HBV transgenic mice have illustrated, for example, that fasting decreases glucose levels but increases HBeAg synthesis in serum. PGC1α transcripts are induced by fasting in HBV transgenic mice[161]. In this study, the expression of transcription factors, including PGC1α, CREB, and ChREBP,

was found to be altered by these indicated glucose concentrations in the cell cultures and correlated with changes in the HBV RNAs levels. This is consistent with previous studies regarding to the importance of HBV transcriptional control. HBV transcriptional activity is regulated by HBV promoters and two additional enhancers and the abundance of specific hepatic transcription factors. The expression of relevant transcription factors is inversely determined by glucose concentrations and correlated to the steady state levels of HBV RNAs. However, the posttranscriptional control of HBV replication at the steps of assembly, release, and degradation by autophagy has emerged as relevant and effective mechanisms that require attention in future studies on the HBV life cycle. In a number of studies, the production of HBeAg has been considered as a marker of HBV replication. However, autophagy significantly promotes HBsAg and virion production but not HBeAg production, as shown in several early studies[120, 126, 162]. HBeAg production occurs in the ER-Golgi compartment and does not have a connection with autophagy. In this study, HBsAg but not HBeAg production was significantly regulated by glucose concentrations, again consistent with the major role of autophagy under these conditions.

Data from other studies demonstrated that autophagy is an essential part of host defense against infections by pathogens such as Sindbis virus[107, 108]. By contrast, other viruses, including HBV, can induce autophagy processes to enhance their own replication[114, 115]. HBV induces early stages of autophagy pathways in hepatocytes[71, 116, 117]. However, the late stages of autophagy (e.g., autophagic degradation) could degrade HBV virions and HBsAg but may be inhibited by HBx protein[120, 121]. In this study, we found that AMPK, a key player in energy homeostasis, induces autophagy under conditions of reduced nutrient supply[163, 164]. AMPK stimulation is reported to inactivate mTOR by AMPK-mediated phosphorylation of both TSC2 and Raptor. ULK1 can subsequently interact with and be phosphorylated by AMPK to initiate autophagy[96, 133, 165, 166]. Consistent with this notion, AMPK activation occurred at low glucose concentration and in the presence of the GLUT inhibitor phloretin, along with inhibited mTOR activity, ULK1 phosphorylation, and autophagy induction. Taken together, our results reveal a novel regulatory mechanism by which glucose supply regulates HBV replication.

Glucose is an essential nutrient and energy source in living organisms. Maintaining energy homeostasis is very important in mammalian physiology. Glycolysis is considered as a “central” carbon metabolic pathway because it is the backbone of

several metabolic pathways and is pivotal for energy homeostasis[4, 5, 26]. Herein, HBV replication decreased after 2-DG treatment in HepG2.2.15 cells. This observation highlights the notion that HBV replication requires glycolysis in host cells. Treatment with 2-DG induced AMPK and Akt/mTOR activation, two processes that may regulate HBV replication in opposite ways. Activation of the Akt/mTOR signaling pathway negatively regulates HBV replication[131, 167, 168] and blocks glycolysis through the regulation of GLUT transport[169], while AMPK acts through downstream autophagic pathway to regulate HBV replication. Treatment with 2-DG strongly inhibited HBV replication, but promoted autophagy (Figure 4.17-Figure 4.21). We assume that other pathways in the downstream of AMPK and Akt/mTOR are also involved in regulation of HBV replication. Previously, we tested several mTOR-related pathways and found that SREBP1 was also partly activated to regulate HBV replication[126]. Therefore, a detailed analysis is needed to completely dissect the functions of different pathways and their relative contributions to the control of HBV replication. On the other hand, 2-DG may markedly inhibit glycolysis that is essential for viral replication[170-172]. Our results in this study did not support the role of reduced nutrient supply in HBV suppression as the cellular protein synthesis was not affected by 2-DG. However, these questions remain to be answered in future studies.

5.2 Decreasing the levels of *O*-GlcNAcylation promotes HBV replication by suppressing autophagic degradation and inhibiting mTOR signaling

Post-translational *O*-GlcNAcylation of OGT plays an important role in the regulation of intracellular signaling by altering the activity, stability and localization of *O*-GlcNAc-modified proteins[11]. *O*-GlcNAcylation is one of the most abundant post-translational modifications, which is similar to the phosphorylation, in mammalian cells, with more than 30% of human proteins being modified with *O*-GlcNAc group[173]. *O*-GlcNAcylation is a key regulator of the temporal dynamics of various cellular signaling pathways. Thousands of *O*-GlcNAcylated proteins have been identified, including kinases and phosphatases[143]. In fact, *O*-GlcNAcylation and phosphorylation can modulate each other at the same or adjacent sites[144]. In the present study, we found that Akt and mTOR were *O*-GlcNAcylation. Inhibiting *O*-GlcNAcylation by OSMI-1 markedly decreased the levels of *O*-GlcNAcylation for Akt and mTOR, and also inhibited the activity of Akt and mTOR, suggesting that *O*-GlcNAcylation of Akt and mTOR and their phosphorylation modulate each other. In addition to the many

O-GlcNAcylated cellular proteins, OGT-modified residues have been found on proteins from several human viruses. This is not surprising since many viruses typically utilize cellular post-translational modifications like phosphorylation and ubiquitination to alter cellular pathways or to modify the activity of viral protein activity. However, little is known about the role of *O*-GlcNAcylation in viral infection, and the biological effect of this modification on viruses is unclear. Previous reports have shown that *O*-GlcNAcylation promotes replication of Herpes Simplex Virus and Human Cytomegalovirus[174], suggesting that *O*-GlcNAcylation can positively regulate viral replication. However, in this study, we demonstrated that inhibition of OGT's glycosyltransferase activity with a small molecule inhibitor OSMI-1 or silencing of OGT with a small interfering RNA notably increased HBV replication and autophagosome formation, but inhibited autophagic degradation. In addition, silencing of OGA with a small interfering RNA slightly decreased HBV replication.

Previous studies have demonstrated the essential role of autophagy initiation for efficient HBV replication[71, 126, 162]. However, our results also suggest that autophagic degradation plays a significant role in HBV replication. In this study, we provide evidence that inhibition of *O*-GlcNAcylation plays an essential role not only in initial HBV replication but also in the autophagic degradation of HBV virions and HBsAg. Inhibition of *O*-GlcNAcylation blocked autophagic degradation of HBV virions and proteins by inhibiting mTORC1 signaling and autophagosome-lysosomal fusion, followed by promotion of HBV replication. Thus, inhibition of *O*-GlcNAcylation can modulate autophagy in hepatocytes in a dual way. The mechanism by which Akt/mTOR regulates the initiation of autophagy is very clear, but the mechanism by which *O*-GlcNAcylation inhibits autophagy degradation remains to be further elucidated. Previous studies have revealed that *O*-GlcNAcylation of SNAP-29 reduced formation of the Stx17-SNAP-29-VAMP8 SNARE complex, blocking the autophagosome-lysosomal fusion[175]. Therefore, we hypothesized that some proteins that regulate autophagosome-lysosomal fusion reduce O-GlcNAc levels by inhibiting OGT, leading to autophagosome-lysosomal fusion blockade, thereby promoting HBV replication.

Small chemical molecule that modulates protein activity are useful tools for studying protein function. It selectively inhibits >80% of OGT's activity in vitro and has high cell permeability, allowing us to efficiently probe the function of OGT in the context of HBV infection. Treatment with OSMI-1 significantly increased replication of HBV in

HepG2.2.15 cells and PHHs. Consistently, silencing of OGT obviously increased replication of HBV in HepG2.2.15 and Huh7 cells. On the other hand, silencing of OGA slightly decreased HBV replication. These data suggest that inhibition of *O*-GlcNAcylation plays a positive role in HBV replication.

Some studies have shown that *O*-GlcNAcylation is an important modification that regulates the viral replication cycles. *O*-GlcNAc modification has been found on many viral proteins, including HBV surface proteins[176], HCMV UL32 tegument protein[177], adenovirus fiber protein[178], baculovirus tegument protein gp41[179], rotavirus NS26 protein[180], and several KSHV proteins involved in DNA replication[181, 182]. A few studies have suggested that high *O*-GlcNAc levels have an inhibitory effect on viral replication. Increased *O*-GlcNAcylation of the cellular protein Sp1, a key transcription factor for HIV-1 gene expression, has been shown to inhibit transcription of the HIV-1 long terminal repeat (LTR) promoter[183]. Furthermore, increased *O*-GlcNAcylation by overexpression of OGT reduces KSHV replication[182]. In addition, increased *O*-GlcNAcylation of the KSHV major transcriptional activator (RTA) reduced its ability to transactivate viral genes[181]. Unlike the positive effect of *O*-GlcNAc modification for SHV and HCMV, we demonstrated that inhibition of OGT is needed for the efficient replication of HBV, as the OGT inhibitor OSMI-1 significantly increased HBV replication. The results from this study demonstrated that OGT is involved in the HBV replication cycle. In summary, the results described here implicate *O*-GlcNAcylation as a novel factor involved in HBV replication, and further studies are needed to define its precise role in the viral cycle.

5.3 Decreasing the levels of *N*-glycosylation by TM promotes HBV replication by suppressing autophagic degradation

N-glycosylation, is the attachment of an oligosaccharide, a carbohydrate consisting of several sugar molecules, sometimes also referred to as glycan, to a nitrogen atom (the amide nitrogen of an asparagine (Asn) residue of a protein). This type of linkage is important for both the structure and function of some eukaryotic proteins[184, 185]. The data obtained with TM suggest the importance of *N*-glycosylation for the HBV replication. Using TM to inhibit the levels of *N*-glycosylation could promote autophagosome formation and inhibit autophagosome-lysosome fusion, thereby increasing HBV production and replication. Previous studies showed that inhibition of *N*-glycosylation could induce ER stress, thereby trigger autophagy pathway. As

mentioned before, autophagy plays an essential role in HBV replication. However, our data also show that a large proportion of HBsAg and HBV DNA capsids and virions are not degraded after TM treatment. In the present study, we provide evidence that *N*-glycosylation plays a key role in the autophagic degradation of HBV virions and HBsAg. Previous studies have reported the important role of Rab7 and SNAP29 in HBV degradation by autophagy[120, 162]. CQ is known to prevent autophagosome maturation and degradation of autophagic cargo by altering the pH of lysosomes. However, inhibition of *N*-glycosylation by TM led to blockade of autophagosome-lysosome fusion without altering lysosomal acidification. Thus, both CQ and TM treatment in hepatoma cells resulted in enhanced HBV replication and HBsAg production by reducing lysosomal degradation. However, these treatments were very effective individually, and therefore, their synergistic effects, if any existed, were no strong. As previously reported, the mechanism may be that inhibition of *N*-glycosylation increases the formation of autophagosomes by inhibiting autophagosome-lysosomal fusion. It is possible that *N*-glycosylation of proteins involved in autophagosome-lysosomal fusion. However, the detailed function of *N*-glycosylation in autophagosome-lysosomal fusion remains to be studied in the future.

6. Summary

In the present study, we investigated the influence of glucose on HBV replication. We found that increasing glucose concentration could markedly decrease HBV replication, progeny secretion and antigen expression in hepatoma cells and primary hepatocytes. However, the indicated glucose concentrations showed a slight effect on modulating HBV transcription and HBV promoter activities, suggesting that they may regulate HBV replication through other mechanisms. Consistent with recent reports, we found that low glucose concentration could activate AMPK signaling pathway and inactivate Akt/mTOR signaling pathway in hepatoma cells. Moreover, the experimental data revealed that a low glucose concentration of 5 mM promoted the formation of autophagosomes through increasing the phosphorylation of ULK1 on Ser 555. These results imply that the low glucose concentration enhanced HBV replication through AMPK-, mTOR-ULK1 signaling induced autophagy flux. In addition, we further explored the effect of *O*-GlcNAcylation levels on HBV production. We found that HBV replication and HBsAg production were significantly increased by inhibition or silencing of OGT, with markedly increased autophagosome formation and a blockade of autophagic degradation. Similarly, inhibition of N-glycosylation by TM also promoted HBV replication and HBsAg production by blocking autophagic degradation. Thus, increasing autophagosome formation and blocking autophagic degradation are the processes leading to promotion of HBV production if the cellular glycosylation is disturbed.

Taken together, our results demonstrated that the different concentrations of glucose and inhibition the levels of *O*-GlcNAcylation promote HBV replication through Akt/mTOR-ULK1 signaling-induced autophagy. We provide new evidence that cellular glycosylation is required for autophagy degradation.

7. Zusammenfassung

In der vorliegenden Studie untersuchten wir den Einfluss von Glucose auf die HBV-Replikation. Wir fanden heraus, dass eine Erhöhung der Glucosekonzentration die HBV-Replikation, die Produktion der HBV Virions und die Antigenexpression in Hepatomzellen und primären Hepatozyten deutlich verringern kann. Diese verwendeten Glucose-Konzentrationen zeigten jedoch einen geringen Effekt auf die Modulation der HBV-Transkriptions- und HBV-Promotoraktivitäten, was darauf hindeutet, dass sie die HBV-Replikation durch andere Mechanismen regulieren können. In Übereinstimmung mit jüngsten Berichten fanden wir ferner, dass eine niedrige Glukose-Konzentration den AMPK-Signalweg aktiviert und den Akt/mTOR-Signalweg in Hepatomzellen inhibiert. Darüber hinaus zeigten die experimentellen Daten, dass die niedrige Glucose-Konzentration bei 5 mM die Bildung von Autophagosomen durch Erhöhen der Phosphorylierung von ULK1 auf Ser 555 förderte. Diese Ergebnisse impizieren, dass die niedrige Glucose-Konzentration die HBV-Replikation durch AMPK-, mTOR-ULK1-Signaltransduktion und Induktion der Autophagie erhöht. Darüber hinaus untersuchten wir den Effekt der *O*-Glykosylierung auf die HBV-Produktion. Wir fanden heraus, dass die HBV-Replikation und die HBsAg-Produktion durch die Hemmung der OGT signifikant erhöht wurden. Dabei nahm die Bildung von Autophagosomen deutlich zu, während die autophagische Degradation blockiert wurde. Darüber hinaus förderte die Hemmung der N-Glykosylierung durch Tunicamycin sowohl die HBV-Replikation als auch die HBsAg-Produktion, indem sie den autophagischen Abbau blockierte. Diese Daten zeigten, dass eine Erhöhung der Bildung von Autophagosomen und ein Blockieren des autophagischen Abbaus die HBV-Produktion fördern.

Zusammengenommen zeigten unsere Ergebnisse, dass die unterschiedliche Konzentrationen von Glucose und die Hemmung der *O*-Glykosylierung die HBV-Replikation durch Akt/mTOR-ULK1-signalinduzierte Autophagie verstärken. Wir bringen auch den Nachweis dafür, dass die zelluläre Glykosylisierung für den Abbauprozess der Autophagie erforderlich ist.

8. References

1. Hay N. Reprogramming glucose metabolism in cancer: can it be exploited for cancer therapy? Nature reviews Cancer 2016; 16:635-49.
2. Jones W, Bianchi K. Aerobic glycolysis: beyond proliferation. Frontiers in immunology 2015; 6:227.
3. Yang W, Lu Z. Regulation and function of pyruvate kinase M2 in cancer. Cancer letters 2013; 339:153-8.
4. Akram M. Citric acid cycle and role of its intermediates in metabolism. Cell biochemistry and biophysics 2014; 68:475-8.
5. Kornberg H. Krebs and his trinity of cycles. Nature reviews Molecular cell biology 2000; 1:225-8.
6. Lane AN, Fan TW. Regulation of mammalian nucleotide metabolism and biosynthesis. Nucleic acids research 2015; 43:2466-85.
7. Bonkovsky HL, Guo JT, Hou W, Li T, Narang T, Thapar M. Porphyrin and heme metabolism and the porphyrias. Comprehensive Physiology 2013; 3:365-401.
8. Buchakjian MR, Kornbluth S. The engine driving the ship: metabolic steering of cell proliferation and death. Nature reviews Molecular cell biology 2010; 11:715-27.
9. Patra KC, Hay N. The pentose phosphate pathway and cancer. Trends in biochemical sciences 2014; 39:347-54.
10. Buse MG. Hexosamines, insulin resistance, and the complications of diabetes: current status. American journal of physiology Endocrinology and metabolism 2006; 290:E1-E8.
11. Hart GW, Housley MP, Slawson C. Cycling of O-linked beta-N-acetylglucosamine on nucleocytoplasmic proteins. Nature 2007; 446:1017-22.
12. Love DC, Hanover JA. The hexosamine signaling pathway: deciphering the "O-GlcNAc code". Science's STKE : signal transduction knowledge environment 2005; 2005:re13.
13. Issad T, Kuo M. O-GlcNAc modification of transcription factors, glucose sensing and glucotoxicity. Trends in endocrinology and metabolism: TEM 2008; 19:380-9.
14. Zeidan Q, Hart GW. The intersections between O-GlcNAcylation and phosphorylation: implications for multiple signaling pathways. Journal of cell science 2010; 123:13-22.
15. Ozcan S, Andrali SS, Cantrell JE. Modulation of transcription factor function by O-GlcNAc modification. Biochimica et biophysica acta 2010; 1799:353-64.

16. Gonzalez GA, Montminy MR. Cyclic AMP stimulates somatostatin gene transcription by phosphorylation of CREB at serine 133. Cell 1989; 59:675-80.
17. Goodman RH, Smolik S. CBP/p300 in cell growth, transformation, and development. Genes & development 2000; 14:1553-77.
18. Parker D, Ferreri K, Nakajima T, LaMorte VJ, Evans R, Koerber SC, et al. Phosphorylation of CREB at Ser-133 induces complex formation with CREB-binding protein via a direct mechanism. Molecular and cellular biology 1996; 16:694-703.
19. Asahara H, Santoso B, Guzman E, Du K, Cole PA, Davidson I, et al. Chromatin-dependent cooperativity between constitutive and inducible activation domains in CREB. Molecular and cellular biology 2001; 21:7892-900.
20. Michael LF, Asahara H, Shulman AI, Kraus WL, Montminy M. The phosphorylation status of a cyclic AMP-responsive activator is modulated via a chromatin-dependent mechanism. Molecular and cellular biology 2000; 20:1596-603.
21. Herzig S, Long F, Jhala US, Hedrick S, Quinn R, Bauer A, et al. CREB regulates hepatic gluconeogenesis through the coactivator PGC-1. Nature 2001; 413:179-83.
22. Uebi T, Tamura M, Horike N, Hashimoto YK, Takemori H. Phosphorylation of the CREB-specific coactivator TORC2 at Ser(307) regulates its intracellular localization in COS-7 cells and in the mouse liver. American journal of physiology Endocrinology and metabolism 2010; 299:E413-25.
23. Dentin R, Hedrick S, Xie J, Yates J, 3rd, Montminy M. Hepatic glucose sensing via the CREB coactivator CRTC2. Science 2008; 319:1402-5.
24. Housley MP, Udeshi ND, Rodgers JT, Shabanowitz J, Puigserver P, Hunt DF, et al. A PGC-1alpha-O-GlcNAc transferase complex regulates FoxO transcription factor activity in response to glucose. The Journal of biological chemistry 2009; 284:5148-57.
25. Li MD, Ruan HB, Singh JP, Zhao L, Zhao T, Azarhoush S, et al. O-GlcNAc transferase is involved in glucocorticoid receptor-mediated transrepression. The Journal of biological chemistry 2012; 287:12904-12.
26. Dashty M. A quick look at biochemistry: carbohydrate metabolism. Clinical biochemistry 2013; 46:1339-52.
27. Klover PJ, Mooney RA. Hepatocytes: critical for glucose homeostasis. The international journal of biochemistry & cell biology 2004; 36:753-8.
28. Li H, Zhu W, Zhang L, Lei H, Wu X, Guo L, et al. The metabolic responses to hepatitis B virus infection shed new light on pathogenesis and targets for treatment.

Scientific reports 2015; 5:8421.
29. Nguyen P, Leray V, Diez M, Serisier S, Le Bloc'h J, Siliart B, et al. Liver lipid metabolism. Journal of animal physiology and animal nutrition 2008; 92:272-83.
30. Chiang JY. Bile acids: regulation of synthesis. Journal of lipid research 2009; 50:1955-66.
31. Yan H, Peng B, Liu Y, Xu G, He W, Ren B, et al. Viral entry of hepatitis B and D viruses and bile salts transportation share common molecular determinants on sodium taurocholate cotransporting polypeptide. Journal of virology 2014; 88:3273-84.
32. Geier A. Hepatitis B virus: the "metabolovirus" highjacks cholesterol and bile acid metabolism. Hepatology 2014; 60:1458-60.
33. Patman G. Hepatitis: HBV infection alters bile acid metabolism gene profile. Nature reviews Gastroenterology & hepatology 2014; 11:332.
34. Zheng G, Fu Y, He C. Nucleic acid oxidation in DNA damage repair and epigenetics. Chemical reviews 2014; 114:4602-20.
35. Na TY, Ka NL, Rhee H, Kyeong D, Kim MH, Seong JK, et al. Interaction of hepatitis B virus X protein with PARP1 results in inhibition of DNA repair in hepatocellular carcinoma. Oncogene 2016; 35:5435-45.
36. Liang TJ. Hepatitis B: the virus and disease. Hepatology 2009; 49:S13-21.
37. Gish RG, Given BD, Lai CL, Locarnini SA, Lau JY, Lewis DL, et al. Chronic hepatitis B: Virology, natural history, current management and a glimpse at future opportunities. Antiviral research 2015; 121:47-58.
38. Tong S, Revill P. Overview of hepatitis B viral replication and genetic variability. Journal of hepatology 2016; 64:S4-S16.
39. Glebe D, Bremer CM. The molecular virology of hepatitis B virus. Seminars in liver disease 2013; 33:103-12.
40. Tong S, Revill P. Overview of hepatitis B viral replication and genetic variability. Journal of hepatology 2016; 64:S4-16.
41. Yan H, Zhong G, Xu G, He W, Jing Z, Gao Z, et al. Sodium taurocholate cotransporting polypeptide is a functional receptor for human hepatitis B and D virus. Elife 2012; 3.
42. Ni Y, Lempp FA, Mehrle S, Nkongolo S, Kaufman C, Falth M, et al. Hepatitis B and D viruses exploit sodium taurocholate co-transporting polypeptide for species-specific entry into hepatocytes. Gastroenterology 2014; 146:1070-83.

43. McMahon BJ. The Natural History of Chronic Hepatitis B Virus Infection. Hepatology 2009; 49:S45-S55.
44. Urban S, Schulze A, Dandri M, Petersen J. The replication cycle of hepatitis B virus. Journal of hepatology 2010; 52:282-4.
45. Nassal M. HBV cccDNA: viral persistence reservoir and key obstacle for a cure of chronic hepatitis B. Gut 2015; 64:1972-84.
46. Decorsiere A, Mueller H, van Breugel PC, Abdul F, Gerossier L, Beran RK, et al. Hepatitis B virus X protein identifies the Smc5/6 complex as a host restriction factor. Nature 2016; 531:386-9.
47. Nassal M. Hepatitis B viruses: reverse transcription a different way. Virus Res 2008; 134:235-49.
48. Lucifora FZJ. The life cycle of hepatitis B virus and antiviral targets. Future Virology 2011; 6:599-614.
49. Beck J, Nassal M. Hepatitis B virus replication. World J Gastroenterol 2007; 13:48-64.
50. Bruss V. Hepatitis B virus morphogenesis. World J Gastroenterol 2007; 13:65-73.
51. Guidotti LG, Chisari FV. Immunobiology and pathogenesis of viral hepatitis. Annu Rev Pathol 2006; 1:23-61.
52. Prange R. Host factors involved in hepatitis B virus maturation, assembly, and egress. Med Microbiol Immun 2012; 201:449-61.
53. Ma SW, Huang X, Li YY, Tang LB, Sun XF, Jiang XT, et al. High serum IL-21 levels after 12 weeks of antiviral therapy predict HBeAg seroconversion in chronic hepatitis B. Journal of hepatology 2012; 56:775-81.
54. Schoggins JW, Rice CM. Interferon-stimulated genes and their antiviral effector functions. Curr Opin Virol 2011; 1:519-25.
55. Wang SH, Yeh SH, Lin WH, Yeh KH, Yuan Q, Xia NS, et al. Estrogen receptor alpha represses transcription of HBV genes via interaction with hepatocyte nuclear factor 4alpha. Gastroenterology 2012; 142:989-98 e4.
56. Levrero M, Pollicino T, Petersen J, Belloni L, Raimondo G, Dandri M. Control of cccDNA function in hepatitis B virus infection. Journal of hepatology 2009; 51:581-92.
57. Pollicino T, Belloni L, Raffa G, Pediconi N, Squadrito G, Raimondo G, et al. Hepatitis B virus replication is regulated by the acetylation status of hepatitis B virus cccDNA-bound H3 and H4 histones. Gastroenterology 2006; 130:823-37.
58. Zhang X, Zhang E, Ma Z, Pei R, Jiang M, Schlaak JF, et al. Modulation of

hepatitis B virus replication and hepatocyte differentiation by MicroRNA-1. Hepatology 2011; 53:1476-85.
59. Zhang X, Liu H, Xie Z, Deng W, Wu C, Qin B, et al. Epigenetically regulated miR-449a enhances hepatitis B virus replication by targeting cAMP-responsive element binding protein 5 and modulating hepatocytes phenotype. Scientific reports 2016; 6:25389.
60. Zhang X, Hou J, Lu M. Regulation of hepatitis B virus replication by epigenetic mechanisms and microRNAs. Frontiers in genetics 2013; 4:202.
61. Zoulim F, Luangsay S, Durantel D. Targeting innate immunity: a new step in the development of combination therapy for chronic hepatitis B. Gastroenterology 2013; 144:1342-4.
62. Chang J, Block TM, Guo JT. The innate immune response to hepatitis B virus infection: implications for pathogenesis and therapy. Antiviral research 2012; 96:405-13.
63. Guo HT, Zhou TL, Jiang D, Cuconati A, Xiao GH, Block TM, et al. Regulation of hepatitis B virus replication by the phosphatidylinositol 3-kinase-Akt signal transduction pathway. Journal of virology 2007; 81:10072-80.
64. Rawat S, Bouchard MJ. The hepatitis B virus (HBV) HBx protein activates AKT To simultaneously regulate HBV replication and hepatocyte survival. Journal of virology 2015; 89:999-1012.
65. Teng CF, Wu HC, Tsai HW, Shiah HS, Huang WY, Su IJ. Novel feedback inhibition of surface antigen synthesis by mammalian target of rapamycin (mTOR) signal and its implication for hepatitis B virus tumorigenesis and therapy. Hepatology 2011; 54:1199-207.
66. Su X, Yu Y, Zhong Y, Giannopoulou EG, Hu X, Liu H, et al. Interferon-gamma regulates cellular metabolism and mRNA translation to potentiate macrophage activation. Nature immunology 2015; 16:838-49.
67. Sir D, Ann DK, Ou JH. Autophagy by hepatitis B virus and for hepatitis B virus. Autophagy 2010; 6:548-9.
68. Wang P, Guo QS, Wang ZW, Qian HX. HBx induces HepG-2 cells autophagy through PI3K/Akt-mTOR pathway. Mol Cell Biochem 2013; 372:161-8.
69. Sir D, Tian YJ, Chen WL, Ann DK, Yen TSB, Ou JHJ. The early autophagic pathway is activated by hepatitis B virus and required for viral DNA replication. P Natl Acad Sci USA 2010; 107:4383-8.

70. Tian Y, Sir D, Kuo CF, Ann DK, Ou JH. Autophagy required for hepatitis B virus replication in transgenic mice. Journal of virology 2011; 85:13453-6.
71. Li J, Liu Y, Wang Z, Liu K, Wang Y, Liu J, et al. Subversion of cellular autophagy machinery by hepatitis B virus for viral envelopment. Journal of virology 2011; 85:6319-33.
72. Schweitzer A, Horn J, Mikolajczyk RT, Krause G, Ott JJ. Estimations of worldwide prevalence of chronic hepatitis B virus infection: a systematic review of data published between 1965 and 2013. Lancet 2015; 386:1546-55.
73. McMahon BJ. Natural history of chronic hepatitis B. Clinics in liver disease 2010; 14:381-96.
74. Hoofnagle JH, Doo E, Liang TJ, Fleischer R, Lok AS. Management of hepatitis B: summary of a clinical research workshop. Hepatology 2007; 45:1056-75.
75. Giordano S, Columbano A. MicroRNAs: new tools for diagnosis, prognosis, and therapy in hepatocellular carcinoma? Hepatology 2013; 57:840-7.
76. Parkin DM. The global health burden of infection-associated cancers in the year 2002. International journal of cancer 2006; 118:3030-44.
77. Fattovich G, Stroffolini T, Zagni I, Donato F. Hepatocellular carcinoma in cirrhosis: incidence and risk factors. Gastroenterology 2004; 127:S35-50.
78. Tan YJ. Hepatitis B virus infection and the risk of hepatocellular carcinoma. World J Gastroenterol 2011; 17:4853-7.
79. Kuo TC, Chao CC. Hepatitis B virus X protein prevents apoptosis of hepatocellular carcinoma cells by upregulating SATB1 and HURP expression. Biochem Pharmacol 2010; 80:1093-102.
80. Zhu YZ, Zhu R, Shi LG, Mao Y, Zheng GJ, Chen Q, et al. Hepatitis B virus X protein promotes hypermethylation of p16(INK4A) promoter through upregulation of DNA methyltransferases in hepatocarcinogenesis. Exp Mol Pathol 2010; 89:268-75.
81. Zhang XD, Zhang H, Ye LH. Effects of hepatitis B virus X protein on the development of liver cancer. J Lab Clin Med 2006; 147:58-66.
82. Nguyen DH, Ludgate L, Hu J. Hepatitis B virus-cell interactions and pathogenesis. J Cell Physiol 2008; 216:289-94.
83. Hino O, Kajino K. Hepatitis virus-related hepatocarcinogenesis. Intervirology 1994; 37:133-5.
84. Faria LC, Gigou M, Roque-Afonso AM, Sebagh M, Roche B, Fallot G, et al. Hepatocellular carcinoma is associated with an increased risk of hepatitis B virus

recurrence after liver transplantation. Gastroenterology 2008; 134:1890-9; quiz 2155.
85. Ni YH, Huang LM, Chang MH, Yen CJ, Lu CY, You SL, et al. Two decades of universal hepatitis B vaccination in taiwan: impact and implication for future strategies. Gastroenterology 2007; 132:1287-93.
86. Trepo C, Chan HL, Lok A. Hepatitis B virus infection. Lancet 2014; 384:2053-63.
87. Zoulim F, Durantel D. Antiviral therapies and prospects for a cure of chronic hepatitis B. Csh Perspect Med 2015; 5.
88. Lucifora J, Xia Y, Reisinger F, Zhang K, Stadler D, Cheng X, et al. Specific and nonhepatotoxic degradation of nuclear hepatitis B virus cccDNA. Science 2014; 343:1221-8.
89. Mizushima N, Yoshimori T, Ohsumi Y. The role of Atg proteins in autophagosome formation. Annual review of cell and developmental biology 2011; 27:107-32.
90. Mizushima N. Autophagy: process and function. Genes & development 2007; 21:2861-73.
91. Mizushima N, Komatsu M. Autophagy: renovation of cells and tissues. Cell 2011; 147:728-41.
92. Hansen M, Rubinsztein DC, Walker DW. Autophagy as a promoter of longevity: insights from model organisms. Nature reviews Molecular cell biology 2018; 19:579-93.
93. Feng Y, He D, Yao Z, Klionsky DJ. The machinery of macroautophagy. Cell research 2014; 24:24-41.
94. Liang XH, Jackson S, Seaman M, Brown K, Kempkes B, Hibshoosh H, et al. Induction of autophagy and inhibition of tumorigenesis by beclin 1. Nature 1999; 402:672-6.
95. Klionsky DJ, Abdelmohsen K, Abe A, Abedin MJ, Abeliovich H, Acevedo Arozena A, et al. Guidelines for the use and interpretation of assays for monitoring autophagy (3rd edition). Autophagy 2016; 12:1-222.
96. Kim J, Kundu M, Viollet B, Guan KL. AMPK and mTOR regulate autophagy through direct phosphorylation of Ulk1. Nature cell biology 2011; 13:132-41.
97. Hosokawa N, Hara T, Kaizuka T, Kishi C, Takamura A, Miura Y, et al. Nutrient-dependent mTORC1 association with the ULK1-Atg13-FIP200 complex required for autophagy. Molecular biology of the cell 2009; 20:1981-91.
98. Jung CH, Jun CB, Ro SH, Kim YM, Otto NM, Cao J, et al. ULK-Atg13-FIP200 complexes mediate mTOR signaling to the autophagy machinery. Molecular biology

of the cell 2009; 20:1992-2003.
99. Hara T, Takamura A, Kishi C, Iemura S, Natsume T, Guan JL, et al. FIP200, a ULK-interacting protein, is required for autophagosome formation in mammalian cells. The Journal of cell biology 2008; 181:497-510.
100. Russell RC, Tian Y, Yuan H, Park HW, Chang YY, Kim J, et al. ULK1 induces autophagy by phosphorylating Beclin-1 and activating VPS34 lipid kinase. Nature cell biology 2013; 15:741-50.
101. Di Bartolomeo S, Corazzari M, Nazio F, Oliverio S, Lisi G, Antonioli M, et al. The dynamic interaction of AMBRA1 with the dynein motor complex regulates mammalian autophagy. The Journal of cell biology 2010; 191:155-68.
102. Kanazawa T, Taneike I, Akaishi R, Yoshizawa F, Furuya N, Fujimura S, et al. Amino acids and insulin control autophagic proteolysis through different signaling pathways in relation to mTOR in isolated rat hepatocytes. J Biol Chem 2004; 279:8452-9.
103. Wei Y, Pattingre S, Sinha S, Bassik M, Levine B. JNK1-mediated phosphorylation of Bcl-2 regulates starvation-induced autophagy. Mol Cell 2008; 30:678-88.
104. Zalckvar E, Berissi H, Mizrachy L, Idelchuk Y, Koren I, Eisenstein M, et al. DAP-kinase-mediated phosphorylation on the BH3 domain of beclin 1 promotes dissociation of beclin 1 from Bcl-XL and induction of autophagy. EMBO Rep 2009; 10:285-92.
105. Yang Z, Klionsky DJ. Eaten alive: a history of macroautophagy. Nature cell biology 2010; 12:814-22.
106. Pareja ME, Colombo MI. Autophagic clearance of bacterial pathogens: molecular recognition of intracellular microorganisms. Front Cell Infect Microbiol 2013; 3:54.
107. Orvedahl A, MacPherson S, Sumpter R, Jr., Talloczy Z, Zou Z, Levine B. Autophagy protects against Sindbis virus infection of the central nervous system. Cell host & microbe 2010; 7:115-27.
108. Rey-Jurado E, Riedel CA, Gonzalez PA, Bueno SM, Kalergis AM. Contribution of autophagy to antiviral immunity. FEBS letters 2015; 589:3461-70.
109. Shelly S, Lukinova N, Bambina S, Berman A, Cherry S. Autophagy is an essential component of Drosophila immunity against vesicular stomatitis virus. Immunity 2009; 30:588-98.

110. Sir D, Ou JH. Autophagy in viral replication and pathogenesis. Molecules and cells 2010; 29:1-7.
111. Ravikumar B, Sarkar S, Davies JE, Futter M, Garcia-Arencibia M, Green-Thompson ZW, et al. Regulation of mammalian autophagy in physiology and pathophysiology. Physiological reviews 2010; 90:1383-435.
112. Orvedahl A, Alexander D, Talloczy Z, Sun Q, Wei Y, Zhang W, et al. HSV-1 ICP34.5 confers neurovirulence by targeting the Beclin 1 autophagy protein. Cell host & microbe 2007; 1:23-35.
113. Talloczy Z, Virgin HWt, Levine B. PKR-dependent autophagic degradation of herpes simplex virus type 1. Autophagy 2006; 2:24-9.
114. Tanida I, Fukasawa M, Ueno T, Kominami E, Wakita T, Hanada K. Knockdown of autophagy-related gene decreases the production of infectious hepatitis C virus particles. Autophagy 2009; 5:937-45.
115. Mizui T, Yamashina S, Tanida I, Takei Y, Ueno T, Sakamoto N, et al. Inhibition of hepatitis C virus replication by chloroquine targeting virus-associated autophagy. Journal of gastroenterology 2010; 45:195-203.
116. Sir D, Tian Y, Chen WL, Ann DK, Yen TS, Ou JH. The early autophagic pathway is activated by hepatitis B virus and required for viral DNA replication. Proceedings of the National Academy of Sciences of the United States of America 2010; 107:4383-8.
117. Wang J, Chen J, Liu Y, Zeng X, Wei M, Wu S, et al. Hepatitis B Virus Induces Autophagy to Promote its Replication by the Axis of miR-192-3p-XIAP Through NF kappa B Signaling. Hepatology 2019; 69:974-92.
118. Jiang H, White EJ, Rios-Vicil CI, Xu J, Gomez-Manzano C, Fueyo J. Human adenovirus type 5 induces cell lysis through autophagy and autophagy-triggered caspase activity. Journal of virology 2011; 85:4720-9.
119. Kim CW, Addy C, Kusunoki J, Anderson NN, Deja S, Fu X, et al. Acetyl CoA Carboxylase Inhibition Reduces Hepatic Steatosis but Elevates Plasma Triglycerides in Mice and Humans: A Bedside to Bench Investigation. Cell metabolism 2017; 26:394-406 e6.
120. Lin Y, Wu C, Wang X, Liu S, Kemper T, Li F, et al. Synaptosomal-associated protein 29 is required for the autophagic degradation of hepatitis B virus. FASEB journal : official publication of the Federation of American Societies for Experimental Biology 2019:fj201801995RR.

121. Liu B, Fang M, Hu Y, Huang B, Li N, Chang C, et al. Hepatitis B virus X protein inhibits autophagic degradation by impairing lysosomal maturation. Autophagy 2014; 10:416-30.
122. Tang SW, Ducroux A, Jeang KT, Neuveut C. Impact of cellular autophagy on viruses: Insights from hepatitis B virus and human retroviruses. Journal of biomedical science 2012; 19:92.
123. Pehar M, Jonas MC, Hare TM, Puglielli L. SLC33A1/AT-1 protein regulates the induction of autophagy downstream of IRE1/XBP1 pathway. The Journal of biological chemistry 2012; 287:29921-30.
124. Kroemer G, Marino G, Levine B. Autophagy and the integrated stress response. Molecular cell 2010; 40:280-93.
125. Stanssens P, Opsomer C, Mckeown YM, Kramer W, Zabeau M, Fritz HJ. Efficient oligonucleotide-directed construction of mutations in expression vectors by the gapped duplex DNA method using alternating selectable markers. Nucleic acids research 1989; 17:4441-54.
126. Lin Y, Deng W, Pang J, Kemper T, Hu J, Yin J, et al. The microRNA-99 family modulates hepatitis B virus replication by promoting IGF-1R/PI3K/Akt/mTOR/ULK1 signaling-induced autophagy. Cellular microbiology 2017; 19.
127. Galle PR, Hagelstein J, Kommerell B, Volkmann M, Schranz P, Zentgraf H. In vitro experimental infection of primary human hepatocytes with hepatitis B virus. Gastroenterology 1994; 106:664-73.
128. Ryu JM, Lee MY, Yun SP, Han HJ. High glucose regulates cyclin D1/E of human mesenchymal stem cells through TGF-beta1 expression via Ca2+/PKC/MAPKs and PI3K/Akt/mTOR signal pathways. Journal of cellular physiology 2010; 224:59-70.
129. Harada H, Itasaka S, Kizaka-Kondoh S, Shibuya K, Morinibu A, Shinomiya K, et al. The Akt/mTOR pathway assures the synthesis of HIF-1alpha protein in a glucose- and reoxygenation-dependent manner in irradiated tumors. The Journal of biological chemistry 2009; 284:5332-42.
130. Bagga S, Rawat S, Ajenjo M, Bouchard MJ. Hepatitis B virus (HBV) X protein-mediated regulation of hepatocyte metabolic pathways affects viral replication. Virology 2016; 498:9-22.
131. Rawat S, Bouchard MJ. The hepatitis B virus (HBV) HBx protein activates AKT to simultaneously regulate HBV replication and hepatocyte survival. Journal of

virology 2015; 89:999-1012.
132. Xie N, Yuan K, Zhou L, Wang K, Chen HN, Lei Y, et al. PRKAA/AMPK restricts HBV replication through promotion of autophagic degradation. Autophagy 2016; 12:1507-20.
133. Nwadike C, Williamson LE, Gallagher LE, Guan JL, Chan EYW. AMPK Inhibits ULK1-Dependent Autophagosome Formation and Lysosomal Acidification via Distinct Mechanisms. Molecular and cellular biology 2018; 38: e00023-18.
134. Xu DQ, Wang Z, Wang CY, Zhang DY, Wan HD, Zhao ZL, et al. PAQR3 controls autophagy by integrating AMPK signaling to enhance ATG14L-associated PI3K activity. The EMBO journal 2016; 35:496-514.
135. Xintaropoulou C, Ward C, Wise A, Marston H, Turnbull A, Langdon SP. A comparative analysis of inhibitors of the glycolysis pathway in breast and ovarian cancer cell line models. Oncotarget 2015; 6:25677-95.
136. Brown J. Effects of 2-deoxyglucose on carbohydrate metablism: review of the literature and studies in the rat. Metabolism: clinical and experimental 1962; 11:1098-112.
137. Xi H, Kurtoglu M, Liu H, Wangpaichitr M, You M, Liu X, et al. 2-Deoxy-D-glucose activates autophagy via endoplasmic reticulum stress rather than ATP depletion. Cancer chemotherapy and pharmacology 2011; 67:899-910.
138. Jeon JY, Kim SW, Park KC, Yun M. The bifunctional autophagic flux by 2-deoxyglucose to control survival or growth of prostate cancer cells. BMC cancer 2015; 15:623.
139. Hardiville S, Hart GW. Nutrient regulation of signaling, transcription, and cell physiology by O-GlcNAcylation. Cell metabolism 2014; 20:208-13.
140. Xu W, Zhang X, Wu JL, Fu L, Liu K, Liu D, et al. O-GlcNAc transferase promotes fatty liver-associated liver cancer through inducing palmitic acid and activating endoplasmic reticulum stress. Journal of hepatology 2017; 67:310-20.
141. Alejandro EU, Bozadjieva N, Kumusoglu D, Abdulhamid S, Levine H, Haataja L, et al. Disruption of O-linked N-Acetylglucosamine Signaling Induces ER Stress and beta Cell Failure. Cell reports 2015; 13:2527-38.
142. Jang I, Kim HB, Seo H, Kim JY, Choi H, Yoo JS, et al. O-GlcNAcylation of eIF2alpha regulates the phospho-eIF2alpha-mediated ER stress response. Biochimica et biophysica acta 2015; 1853:1860-9.
143. Mishra S, Ande SR, Salter NW. O-GlcNAc modification: why so intimately

associated with phosphorylation? Cell communication and signaling : CCS 2011; 9:1.
144. Wang Z, Gucek M, Hart GW. Cross-talk between GlcNAcylation and phosphorylation: site-specific phosphorylation dynamics in response to globally elevated O-GlcNAc. Proceedings of the National Academy of Sciences of the United States of America 2008; 105:13793-8.
145. Timothy M. Block XL, Frances M. Platt, Graham R. Foster, Wolfram H. Gerlich, Baruch S. Blumberg, Raymond A. Dwek. Secretion of human hepatitis B virus is inhibited by the imino sugar N-butyldeoxynojirimycin. Proceedings of the National Academy of Sciences of the United States of America 1994; 91:2235-9.
146. Sigrid Schmitt DG, Kim Alving, Tanja K. Tolle, Monica Linder, Hildegard Geyer, Dietmar Linder, Jasna Peter-Katalinic, Wolfram H. Gerlich, and Rudolf Geyeri. Analysis of the Pre-S2 N- and O-Linked Glycans of the M Surface Protein from Human Hepatitis B Virus. The Journal of biological chemistry 1999; 274:11945-57.
147. Bermingham ML, Colombo M, McGurnaghan SJ, Blackbourn LAK, Vuckovic F, Pucic Bakovic M, et al. N-Glycan Profile and Kidney Disease in Type 1 Diabetes. Diabetes care 2018; 41:79-87.
148. Trbojevic Akmacic I, Ventham NT, Theodoratou E, Vuckovic F, Kennedy NA, Kristic J, et al. Inflammatory bowel disease associates with proinflammatory potential of the immunoglobulin G glycome. Inflammatory bowel diseases 2015; 21:1237-47.
149. Chen G, Wang Y, Qin X, Li H, Guo Y, Wang Y, et al. Change in IgG1 Fc N-linked glycosylation in human lung cancer: age- and sex-related diagnostic potential. Electrophoresis 2013; 34:2407-16.
150. Kodar K, Stadlmann J, Klaamas K, Sergeyev B, Kurtenkov O. Immunoglobulin G Fc N-glycan profiling in patients with gastric cancer by LC-ESI-MS: relation to tumor progression and survival. Glycoconjugate journal 2012; 29:57-66.
151. Nakagawa H, Hato M, Takegawa Y, Deguchi K, Ito H, Takahata M, et al. Detection of altered N-glycan profiles in whole serum from rheumatoid arthritis patients. Journal of chromatography B, Analytical technologies in the biomedical and life sciences 2007; 853:133-7.
152. Mahmoudabadi G, Milo R, Phillips R. Energetic cost of building a virus. Proceedings of the National Academy of Sciences of the United States of America 2017; 114:E4324-E33.
153. Fontaine KA, Sanchez EL, Camarda R, Lagunoff M. Dengue virus induces and requires glycolysis for optimal replication. Journal of virology 2015; 89:2358-66.

154. Ikeda M, Kato N. Modulation of host metabolism as a target of new antivirals. Advanced drug delivery reviews 2007; 59:1277-89.
155. Shlomai A, Shaul Y. The "metabolovirus" model of hepatitis B virus suggests nutritional therapy as an effective anti-viral weapon. Medical hypotheses 2008; 71:53-7.
156. Tacke F, Liedtke C, Bocklage S, Manns MP, Trautwein C. CREB/PKA sensitive signalling pathways activate and maintain expression levels of the hepatitis B virus pre-S2/S promoter. Gut 2005; 54:1309-17.
157. Bar-Yishay I, Shaul Y, Shlomai A. Hepatocyte metabolic signalling pathways and regulation of hepatitis B virus expression. Liver international : official journal of the International Association for the Study of the Liver 2011; 31:282-90.
158. Ramiere C, Scholtes C, Diaz O, Icard V, Perrin-Cocon L, Trabaud MA, et al. Transactivation of the hepatitis B virus core promoter by the nuclear receptor FXRalpha. Journal of virology 2008; 82:10832-40.
159. Ondracek CR, McLachlan A. Role of peroxisome proliferator-activated receptor gamma coactivator 1alpha in AKT/PKB-mediated inhibition of hepatitis B virus biosynthesis. Journal of virology 2011; 85:11891-900.
160. Quasdorff M, Protzer U. Control of hepatitis B virus at the level of transcription. Journal of viral hepatitis 2010; 17:527-36.
161. Li L, Oropeza CE, Kaestner KH, McLachlan A. Limited effects of fasting on hepatitis B virus (HBV) biosynthesis in HBV transgenic mice. Journal of virology 2009; 83:1682-8.
162. Lin Y, Wu C, Wang X, Kemper T, Squire A, Gunzer M, et al. Hepatitis B virus is degraded by autophagosome-lysosome fusion mediated by Rab7 and related components. Protein & cell 2019; 10:60-6.
163. Boroughs LK, DeBerardinis RJ. Metabolic pathways promoting cancer cell survival and growth. Nature cell biology 2015; 17:351-9.
164. Meijer AJ, Codogno P. Autophagy: regulation by energy sensing. Current biology : CB 2011; 21:R227-9.
165. Corradetti MN, Inoki K, Bardeesy N, DePinho RA, Guan KL. Regulation of the TSC pathway by LKB1: evidence of a molecular link between tuberous sclerosis complex and Peutz-Jeghers syndrome. Genes & development 2004; 18:1533-8.
166. Gwinn DM, Shackelford DB, Egan DF, Mihaylova MM, Mery A, Vasquez DS, et al. AMPK phosphorylation of raptor mediates a metabolic checkpoint. Molecular cell

2008; 30:214-26.
167. Guo H, Zhou T, Jiang D, Cuconati A, Xiao GH, Block TM, et al. Regulation of hepatitis B virus replication by the phosphatidylinositol 3-kinase-akt signal transduction pathway. Journal of virology 2007; 81:10072-80.
168. Xiang K, Wang B. Role of the PI3KAKTmTOR pathway in hepatitis B virus infection and replication. Molecular medicine reports 2018; 17:4713-9.
169. Altomare DA, Khaled AR. Homeostasis and the importance for a balance between AKT/mTOR activity and intracellular signaling. Current medicinal chemistry 2012; 19:3748-62.
170. Gardner TW, Abcouwer SF, Losiewicz MK, Fort PE. Phosphatase control of 4E-BP1 phosphorylation state is central for glycolytic regulation of retinal protein synthesis. American journal of physiology Endocrinology and metabolism 2015; 309:E546-56.
171. Muaddi H, Majumder M, Peidis P, Papadakis AI, Holcik M, Scheuner D, et al. Phosphorylation of eIF2alpha at serine 51 is an important determinant of cell survival and adaptation to glucose deficiency. Molecular biology of the cell 2010; 21:3220-31.
172. Maus M, Torrens Y, Gauchy C, Bretin S, Nairn AC, Glowinski J, et al. 2-Deoxyglucose and NMDA inhibit protein synthesis in neurons and regulate phosphorylation of elongation factor-2 by distinct mechanisms. Journal of neurochemistry 2006; 96:815-24.
173. Lima VV, Rigsby CS, Hardy DM, Webb RC, Tostes RC. O-GlcNAcylation: a novel post-translational mechanism to alter vascular cellular signaling in health and disease: focus on hypertension. Journal of the American Society of Hypertension : JASH 2009; 3:374-87.
174. Angelova M, Ortiz-Meoz RF, Walker S, Knipe DM. Inhibition of O-Linked N-Acetylglucosamine Transferase Reduces Replication of Herpes Simplex Virus and Human Cytomegalovirus. Journal of virology 2015; 89:8474-83.
175. Guo B, Liang Q, Li L, Hu Z, Wu F, Zhang P, et al. O-GlcNAc-modification of SNAP-29 regulates autophagosome maturation. Nature cell biology 2014; 16:1215-26.
176. Lin Z, Zhou P, von Gise A, Gu F, Ma Q, Chen J, et al. Pi3kcb links Hippo-YAP and PI3K-AKT signaling pathways to promote cardiomyocyte proliferation and survival. Circulation research 2015; 116:35-45.
177. Gumbiner BM, Kim NG. The Hippo-YAP signaling pathway and contact

inhibition of growth. Journal of cell science 2014; 127:709-17.
178. Liang N, Zhang C, Dill P, Panasyuk G, Pion D, Koka V, et al. Regulation of YAP by mTOR and autophagy reveals a therapeutic target of tuberous sclerosis complex. The Journal of experimental medicine 2014; 211:2249-63.
179. Novelli A, Boulanger PA. Deletion analysis of functional domains in baculovirus-expressed adenovirus type 2 fiber. Virology 1991; 185:365-76.
180. Gonzalez SA, Burrone OR. Rotavirus NS26 is modified by addition of single O-linked residues of N-acetylglucosamine. Virology 1991; 182:8-16.
181. Ko YC, Tsai WH, Wang PW, Wu IL, Lin SY, Chen YL, et al. Suppressive regulation of KSHV RTA with O-GlcNAcylation. Journal of biomedical science 2012; 19:12.
182. Jochmann R, Pfannstiel J, Chudasama P, Kuhn E, Konrad A, Sturzl M. O-GlcNAc transferase inhibits KSHV propagation and modifies replication relevant viral proteins as detected by systematic O-GlcNAcylation analysis. Glycobiology 2013; 23:1114-30.
183. Jochmann R, Thurau M, Jung S, Hofmann C, Naschberger E, Kremmer E, et al. O-linked N-acetylglucosaminylation of Sp1 inhibits the human immunodeficiency virus type 1 promoter. Journal of virology 2009; 83:3704-18.
184. Patterson MC. Metabolic mimics: the disorders of N-linked glycosylation. Seminars in pediatric neurology 2005; 12:144-51.
185. Imperiali B, O'Connor SE. Effect of N-linked glycosylation on glycopeptide and glycoprotein structure. Current opinion in chemical biology 1999; 3:643-9.

9. Abbreviations

Abbreviations	Full name
1,3BPG	1,3-bisphosphoglycerate
2PG	2-phosphoglycerate
3PG	3-phosphoglycerate
α-KG	α-ketoglutarate
AcCoA	acetyl-CoA
DHAP	dihydroxyacetone-phosphate
F1,6BP	fructose-1,6-bisphosphate
F2,6BP	fructose-2,6-bisphosphate
F6P	fructose-6-phosphate

FAS	fatty acid synthesis
G6P	glucose-6-phosphate
LDH	lactate dehydrogenase
PEP	phosphoenolpyruvate
PFK1	phosphofructokinase 1
PFKFB	6-phosphofructo 2-kinase/fructose-2,6-bisphosphatase
PK	pyruvate kinase
PPP	pentose phosphate pathway
TCA	tricarboxylic acid
TPI	triosephosphate isomerase
cccDNA	circular covalently closed DNA
CHB	chronic hepatitis B
CMIA	chemiluminescence immunoassay
GFP	green fluorescence protein
DMEM	Dulbecco’s Modified Eagles’s Medium
DMSO	dimethylsulfoxide
CQ	chloroquine
AICAR	5-Aminoimidazole-4-carboxamide 1-β-D-ribofuranoside
OSMI-1	(αR)-α-[[(1,2-Dihydro-2-oxo-6-quinolinyl)sulfonyl]amino]-N-(2-furanylmethyl)-2-methoxy-N-(2-thienylmethyl)-benzeneacetamide
BADGP	Benzyl 2-acetamido-2-deoxy-α-D-galactopyranoside
PUGNAc	O-(2-Acetamido-2-deoxy-D-glucopyranosylidenamino) N-phenylcarbamate
3-MA	3-Methyladenine
2-DG	2-Deoxy-D-glucose
TM	Tunicamycin
DNA	deoxyribonucleic acid
E.coli	*Escherichia coli*
EDTA	ethylenediaminetetraaceticacid
FBS	fetal bovine serum
g	gram
HBsAg	hepatitis B surface antigen
HBeAg	hepatitis B e antigen
HBV	hepatitis B virus

HBV RIs	hepatitis B virus replicative intermediates
HBx	hepatitis B x antigen
HCC	hepatocellular carcinoma
HCV	hepatitis C virus
HIV	human immunodeficiency virus
IFN	interferon
IGF1R	insulin-like growth factor 1 receptor
PI3K	phosphatidylinositol 3-kinase
mTOR	mammalian target of rapamycin
LC3	MAP1LC3, microtubule-associated protein 1 light chain 3 beta
p62/SQSTM1	Sequestosome-1
LXRs	liver X receptors
m	milli
kb	kilo base pair
l	liter
MEM	Dulbecco’s Modified Eagle Medium
min	minute
PBS	phosphate buffered saline
pSP1	plasmid contains HBV pre S1 promoter region
pSP2	plasmid contains HBV pre S2 promoter region
pCP	plasmid contains HBV core promoter region
pXP	plasmid contains HBV X promoter region
PCR	polymerase chain reaction
pgRNA	pregenomic RNA
PHH	primary human hepatocyte
RT-PCR	reverse transcriptase polymerase chain reaction
siR-C	control small interfering RNA
siRNA	small interfering RNA

10. List of figures

11. Acknowledgements

I am deeply grateful to my supervisor, Prof. Dr. rer. nat. Mengji Lu for providing me the opportunity to study and finish my PhD project in the Institute of Virology, University Hospital Essen. I strongly appreciate his patient guidance and strict attitude in scientific work. With his help, I have not only gained a lot of knowledge and skills, but also learned to communicate with other people and exchange ideas.

I also would like to thank Prof. Dr. Ulf Dittmer in the Institute of Virology. He has provided me good welfare and a lot of help in Germany in the past four years. Moreover, I want to appreciate the support and help from Ms. Ursula Schrammel and Ms. Katrin Palupsky in my work and daily life during my stay in Germany.

Many thanks go to our technicians Mrs. Thekla Kemper and Mrs. Barbara Bleekmann. Their technical assistance and help were very important for my PhD project. I also would like to appreciate my colleagues Dr. Yong Lin, Mrs. Qian Li and all the other Chinese colleagues in the University Hospital Essen. Their grateful help and care made my life much more joyous in Germany.

I also would like to thank my parents, sister, relatives and friends for their sustained encouragement and help.

I appreciate the support and help from the Graduate School of Biomedical Science. Many thanks to my other classmates in the Graduate School of Biomedical Science for their friendship and help. Finally, I want to convey my thanks to the financial support provided by Deutsche Forschungsgemeinschaft (TRR60).

Curriculum vitae

The biography is not included in the online version for reasons of data protection

Erklärung:

Hiermit erkläre ich, gem. § 6 Abs. (2) g) der Promotionsordnung der Fakultät für Biologie zur Erlangung der Dr. rer. nat., dass ich das Arbeitsgebiet, dem das Thema „Hepatitis B virus production is modulated through autophagy pathway in response to glucose“ zuzuordnen ist, in Forschung und Lehre vertrete und den Antrag von (Xueyu Wang) befürworte und die Betreuung auch im Falle eines Weggangs, wenn nicht wichtige Gründe dem entgegenstehen, weiterführen werde.

Essen, den _____ _____

Unterschrift des Betreuers (Prof. oder PD) an der Universität Duisburg-Essen

Erklärung:

Hiermit erkläre ich, gem. § 7 Abs. (2) d) + f) der Promotionsordnung der Fakultät für Biologie zur Erlangung des Dr. rer. nat., dass ich die vorliegende Dissertation selbständig verfasst und mich keiner anderen als der angegebenen Hilfsmittel bedient, bei der Abfassung der Dissertation nur die angegeben Hilfsmittel benutzt und alle wörtlich oder inhaltlich übernommenen Stellen als solche gekennzeichnet habe.

Essen, den _____ _____

Unterschrift des/r Doktoranden/in

Erklärung:

Hiermit erkläre ich, gem. § 7 Abs. (2) e) + g) der Promotionsordnung der Fakultät für Biologie zur Erlangung des Dr. rer. nat., dass ich keine anderen Promotionen bzw. Promotionsversuche in der Vergangenheit durchgeführt habe und dass diese Arbeit von keiner anderen Fakultät/Fachbereich abgelehnt worden ist.

Essen, den _____ _____

Unterschrift des/r Doktoranden/in